Theses and Dissertations

1-1-2013

A Novel Approach to the Design of Selective Inhibitors for Cell Cycle Cyclin Dependent Kinases

Tracy Perkins
University of South Carolina

Follow this and additional works at: https://scholarcommons.sc.edu/etd

Part of the Pharmacy and Pharmaceutical Sciences Commons

Recommended Citation

A NOVEL APPROACH TO THE DESIGN OF SELECTIVE INHIBITORS FOR CELL
CYCLE CYCLIN DEPENDENT KINASES

by

Tracy Perkins

Bachelor of Science
University of Pittsburgh, 2010

_____

Submitted in Partial Fulfillment of the Requirements

For the Degree of Master of Science in

Pharmaceutical Sciences

College of Pharmacy

University of South Carolina

2013

Accepted by:

Campbell McInnes, Major Professor

James Chapman, Chair of Examining Committee

Kim Creek, Committee Member

Thomas Dix, Committee Member

John Lavigne, Committee Member

Lacy Ford, Vice Provost and Dean of Graduate Studies

ABSTRACT

CDK2/cyclin A and CDK4/cyclin D1 are proven targets for cancer drug discovery. The development of novel CDK inhibitors, with high selectivity, are being investigated by targeting the cyclin binding groove (CBG) located on the cyclin, the regulatory subunit of CDK. The CBG is a shallow area that is involved in signaling and the inhibition of cell cycle CDKs via endogenous tumor suppressors. Currently, non-peptidic inhibitors are being developed based on the recognition amino acid sequence, HAKRRLIF, of the C-terminal peptide sequence of the CDK inhibitor p21^{WAF1}. Computational design and the utilization of non-natural amino acids are being proposed in identifing small molecules to replace the C-terminal amino acids (RLIF) via the REPLACE methodology. Such small molecules, known as capping groups, have significant potential for converting the octamer into a more drug-like molecule. The REPLACE methodology has been applied and used to identify novel Ccaps to replace RLIF and these Ccaps have IC$_{50}$ values in the 40-100 μM range against the cell cycle CDK/cyclin complexes of interest. Fragment ligated inhibitory peptides (FLIPs) have been synthesized, coupled with a potent small molecule N-terminal capping group (Ncap), and their binding affinities have been tested using a Fluorescence Polarization (FP) assay. The results reported here enhance the development of a selective, drug-like, cell permeable small molecule CDK cyclin groove inhibitors by generating promising Ccaps and by identifying a novel approach to the designing of potential partial ligand alternatives. Further, these results bring us closer to achieving the ultimate goal of developing a novel class of cancer therapeutics based on

iv

cell cycle inhibition through cyclin dependent kinases.

TABLE OF CONTENTS

LIST OF TABLES

LIST OF FIGURES

LIST OF SCHEMES

LIST OF ABBREVIATIONS

CHAPTER 1
INTRODUCTION

Cyclin dependent kinases (CDKs) play a major role in many cellular processes including the mammalian cell cycle. CDKs are heterodimeric structures that contain two subunits, the catalytic kinase and the regulatory cyclin. This complex is responsible for the phosphorylation of various substrates to tightly control cell proliferation. Other proteins also regulate the cell cycle such as CDK inhibitors and tumor suppressor proteins. These proteins, among others, work together to promote or suppress DNA replication and in a perfect world this is done without disruptions or damage. However, through genetic or environmental disturbance, many aspects of the cell cycle can be deregulated or disrupted by mutation, overexpression, or amplification. Currently, several approaches are being studied to identify potential CDK inhibitors to help restore regulation in cells with uncontrolled proliferation. These include, but are not limited to, targeting the ATP binding pocket on the kinase and the substrate recruitment site located on the cyclin. In this chapter, the details of the cell cycle, altered functions of endogenous proteins and the current therapeutic approaches will be discussed.

1.1 ROLE OF CDK/CYCLIN COMPLEXES IN THE CELL CYCLE

The mammalian cell cycle is the process in which cells replicate and divide to form two daughter cells from a single parental cell. There are four consecutive phases of the cell cycle that must occur in order for the cell to properly divide. These phases are Gap 1

(G1), Synthesis (S), Gap 2 (G2), and Mitosis (M). Additionally, there is a resting phase known as Gap 0 (G0) which is considered to be a sub-phase of G1 and contains non-proliferating cells[1]. During G1 phase the cell prepares for the entry into S phase by expressing proteins required for S phase[1]. During S phase, DNA is replicated, in G2 phase the cell prepares for the entry into M phase, and during M phase the cell undergoes cellular division[1].

Each phase of the cell cycle is tightly controlled by specific CDKs. This protein family contains more than 20 members and individual isoforms can be involved in distinct cellular functions including both cell cycle progression and/or transcription. During the cell cycle, CDKs complex with a regulatory cyclin and phosphorylate various substrates to promote cell proliferation. During G1, CDK4 and CDK6 complex with the D-type cyclins and these heterodimers are essential for progression through this phase[1]. Late in G1, CDK2 binds to cyclin E to regulate the transition from G1 to S phase. In G2, CDK1 complexes with cyclin A to promote entry into M phase and in M phase, CDK1 binds to cyclin B to help promote cellular division[1] (Figure 1.1 and Table 1.1). CDK protein levels remain constant throughout the cell cycle unlike the cyclins whose levels oscillate to activate specific CDKs and to tightly control each phase of cell proliferation. Unlike most others, the D-type cyclin (D1, D2, and D3) levels are maintained throughout the cell cycle and their activity is regulated by growth factors/mitogenic stimulation[1-2].

During transcription, two other CDKs (7 and 9) are active[3]. These CDKs promote the initiation and elongation of nascent RNA transcripts by phosphorylating the carboxy-terminal domain (CTD) of RNA polymerase II[2a]. CDK7 and 9 are subunits of TFIIH and p-TEFb, respectively, in which they activate RNA polymerase II[4]. TFIIH is critical for

stabilizing of the elongation factors and p-TEFb promotes productive elongation[5].
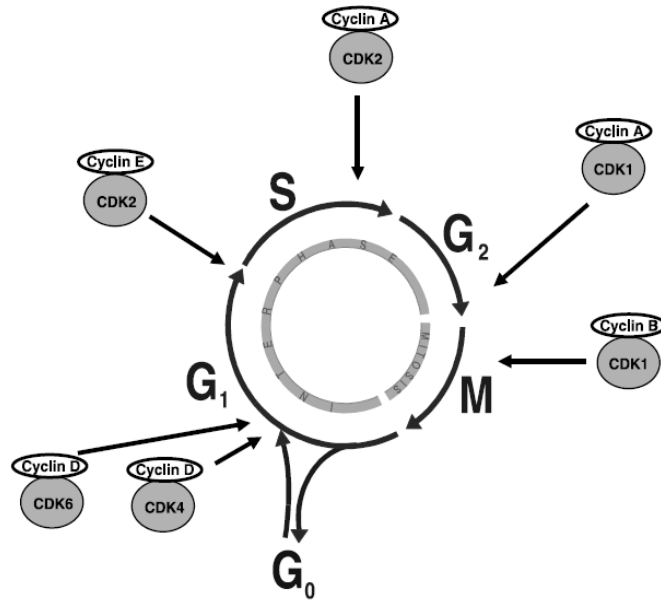
FIGURE 1.1. STAGES OF THE CELL CYCLE The four stages of the mammalian cell cycle consist of Gap 1 (G1), Synthesis (S), Gap 2 (G2), and Mitosis (M) phases. G0 is a sub-phase of G1 and contains non-proliferating cells. During G1 phase, CDK4/cyclin D and CDK6/cyclin D complexes are active. During S, G2, and M phases, CDK2/cyclin E and CDK2/cyclin A, CDK1/cyclin A, and CDK1/cyclin B are active, respectively (Vermeulen, *et al*. 2003). [Figure reproduced with permission from John Wiley and Sons.]

TABLE 1.1. SUMMARY OF CDK/CYCLIN COMPLEXES DURING EACH PHASE OF THE CELL CYCLE.

CDK	Cyclin	Cell Cycle Phase
4	D	G1
6	D	G1
2	E	Late G1 into S
2	A	S
1	A	G2 into M
1	B	M

The G1/S phase transition is a critical point in the cell cycle. Cells either commit to or abandon cell cycle progression. This process is complex and the retinoblastoma protein (pRb) is at the center of all the action. pRb is a tumor suppressor protein whose primary function is to tightly regulate cell proliferation during the G1 phase[6]. When

hypophosphorylated, pRb is able to interact with a transcription factor, E2F-1, and also with histone deacetylase-1 (HDAC1) to inhibit progression through the cell cycle[2a]. When pRb is bound to E2F-1, the transcription of genes necessary for entry into S phase is inhibited. When pRb is hyperphosphorylated by CDK4/6-cyclin D complexes late in G1, the inhibitory effects of pRb are abolished and transcription is promoted. Phosphorylation of pRb causes a disruption of the trimeric complex of pRb, HDAC1 and E2F-1[1-2]. E2F-1 is therefore released, able to bind with its heterodimeric partner, DP-1, and together they direct the transcription of genes required for S phase. The cell can then pass through what is known as the restriction point and from this point the cell is committed to a single round of replication[2a, 7]. As a result of E2F-1 promoting transcription, cyclin E is expressed and is able to complex with CDK2 to maintain pRb in a hyperphosphorylated state for the remainder of the cell cycle[1, 2b].

During S phase of normal cells, the DNA of a cell must only replicate once and prior to the completion of this replication, E2F-1 activity must be downregulated to avoid potential apoptosis. CDK2/cyclin A phosphorylation of E2F-1 when bound to DNA is a key event in the timely neutralization of E2F-1 activity[2a]. Phosphorylation of E2F-1 causes it to be released from the DNA and is therefore no longer able to function as a transcription factor[2a]. The cell is then able to complete S phase and enter G2 where it prepares for entry into and progression through mitosis.

There are four stages of mitosis (prophase, metaphase, anaphase, and telophase) that result in the division of a single cell into two daughter cells[1]. Prophase is when the chromosomes begin to condense inside the nucleus and the duplicated centrosomes separate to form the poles of the mitotic spindle[7]. A stage prior to metaphase, known as

prometaphase, is when the nuclear envelope breaks down and the chromosomes begin to attach to the mitotic spindles. Metaphase involves the completion of this attachment and alignment of the chromosomes in the center of the cell[7]. To aid in the metaphase/anaphase transition, CDK1/cyclin A and B phosphorylate the anaphase promoting complex (APC)[7]. In turn the APC ubiquitinates cyclins A and B, marking them for degradation, resulting in a repression of CDK activity which is critical for the cell to exit mitosis and for the reentry into G1[7]. Once in anaphase, the cell begins to exit mitosis and the two sets of chromosomes split and approach the mitotic spindle poles, meanwhile the nuclear envelope begins to reform as a precursor to telophase[7]. In telophase, the cell begins to divide in two and the final separation into daughter cells is termed cytokinesis[7].

1.2 ENDOGENOUS CDK/CYCLIN INHIBITORS

Along with the CDK/cyclin complexes, there are other regulators that are required for the cell to successfully progress through the cell cycle. The regulation of cell proliferation is aided by inhibitory proteins which bind to CDKs (CDKIs). There are two distinct families of CDKIs, INK4 and Cip/Kip[1]. The INK4 family preferentially inactivates CDK4/6 and consists of at least four members ($p15^{INK4b}$, $p16^{INK4a}$, $p18^{INK4c}$, and $p19^{INK4d}$)[1]. These proteins bind to monomeric CDK to prevent their association with the D-type cyclins[1]. The activities of the INK4 family results in the inhibition of the cell cycle in G1 by disrupting the ability of CDK4/6 to phosphorylate pRb[2b]. Without pRb phosphorylation, E2F-1 activity is inhibited and the cell never enters S phase[2b]. The mechanism of action in which INK4 inhibitors bind and inhibit the CDK protein is through binding near the adenosine triphosphate (ATP) binding site which alters its

5

conformation and allosterically prevents ATP from binding[2b].

The Cip/Kip family inactivates the CDK/cyclin complexes of CDK1, CDK2, CDK4, and CDK6. These inhibitory proteins include p21[WAF1], p21[Cip1], p27[Cip2], and p57[Kip2] [1]. Each of these proteins contains a conserved sequence known as the cyclin binding motif (CBM)[2b]. These proteins interact with the cyclin through this motif via protein-protein interactions (PPI) at a shallow hydrophobic region on the cyclin known as the cyclin binding groove (CBG). Other proteins (i.e. E2F-1, pRb, etc) also contain the CBM and interact with the CBG in a similar manner prior to their phosphorylation by the CDK/cyclin complexes. These interactions will be discussed in detail in Section 1.5. The expression of p21[WAF1] is under transcriptional control of p53, a tumor suppressor protein[1]. The levels of p53 are generally kept low with in the cell however, when there is DNA damage (replication errors, external damaging agents such as X-rays or UV light) p53 levels accumulate enough for the expression of p21[WAF1] to occur, resulting in cell cycle arrest[8].

To bring all of this into perspective, Figure 1.2 illustrates the stages and regulation of the cell cycle along with a few of the numerous proteins involved. In brief, starting at G1 (far bottom left) we have an INK4 protein bound to CDK4/6, inhibiting the interaction with cyclin D. Upon mitogenic stimuli the transcription of cyclin D occurs. When the INK4 protein is removed from CDK4/6, the kinases are able to complex with cyclin D and upon phosphorylation by a CDK activating kinase (CAK; CDK7/cyclin H – activates many CDK/cyclin complexes), the CDK4/6/cyclin D complexes become fully activated. pRB is phosphorylated by CDK4/6/cyclin D complexes releasing E2F and promoting the transcription of various genes necessary for S phase (i.e. cyclin E). CDK2

associates with cyclin E to further phosphorylate pRb. CDK2 association with cyclin A

is required for DNA replication and this complex can be blocked by the Cip/Kip family

of CDKIs. Late in S phase, CDK1 binds to cyclins A and B, promoting APC (not shown

in the figure) to ubiquitinate cyclins A and B for their necessary degradation and the

progression of the cell cycle. Vermeulen, *et al*. (2003) explains this figure more in

depth[1].   The CDK/cyclin complexes and other protein activities can be inhibited by

Cip/Kip CDKIs by various pathways [2b].
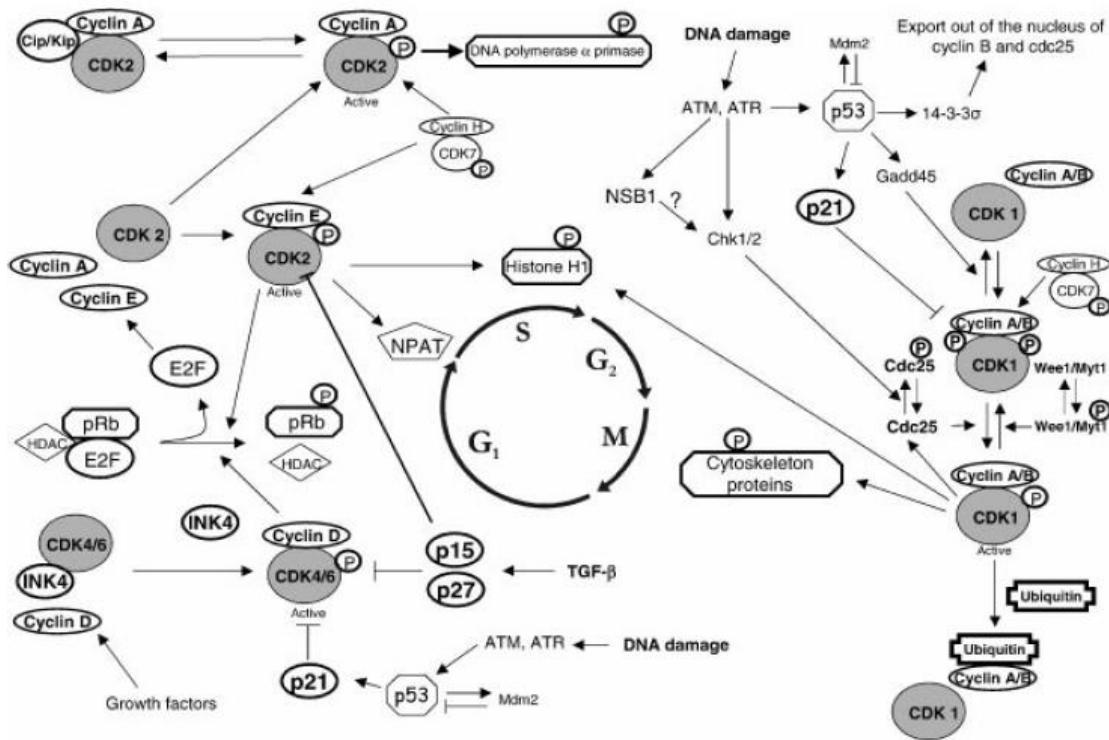
FIGURE 1.2. OVERVIEW OF SOME ESSENTIAL PROTEINS INVOLVED IN CELL CYCLE REGULATION.
Ⓟ: phosphorylated site, →: activation, and |—: inhibition (Vermeulen, *et al*. 2003). [Figure reproduced with permission from John Wiley and Sons.]

Also controlled by CDKs are checkpoints throughout the cell cycle.   These

checkpoints aid in the regulation of proliferation, ensure that the cell is in its optimum

state prior to the transition from one phase to the next, and are sensitive to problems

within DNA replication or within the cellular environment[7]. The first type of checkpoint

is the restriction point late in G1. This checkpoint is sensitive to the physiological state of the cell and its environment and with inappropriate mitogenic signaling, the cell will not transition into S phase[7]. This restriction point is considered the "point of no return" for the cell cycle[1]. It is at this point that the cell either commits to or abandons cell cycle progression. The second type of checkpoint is the DNA damage checkpoint. G1, S, and G2 phases each have this checkpoint which has the ability to block cell proliferation[7]. If DNA damage is detected, the checkpoint will arrest the cell cycle to allow time for DNA repair[1]. If the damage is too advanced the cell will undergo apoptosis[7].

The third type of checkpoint is the DNA replication checkpoint. This checkpoint has the ability to detect unreplicated DNA or malfunctioned replication machinery[7]. If such problems arise, this checkpoint is able to aid in the stabilization of the replication machinery to promote repair or to further DNA replication[7]. The last type of checkpoint is the spindle assembly checkpoint. This checkpoint ensures that all chromosomes have properly attached to the mitotic spindle prior to chromosome segregation[7]. If improper attachment to the spindle is detected, the cell will arrest in mitosis[1].

1.3 ALTERED FUNCTIONS OF CDK/CYCLINS AND ENDOGENOUS INHIBITORS IN TRANSFORMED CELLS

CDKs are key players in regulating many important cellular functions (cell cycle control, cell signaling, apoptosis, gene transcription, etc.) and their deregulation is associated with numerous diseases, in particular cancer[9]. One of the most common deregulation events during the cell cycle involves the CDK4/6-cyclin D-INK4-pRb pathway. This pathway is ubiquitously disrupted in mammalian cancers[2a, 9b]. The functional inactivation of the tumor suppressor gene, pRb causes dysfunction of proteins that endogenously inhibit the

proliferation[1]. Deregulation is most often seen in the G1/S phase CDKs (CDK2/4/6) which occurs by the mutation of CDKIs (p16[INK4a], p21[WAF1], pRb etc.). These mutations provide the means for transformed cells to override the G1 checkpoint resulting in uncontrolled cell proliferation[3, 10].

The CDKI p16 gene has been found to be altered in numerous tumor types and inactivated by a number of mechanisms (deletion, point mutation and hypermethylation)[1-2]. With altered p16, cells lack the ability to inhibit CDK4/6-cyclin D resulting in pRb being hyperphosphorylated and unable to sequester E2F-1, thus promoting uncontrolled cell proliferation[1, 11]. This inappropriate entry into S phase and overactivation of E2F-1 should induce apoptosis[11]. Altered p16 has been noted in glioma, mesothelioma, pancreatic, and many other cancer types[1].

The CDK4 gene has been found to be amplified and CDK4 protein overexpression has been noted in multiple cell lines, particularly in breast cancer[1, 12]. A study conducted on CDK4 null mice determined that the animals were resistant to mammary carcinomas, the continual presence of CDK4 and cyclin D1 was critical in retaining tumor cell proliferation, and the catalytic function of CDK4/cyclin D1 complex is mandatory to sustain the tumorigenic potential of breast cancers cells[12]. Mutant cyclin D1 is able to bind to the appropriate CDKs and to the CDKIs p21[Cip1] and p27[Kip1] however this mutated cyclin lacks the ability to activate the kinase[12].

Cyclin D1 is the most ubiquitously expressed cyclin and is present in many cell types and tissues[9b]. Its gene amplification has been observed in bladder, lung, colon, and many other malignant cancers and cyclin D1 is known to be a critical regulator of breast cancer[1-2]. Cyclin D1 upregulation is often associated with the loss of p16 function and

results in increased levels of CDK4 available to complex with D-type cyclins and endogenous CDKIs[2a]. CDK4/6-cyclin D1 complexes promote the activation of CDK2/cyclin E and the phosphorylation of pRb[2a]. The increased activity of CDK2/cyclin E, as a result of the CDK4/6-cyclin D-INK4-pRb pathway being deregulated, further causing inappropriate levels of E2F activity, leading to uncontrolled cell proliferation. CDK 1 and 2 have been noted to be overexpressed in a subset of colon adenomas, cyclin E is amplified and/or overexpression in breast, colon, and many other cancers, and both cyclin A and E have been found to be overexpressed in lung carcinoma[1].

1.4 ATP Competitive CDK Inhibitors

There are many approaches to the design of kinase inhibitors. These include blocking of the Adenosine Tri-phosphate (ATP) binding pocket, blocking the substrate recruitment site, and stabilizing kinases in their inactive conformations[13]. This section focuses on kinase inhibitors that preferentially block the ATP binding pocket. This pocket is well defined and the generation of small molecules inhibitors to block this hydrophobic pocket has been studied for many years[13c]. The ATP binding pocket is composed of five main sites, (1) central purine binding site, (2) solvent accessible surface, (3) ribose binding site, (4) phosphate binding region, and (5) hinge region[13a]. Each of these sites are important for the binding affinity of ATP, (which is involved in many intermolecular interactions including van der Waals, hydrophobic and hydrogen bonding) and are used as guides for the structure based design of inhibitors[13a, 13c].

CDKs and other proteins have been determined to be critical regulators of the eukaryotic cell cycle[13b], as discussed in Section 1.1. Gain-of-function and/or loss-of-function of such proteins during the cell cycle (i.e. cyclins, endogenous CDK inhibitors,

and other substrates) cause a snowball effect on the regulatory events of the CDKs leading to the transformation of cells[13b]. CDK4/6 have been determined to be frequently amplified or overexpressed in many tumor types and their inhibition would block cell proliferation and avert the transcription of genes necessary for cell cycle progression[13b]. Also, it has been observed that the absence of CDK2/cyclin E complex in both transformed and untransformed cells does not affect cell cycle proliferation[14]. This raises the concern that specific targeting of CDKs may not be of best interest for cancer therapeutics, due to redundancies in kinase activity[14]. There are many kinase inhibitors with single and/or multiple targets in the cell cycle and such targets include cell cycle CDKs, transcriptional CDKs, or both[15]. An alternative strategy that does not target the catalytic domain would evade the problems of redundancy in kinase activity.

PD0332991 (Palbociclib) has recently been approved by the Food and Drug Administration (FDA) as a "Breakthrough Therapy"[16]. Breakthrough therapy allows a drug to be used as treatment while the remainder clinical trials are conducted[16]. CDK4/cyclin D1 has been proven to be disrupted in many tumor types by overexpression and/or amplification and blocking the ability of CDK4/cyclin D1 to phosphorylate substrates necessary for cell cycle progression, is a viable approach to treating cancer[15, 17]. PD0332991 is highly selective for CDK4/6 with IC$_{50}$ values of 11 nM and 15 nM, respectively, and exclusively induces G1 arrest[17-18]. When tested against a panel of serine, threonine, and tyrosine kinases, PD0332991 (Figure 1.3) showed very little to no activity against kinases other than CDK4/6[18].

In retinoblastoma (Rb)-positive cancer cells, it was observed that with treatment of PD0332991 (0.011 μmol/L) there was an induction of G1 arrest, a reduction in tumor

growth, and in human xenograft models there was tumor regression[15, 19]. When PD0332991 was tested against Rb-negative cancer cells there was no activity[15], concluding that PD0332991 has the ability to halt cancer cell growth in patients with Rb-positive cancers[17, 20]. A study was conducted to determine if drug resistance would occur with continued use of PD0332991. Colo-205 human colon carcinoma tumor xenografts in mice were negative for resistance after treatment for 14 days with PD0332991 with doses of 75-150 mg/kg and tumor regression was observed in some tumors at a dose of 37.5 mg/kg[18]. In primary bone marrow myeloma cells, G1 arrest was potently induced with doses as low as 0.3 µM and with higher doses (greater than 5 µmol/L) apoptosis was induced[21].
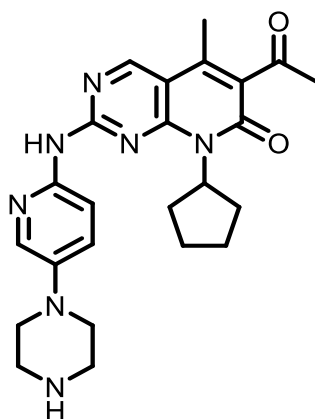
FIGURE 1.3. CHEMICAL STRUCTURE OF PD0332991. Chemical structure of 6-acetyl-8-cyclopentyl-5-methyl-2-((5-(piperazin-1-yl)pyridin-2-yl)amino)pyrido[2,3-d]pyrimidin-7(8H)-one.

When PD0332991 was used in combination with dexamethasone, apoptosis was enhanced with treatment for 48 hours of 0.01µM of drug in bone marrow myeloma cells[21]. In disseminated human myeloma xenografts, tumor growth was completely inhibited[21]. More recently, when used in combination with Femara (Letrozole), an anti-hormonal agent, there was an increase in progression-free survival of about 3.5 fold[20]. A Phase 3 clinical trial is currently recruiting for first-line treatment of postmenopausal

women with ER-positive/HER2-negative advanced breast cancer. Treatment will be conducted with PD0332991 in combination with Letrozole and Letrozole alone.

There are multiple CDK inhibitors targeting the G1 and S phases that are currently in clinical trials, however, PD0332991 is the only orally bioavailable drug that has high specificity for CDK4/6 kinases[17]. During Phase 1 and 2, the most common dose-limiting toxicities were myelosuppression, nausea, vomiting, diarrhea, and fatigue[17]. Neither vascular thrombotic nor neurological adverse events were observed with PD0332991 treatment as has been observed with other CDK inhibitors in clinical trials[17].

A second CDK inhibitor that targets the ATP binding pocket is Flavopiridol (alvocidib, HMR1275; Figure 1.4). This compound is active against multiple kinases but is known to be most potent against the transcriptional CDK, CDK9, relative to other kinases[15].
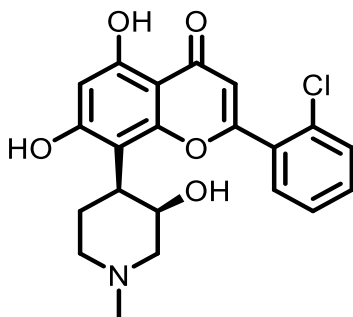
FIGURE 1.4. CHEMICAL STRUCTURE OF FLAVOPIRIDOL. Chemical structure of 2-(2-chlorophenyl)-5,7-dihydroxy-8-((3R,4S)-3-hydroxy-1-methylpiperidin-4-yl)-4H-chromen-4-one.

Early studies showed that flavopiridol potently inhibited CDK2 and CDK4 with IC_{50} values between 50-120 nM[22]. In MCF-7 (p53 and Rb proficient) and MDA-MB-468 (p53 and Rb deficient) cells, G1 arrest was induced, proving that the action of flavopiridol is independent of p53 and Rb[22]. MCF-7 cells showed a significant loss in cyclin D levels without altering the levels of cyclin A, cyclin E, CDK2, or CDK4. These

results led to the conclusion that flavopiridol inhibits CDK2/4 kinase activity resulting in G1 arrest[22]. However, studies conducted in head and neck squamous cell carcinoma (HNSCC) cell lines showed that flavopiridol caused a significant decrease in CDK1/2 activity with IC_{50} values between 43-83 nM[23].

Fischer and Gianella-Borradori (2003) summarizes the potency and selectivity profile of flavopiridol. They summarized that against the transcriptional kinase CDK9/cyclin T1, flavopiridol is most potent with an IC_{50} value of 0.006-0.01 μM. In 2010, studies show that flavopiridol treatment resulted in the inhibition of the C-terminal domain of RNA-polymerase-II causing an inhibition in transcription resulting in apoptosis[24]. When tested against CDK1/cyclin B and CDK4/cyclin D1 flavopiridol showed IC_{50} values of <0.1 μM, and against CDK2/cyclin A, CDK2/cyclin E, CDK7/cyclin H, and other kinases (epidermal growth factor receptor, protein kinase C, etc.) flavopiridol has IC_{50} values of ≥0.1 μM[25].

A study was conducted on a panel of human tumor xenografts[26]. Flavopiridol was proven to be highly potent against prostate and less potent against melanoma, breast, lung, and ovarian cancers[26]. In nude mice containing prostate cancer xenografts (PRXF1369), flavopiridol showed a maximum tolerated dose (MTD) of 10 mg/kg/day and a tumor growth delay of 30 days[26]. In human promyelocytic leukemia (HL-60) xenografts, animals experienced complete regression and remained disease free for several months. In human B-cell follicular lymphoma (SUDHL-4) xeongrafts, animals underwent major or complete regression and were disease free for more than two months at 7.5 mg/kg concentrations[27].

Flavopiridol was the first CDK inhibitor to enter clinical trials. As a single-agent,

in Phase 2 clinica trials, flavopiridol induced pro-inflammatory syndrome at doses of 50 mg/m^2 in patients with advanced cancers[28] and showed to have no effect on advanced colorectal and non-small cell lung cancer as well as several other cancer as first line treatment[29]. Flavopiridol does have a minimal response as a second-line therapy in endometrial adenocarcinoma and advanced renal cell carcinoma[30]. When flavopiridol was used in combination therapy, significant antitumor activity was observed. In the administration of flavopiridol after gemcitabine there was a 10-15 fold increase of apoptosis in pancreatic, gastric, and colon cancer cell lines[31].

A third ATP-competitive inhibitor is JNJ-7706621(Figure 1.5). This compound is a multi-targeted/pan kinase inhibitor that targets CDKs and Aurora kinases[32]. As stated previously, CDKs play a central role in the cell cycle and their activity is dependent upon the regulatory subunit, cyclin. Aurora kinases play an important role during mitosis, in regulating chromosomal movement and organization[33].
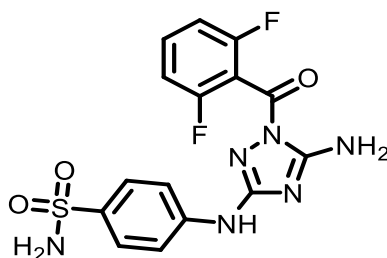
FIGURE 1.5. STRUCTURE OF JNJ-7706621. The chemical structure of 1-(2',6'-difluorobenzoyl)-5-amino-3-(4'aminosulfonylanilino)-1,2,5-triazole.

JNJ-7706621 is a 1,2,4-triazole-3,5-diamine derivative and is moderately potent inhibitor of CDK1 and 2 (moderately potent against CDK4) and Aurora kinases A and B[33-34]. When tested against a large number of other protein kinases JNJ-7706621 had little to no activity[15]. A CDK1 kinase assay was conducted, in the presence of 5 μM ATP and JNJ-7706621 showed to have an IC$_{50}$ value of 17.12±1.03 μM[33]. Against PC3

prostate cancer cells and HCT-116 colon cancer cells, JNJ-7706621 showed potent inhibition with IC_{50} values of 0.112±0.012 μM and 0.189±0.042 μM, respectively. It was observed that JNJ-7706621 resulted in a delay in cell cycle progression in G1 and cell cycle arrest was observed at the G2/ M phases in human cancer cells[33-34]. It was determined that JNJ-7706621 is a potent antiproliferative agent against numerous cancer cell types, irrespective of p53, retinoblastoma (Rb) or P-glycoprotein levels[33]. However, JNJ-7706621 has poor solubility and studies have been conducted on potentially utilizing nanoparticles as non-toxic vehicles for its delivery[34].

1.5 NON-ATP COMPETITIVE CDK INHIBITORS

A different approach to the development of CDK inhibitors is to target alternative sites other than the ATP binding site[35]. Targeting the ATP binding site has proven to be beneficial in the development of cancer therapeutics. It is well known that the ATP binding pocket is conserved across all kinases and present in many proteins that are involved in numerous cellular functions. There are risks in potentially inhibiting transcriptional CDKs by causing effects on normal cells which may account for the toxicities observed with clinically evaluated CDK inhibitors[3]. The ultimate goal in novel chemotherapeutic development is to identify a target that is unique to a specific cancer cell or when inhibited will allow the cancer cell to be sensitized to cell death. It has been established that many biological processes are regulated through protein-protein interactions (PPI) and theoretically, if identifiable, PPIs could be blocked specific proteins or pathways would be inhibited.

During the cell cycle the cyclin binding groove (CBG) of the cyclin subunit is involved in the recruitment of various substrates for phosphorylation[35]. The CBG

recognizes a short peptide sequence known as the cyclin binding motif (CBM). Figure 1.6 illustrates a CDK2/cyclin A heterodimer. This motif is conserved in many cell cycle substrates and inhibitory proteins and has been identified to interact specifically with the CBG through PPIs. Substrates involved in the cell cycle are recognized by the CBG through the CBM, are recruited into close proximity of the groove, and are phosphorylated by the active CDK/cyclin complex.
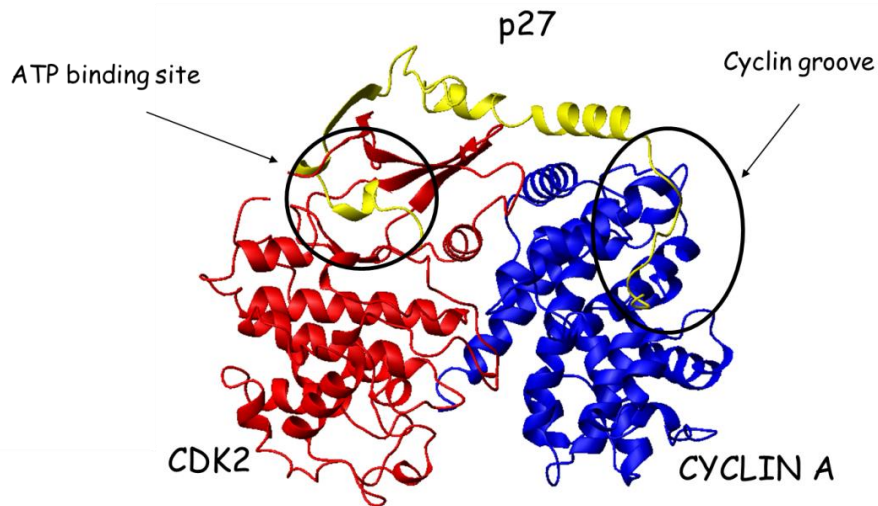
FIGURE 1.6. CDK2/CYCLIN A/P27 TRIMERIC COMPLEX. Illustration of a CDK2/cyclin A complex with the ATP binding site located on the kinase (red) and the cyclin groove on the cyclin (blue). p27 (yellow) is shown interacting with both the ATP binding site and the cyclin groove.

Often times, the negative regulators of the cell cycle (p21, p27, etc.) are inactivated resulting in upregulation of CDK activity. This can cause an override of the phase checkpoints (described in Section 1.2) and may lead to uncontrolled cell proliferation and to the transformation of cells. Cellular response through the inhibition of the CBG is greater in transformed cells because E2F-1 is frequently deregulated in such cells and has been reported to induce apoptosis in combination with CDK2/cyclin A inhibition[36]. Transformed cells depend on CDK2/cyclin A to decrease the activity of E2F-1 to avoid the induction of apoptosis in late S phase[10b].

Due to the CBM being conserved across the Cip/Kip family members (Section 1.2), selective inhibitors can be designed to block the CBG and inhibit the activity of the CDK/cyclin complexes resulting in the induction of apoptosis in transformed cells. Peptides composed of naturally occurring amino acids are useful for lead compounds in discovering new drug therapies but generally speaking are limited as therapeutics by their undesirable pharmacokinetic profiles. These are caused by their poor permeability (blood brain barrier, cell membrane, etc.) and lack of metabolic stability including protease-mediated degradation[37]. Currently, HAKRRLIF, based on the C-terminal domain of p21[WAF1], is being used in structure based design to develop non-peptidic inhibitors for CDK2/cyclin A and CDK4/cyclin D1 references.

Previously mentioned in Section 1.4, selective inhibition of kinases may not be of best interest due to redundancies in the kinase activity. An approach, targeting the CBG, reduces the possibility of such problems because it is the protein kinase that is known to be redundant[14] not the cyclin. Cyclin groove inhibitory compounds should be selective due to cyclins A, D, and E being the only cyclins containing a functional binding groove and thus are potential targets for non-ATP competitive CDK inhibitors[38]. CDK2/cyclin A and CDK4/cyclin D1 are validated anticancer drug targets, targeting the CBG of these kinases provides selectivity, and the kinases involved in other cellular processes will not be affected[38]. However, it has been determined that potent CDK2/cyclin A inhibitors generally are significantly less effective against CDK4/cyclin D1[38]. Due to these differences Liu, *et al*. (2010), set out to determine which structural variants between cyclin A and D1 might affect the potency of CDK inhibitors. In terms of the CBG, there are three major sites of the hydrophobic cleft that are involved the binding of

HAKRRLIF: 1) a primary hydrophobic pocket that interacts with Leu6 and Phe8 (the 6th and 8th amino acids of HAKRRLIF)[38] 2) a secondary hydrophobic pocket that interacts with Ala2 and 3) an acidic region, located between the two lipophilic pockets, that forms ionic contacts with the basic amino acids, Arg4 and Arg5[38].

To determine the differences in the CBG of cyclin A and D1, their crystal structures were overlaid and the following variants were determined (Figure 1.7). On the left-hand side of Figure 1.7, the black chemical structure represents Leu6 and Phe8 of HAKRRLIF. The residues of the primary hydrophobic pocket of the CBG are L214 (Leu) and V60 (Val) for cyclin A and D1, respectively. The residues E220 (Gln) and D216 (Asp) make up the acidic region for cyclin D1 and E66 and T62 (Thr) for cyclin A. As for the secondary hydrophobic pocket, the amino acids W217 (Trp) and W63 constitute this pocket for cyclin A and D1, respectively. The other residues shown are considered to be non-peptide contacting residues. These residues are structurally different between Cyclin A and D1. I281 (Ile) of cyclin A is exchanged for Y127 (Tyr) in cyclin D1 (also seen in the ribbon representation right-hand side of Figure 1.7) within residue region of 116-136 and these differences lead to altered conformations of the CBG in cyclin D1 compared to cyclin A[38]. Cyclin D1 is able to accommodate larger functional groups in the primary hydrophobic pocket because this region is larger and contains an extension, compared to cyclin A[38]. Figure 1.8 illustrates these structural variants using the solvent accessible surface of each cyclin. As a whole, it was determined that cyclin D1 contains a narrower secondary pocket, a shallower yet larger primary hydrophobic, and a less acidic region at Asp283 compared to cyclin A[38]. The variation in the CBG between cyclin A and D1 is significant enough to cause differences in binding affinities

between CDK inhibitors discussed below.
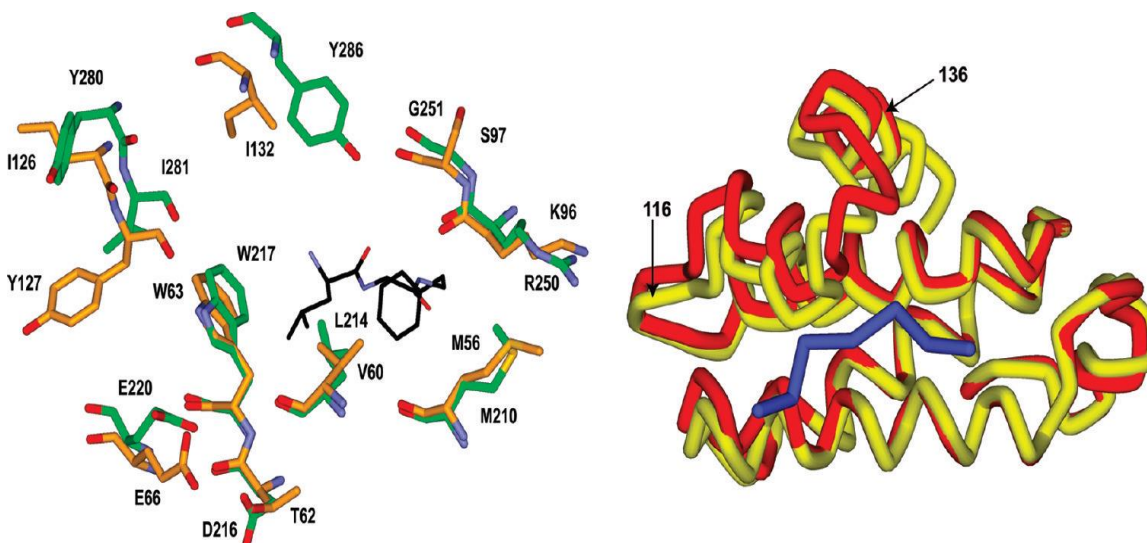
FIGURE 1.7. COMPARING THE CYCLIN BINDING GROOVE OF CYCLIN A AND CYCLIN D1. (Left) Overlay crystal structure of cyclin A2 (PDB 1OKV; Carbon atoms green) and cyclin D1 (PDB 2W96; Carbon atoms orange). (Right) Overlay of the ribbon representation of both cyclin A2 (Red) and cyclin D1 (yellow). An inhibitory peptide (blue) is shown interacting with the CBG. Residues 116 through 136 are where the largest structural differences are located between these two cyclins. [Reprinted with permission from Liu, S., J. K. Bolger, et al. (2010). "Structural and Functional Analysis of Cyclin D1 Reveals p27 and Substrate Inhibitor Binding Requirements." ACS Chemical Biology **5**(12): 1169-1182.. Copyright 2010 American Chemical Society.]

Non-peptidic inhibitors are being developed by the REPLACE (REplacement with Partial Ligand Alternatives through Computational Enrichment) strategy (Figure 1.9). This strategy is an effective way to iteratively convert peptidic analogs involved in PPIs to non-peptidic, drug-like small molecules[3, 10b]. Computational chemistry is utilized to identify partial ligand alternatives (PLAs) by docking small molecule fragments into the cyclin groove and evaluating their interactions compared to that of the native ligand[35]. In brief, REPLACE is carried out by the truncation of the N-terminal amino acids of the lead peptide and computationally designed PLAs are coupled through solid-phase synthesis. These FLIP compounds are then tested in a competitive binding assay and those with substantial activities against CDK/cyclin complexes of interest are further optimized by the truncation and replacement of the central and C-terminal amino acids

with the aim of generating a cell permeable, non-peptidic inhibitor.
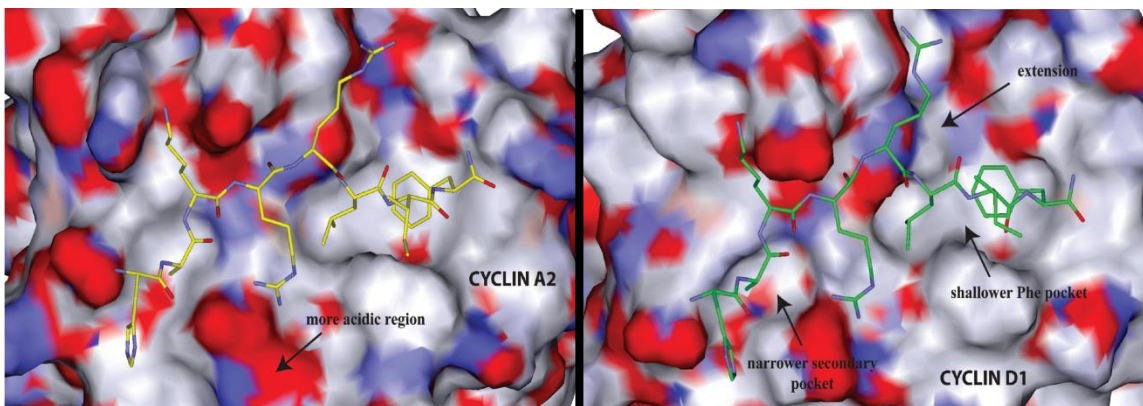
FIGURE 1.8. COMPARING THE PRIMARY AND SECONDARY HYDROPHOBIC POCKETS OF THE CBG OF CYCLIN A AND CYCLIN D1. Solvent accessible representations of the cyclin binding groove. (Left) Cyclin A2 was determined to have a more acidic region around GLU220 of the CBG causing ARG4 of the CBM to interact differently in cyclin A2 compared to cyclin D1. (Right) Cyclin D1 was determined to have a a shallower and an extended primary hydrophobic pocket and a narrower secondary hydrophobic pocket compared to cyclin A2. These structural differences promote different binding affinities for CBG inhibitors. [Reprinted with permission from Liu, S., J. K. Bolger, et al. (2010). "Structural and Functional Analysis of Cyclin D1 Reveals p27 and Substrate Inhibitor Binding Requirements." ACS Chemical Biology **5**(12): 1169-1182.. Copyright 2010 American Chemical Society.]
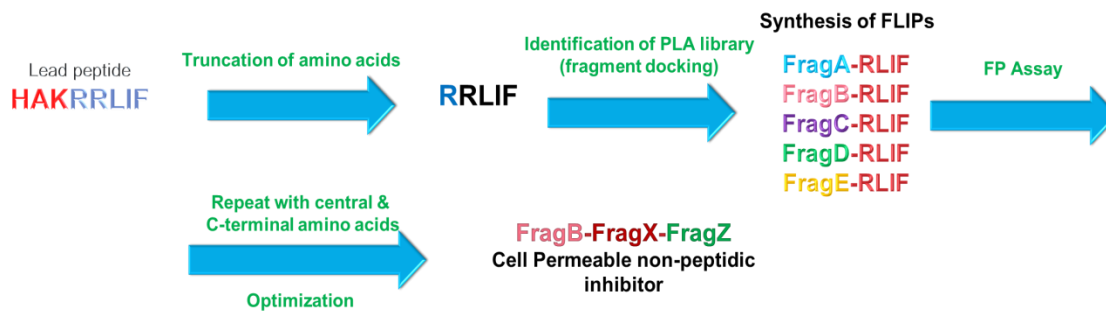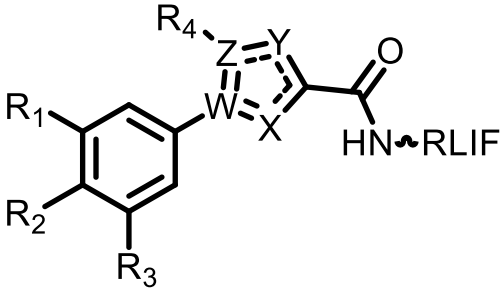
FIGURE 1.9. REPLACE METHODOLOGY. A schematic overview of the REPLACE strategy. The lead peptide is truncated at the N-terminus and computationally designed partial ligand alternatives (PLAs) are coupled through solid-phase peptide synthesis. These FLIP compounds are then tested in a competitive binding assay and those with substantial activities are further optimized by the truncation and replacement of the central and C-terminal amino acids resulting in a cell permeable, non-peptidic inhibitor.

Advantages of the REPLACE strategy are that non-peptidic fragments can be identified for extensive and shallow PPIs while negating the need for highly sensitive binding assay and should be applicable in the replacement of individual amino acids or peptide sequences to generate pharmaceutically adequate lead molecules[10b].

REPLACE has previously been utilized to replace the N-terminal amino acids

(HAKR) with fragment molecules (Ncaps) to create FLIPs[3, 10b]. Much progress has been made in the replacement of these amino acid residues. The most potent Ncap to date is 1-(3,5-dichlorophenyl)-5-methyl-1H-1,2,4-triazole-3-carboxamide (35DCPT) which has decreased the overall charge of the peptidic sequence by eliminating the charged Arg4 residue and has improved potency compared to other FLIP compounds[10b]. When coupled to RLIF (SCCP 5773; Table 1.2), the FLIP compound showed an IC_{50} value of 4.0±0.6 µM against CDK2/cyclin A and 27.3±3.40 µM against CDK4/cyclin D1[3, 35]. These values were directly compared to an optimized peptide sequence that contains the C-terminal amino acids RRLIF of HAKRRLIF[3]. This pentapeptide has an IC_{50} value of 1.4 µM against CDK2/cyclin A and 16.1 µM against CDK4/cyclin D1[3].

TABLE 1.2. Summary of Previously Reported N-terminal Capping Groups Coupled with RLIF.

SCCP ID	R1	R2	R3	R4	W	X	Y	Z	CDK2/cyclin A IC_{50} (µM)	CDK4/cyclin D1 IC_{50} (µM)
5773	Cl	H	Cl	Me	N	N	N	C	4.0±0.6	27.3±3.40
5774	H	Cl	H	Me	N	N	N	N	11.5±3.3	12.0±2.06

Many heterocyclic compounds were designed for the replacement of HAKR and tested against these two cyclins. Such compounds include but are not limited to triazole, pyrazole, pyrrole, furan, imidazole, and thiazole[3, 35]. Variants of each heterocycle were generated with halogens at either the three and five position or at the fourth position of

the phenyl ring[3]. These substitutions were demonstrated to have a significant impact on the binding affinity of these FLIP compounds as measured using a fluorescence polarization assay. The phenyltriazole compounds were determined to be the most potent[3]. A second phenyltriazole FLIP, SCCP 5774, (4-chlorophenyl triazole-RLIF; 4CPT; Table 1.2) was shown to have greater activity in cyclin D1 compared to SCCP 5773 with IC_{50} values of 11.5±3.3 μM and 12.0±2.06 μM against CDK2/cyclin A and CDK4/cyclin D1, respectively[3, 35]. The narrower secondary pocket of cyclin D1 cannot accommodate the 3,5-dichlorophenyl ring of SCCP 5773 to the same degree as the 4-chloro substituted analog[3]. This data demonstrates that critical residues of the octamer can be replaced with small drug-like molecules while decreasing overall charge and increasing potency[9a].

Viable Ncaps have been identified and fragment alternatives are now desired for the replacement of the central and C-terminal amino acids, RLIF, to complete the conversion of HAKRRLIF into a more drug-like molecule. A library of bis(aryl) compounds were generated and it was determined that Ccaps containing a 3-phenoxybenzylamine core structure were the most effective at mimicking the binding mode of Phe8[3]. Structural modifications were conducted to determine how activity could be optimized further and halogens were added at various positions of the aromatic ring contacting the primary hydrophobic pocket[3]. It was determined that the FLIP compound containing a fluorine at the four position of the bis(aryl) Ccap, with 4CPT as Ncap and an arginine linker (SCCP 5823) was the most potent against CDK2/cyclin with an IC_{50} value of 18.1±4.0 μM[3] (Table 1.3). However, neither this FLIP nor others generated have been potent against CDK4/cyclin D1.

TABLE 1.3. Summary of Two Previously Reported Fragment Ligated Inhibitory Peptides.

SCCP ID	R1	X	R2	R3	R4	R5	CDK2/cyclin A IC$_{50}$ (μM)	CDK4/cyclin D1 IC$_{50}$ (μM)
5823	4CPT	N	H	H	F	H	18.1±4.0	>200
5926	35DCPT	N	H	F	F	H	>180	>180

The replacement of Leu6 and Phe8 is imperative for the conversion of HAKRRLIF to a more drug-like molecule based on the work of Liu *et al.* (2013). Small molecule replacements, to enhance the binding affinity of the FLIP molecule, are desired and the following chapters describe further applications of the REPLACE strategy for the design of such novel Ccaps. Towards this goal, computational design has been utilized for structure- and pharmacophore-based design of Leu6 and Phe8 replacements. In addition non-natural arginine isosteres have been incorporated to retain and/or enhance the binding affinity of FLIP compounds while making them more drug-like. Achieving this, will be progressive towards the complete replacement of HAKRRLIF resulting in more drug-like compounds that should have enhanced cell permeability and carry this project into the next phase of *in vivo* testing of such compounds.

CHAPTER 2

DESIGN OF FRAGMENT LIGAND INHIBITORY PEPTIDES FOR THE REPLACEMENT OF THE C-TERMINAL AMINO ACIDS OF THE CYCLIN-BINDING MOTIF

In the effort to convert HAKRRLIF into a more drug-like molecule by utilizing the REPLACE methodology, the replacement of the N-terminal amino acids (HAKR) has been undertaken and significant progress has been achieved. The most effective FLIP compound for the replacement of HAKR to date is 1-(3,5-dichlorophenyl)-5-methyl-1H-1,2,4-triazole-3-carboxamide (35DCPT)-RLIF (SCCP 5773; Table 1.2). However, further replacement of the C-terminal residues (RLIF) is required for the complete conversion of HAKRRLIF into a cell permeable, non-peptidic inhibitor. A library of bis(aryl) ether fragments, coupled with Ncap-Arg5-Leu6 (i.e. the 5th and 6th amino acids of HAKRRLIF), has shown activity in the mid to high micromolar concentrations in inhibiting CDK2/cyclin A. The most potent of these compounds was found to be 4-(4-fluorophenoxy)pyridin-2-yl)methanamine coupled to 1-(4-chlorophenyl)-5-methyl-1H-1,2,4-triazole-3-carboxamide (4CPT)-RL (SCCP 5823, Figure 2.1) which has an IC_{50} value of 18.1±4.0 µM against CDK2/cyclin A but no appreciable activity towards CDK4/cyclin D1. Further optimization to obtain a more effective C-terminal capping group is required for the conversion of HAKRRLIF to a more drug-like, cell permeable small molecule. Currently the Ccaps that have been developed are weakly or not active against CDK2/cyclin A or CDK4/cyclin D1. A new approach for the design and development of such novel Ccaps for the replacement of RLIF of the octamer is desired.

To achieve this, computational design has been used to identify small molecules of interest via structure-based design with Discovery Studio 3.0 and the web-based pharmacophore search software AnchorQuery™.
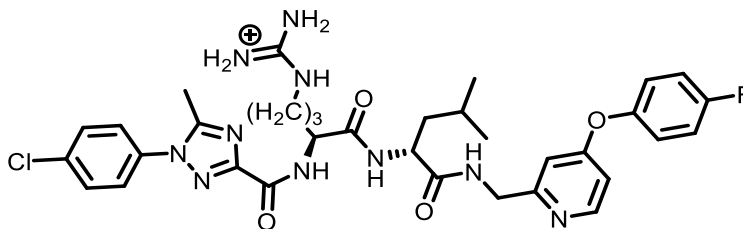
FIGURE 2.1. CHEMICAL STRUCTURE OF SCCP 5823. Chemical structure of 1-(4-chlorophenyl)-N-((S)-1-(((R)-1-(((4-(4-fluorophenoxy)pyridin-2-yl)methyl)amino)-4-methyl-1-oxopentan-2-yl)amino)-5-guanidino-1-oxopentan-2-yl)-5-methyl-1H-1,2,4-triazole-3-carboxamide (SCCP 5823).

2.1 PICOLINAMIDE AND BENZAMIDE NCAP SCAFFOLDS

To continue with the replacement of the amino acid residues of HAKRRLIF, picolinamide and benzamide Ncaps were used to perform substructure searches of online libraries for diverse small molecules that can be used to replace the entire octapeptide (HAKRRLIF) or be used to design potential Ccaps for the replacement of RLIF. The picolinamide and benzamide Ncaps (Figure 2.2) have been modeled and show to have similar intermolecular interactions as the triazole derivative 35DCPT with the CBG at Trp217 and Glu254. These two interactions are of importance to help retain the binding affinity for the FLIP compounds. When tested in a competitive binding assay, picolinamide and benzamide showed adequate IC_{50} values comparable to those of 35DCPT. When coupled with RLIF, 35DCPT (SCCP 5773; Table 1.2) has IC_{50} values of 4.0±0.6 μM against CDK2/cyclin A and 27.3±3.4 μM against CDK4/cyclin D1. To date the most potent picolinamide derivatives, coupled with RLIF, are 6-methoxypicolinamide (SCCP 524) with an IC_{50} value of 70.1±7.9 μM against CDK2/cyclin A and 5-(piperazin-1-ylmethyl)picolinamide (SCCP 5856) with an IC_{50} value of 42.7±12.02 against

26

CDK4/cyclin D1.   Also, to date the most potent benzamide derivative is 3-hydroxy-4-(piperazin-1-ylmethyl)benzamide coupled to R(β-Leu)N-Methyl-Phe-NH2 (SCCP 5966) has been shown to have IC$_{50}$ values of 3.91 µM and 4.93 µM against CDK2/cyclin A and CDK 4/cyclin D1, respectively.   Changing the C-terminal amino acids from RLIF to R(β-Leu)N-Methyl-Phe-NH2 increased the binding affinity for this FLIP compound 1.5-fold.
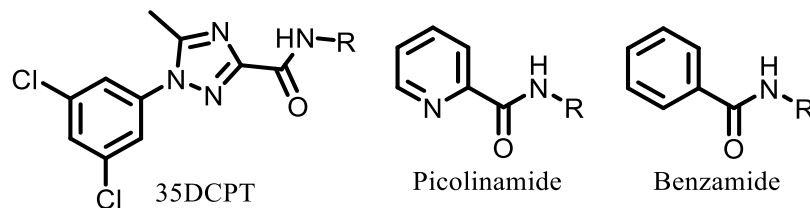
FIGURE 2.2. CHEMICAL STRUCTURES OF N-TERMINAL CAPPING GROUPS. Chemical structures of (left) 1-(3,5-dichlorophenyl)-5-methyl-1H-1,2,4-triazole-3-carboxamide   (35DCPT), (middle) picolinamide, and (right) benzamide.

A library search using these Ncap as scaffolds has identified potential Ccaps of which the small molecules are commercially available.   This allows rapid assessment of activity without investing the time, expense and effort in the laboratory required to synthesize these compounds.   Using this approach, small molecules identified to replace HAKRRLIF are required to have at least one of the desired hydrogen bonding (H-bonding) interactions in the secondary hydrophobic pocket (Trp217 and/or Glu254) to help retain the binding affinity of HAKR and have good complementarity with the primary hydrophobic pocket for the replacement of RLIF.   Of the small molecules identified, those with the best prediction will be sourced commercially and their activities tested in a competitive binding assay.

2.1.1 RESULTS AND DISCUSSION

Previously, validation exercises for LigandFit as a high throughput docking method were conducted to determine the predictability and reproducibility of computationally

designing Ccaps. Along with a negative control, native ligands of both cyclin A and cyclin D (35DCPT and 4CPT, respectively) were used as positive controls and docked into the CBG of CDK2/cyclin A. In conjunction with this docking, a number of parameters were altered such as a) the energy grid (force field that calculates the ligand-receptor interaction energies), b) the minimization sphere (helps minimize the molecular energy), and c) the number of poses (orientation of how the fragment potentially may fit into the pocket) generated. For each of the result sets, the poses generated that were superimposable with the native ligand crystal structure (correct poses; within 2 Angstroms), whose scoring functions (used to provide a consistent interpretation of the data generated) yielded the negative control to be within the top 25 poses, and whose scoring functions yielded the most number of correct poses within the top 25 poses were further studied. The CFF (consistent force field) energy grid with the minimization sphere on, the generation of 20 poses per native ligand, and the scoring functions of LigScore2_Dreiding, -PLP1, and –PLP2 were determined to be the optimized parameters for the LigandFit docking method (Table 2.1).

Picolinamide and benzamide Ncap scaffolds were used in a substructure search of the ChemBridge® library for potential small molecules to replace HAKRRLIF or to aid in the design of novel Ccaps. The validated optimized parameters were used in the docking of the resulting compounds from the search. One of the most interesting fragments is N-(5-guanidino-1-(naphthalen-2-ylamino)-1-oxopentan-2-yl)benzamide (BZ01; Figure 2.3) which contains a benzamide Ncap, a naphthalene Ccap, and an arginine in the Arg5 position.

The benzamide Ncap, of this small molecule, forms an H-bond with Trp217 and the

arginine ion-pairs with Asp283 and H-bonds with Glu254. In addition, the naphthalene Ccap has good complementarity with the primary hydrophobic pocket. This compound also ranks well in the overall scoring functions. LigScore2_Dreiding, -PLP1, and –PLP2 were previously determined to be the optimal scoring functions for the prediction of potent small molecules. This compound is ranked within the top twenty- five percent of all ligands docked with scores of 5, 56.06,and 55.88 for LigScore2_Dreiding, -PLP1, and –PLP2, respectively (Table 2.2). With the observed intermolecular interaction and the resulting scores, this molecule was expected to have activity against both Cyclin A and D1. However, upon testing in the FP assay this fragment was found to be weakly binding. Possible further optimization of the naphthalene group would provide better binding.

TABLE 2.1 VALIDATION RESULTS FOR THE SELECTION OF OPTIMAL PARAMETERS FOR THE LIGANDFIT DOCKING METHOD

Energy Grid	Dreiding	CFF	PLP1
No. of correct poses 3,5-DCPT	7	10	7
No. of correct poses 4-CPT	3	-	1
Negative controls in top 25	-PLP1(5), -PLP2(3), PMF(10), DOCK SCORE(4)	-PMF (21)	-PLP1(1), -PMF(10)
Best scoring functions	LigScore2_Dreiding, -PLP1, -PLP2, DOCKSCORE	LigScore2_Dreiding, -PLP1, -PLP2	LigScore2_Dreiding, -PLP1, -PLP2, DOCKSCORE
3,5-DCPT(rank of top 25 correct/closer poses for the best scoring function)	LigScore2_Dreiding, -PLP1, -PLP2, and DOCKSCORE (22,23,24, 25,26,27), Jain (22)	LigScore2_Dreiding, -PLP1, and –PLP2 (31,32,33,38)	LigScore2_Dreiding, -PLP1, and –PLP2 (39,40,41), DOCKSCORE (23,28,29,30)
4-CPT (rank of top 25 correct/closer poses for the best scoring function)	-	-PLP1 (11,14,15), Jain (11), -PMF (11,12,13,14,15)	-PLP1 (6), -PMF (8,21)

29
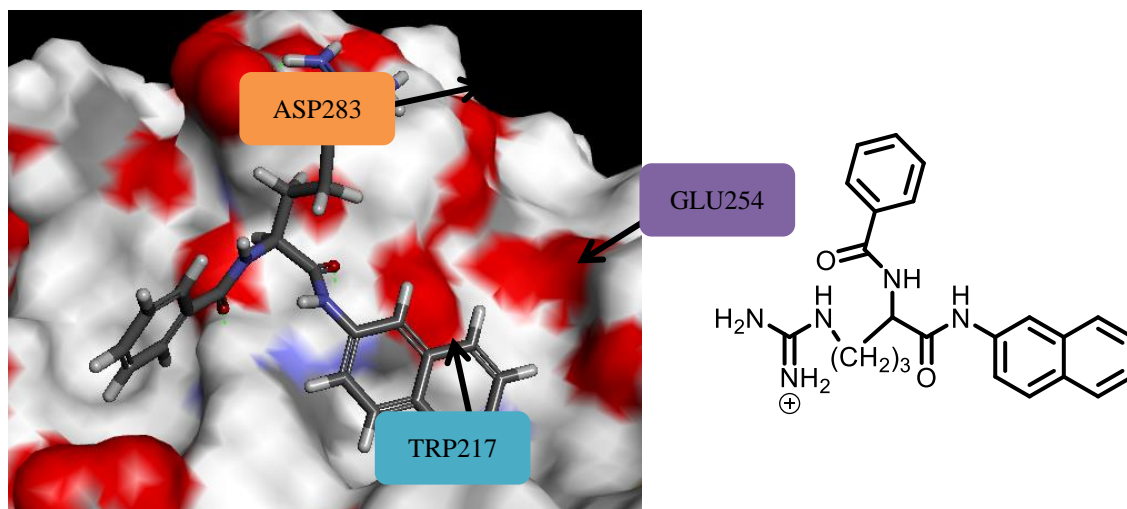
FIGURE 2.3. POTENTIAL SMALL MOLECULE FOR THE REPLACEMENT OF HAKRRLIF (BZ01). N-(5-guanidino-1-(naphthalen-2-ylamino)-1-oxopentan-2-yl)benzamide modeled into the CBG of cyclin A (BZ01; PDB 2UUE). As shown by the light green dotted lines, this small molecule hydrogen bonds and ion-pairs with the CBG at TRP217, GLU254, and ASP283, respectively.

The most potent benzamide Ncap coupled with RLIF contains a 4-methoxypiperidine (SCCP 5851) at the 4 position of the aromatic ring. This functional group and others can easily be added to the benzamide to help retain activity against Cyclin A and D1. Various groups also may be added to the naphthalene Ccap to potentially promote further intermolecular interactions and increase the binding affinity.

TABLE 2.2. The SCORING FUNCTION SUMMARY FOR N-(5-GUANIDINO-1-(NAPHTHALEN-2-YLAMINO)-1-OXOPENTAN-2-YL)BENZAMIDE [BZ01], METHYL 3-BENZAMIDO-5-((5-METHYL-3-PHENYLISOXAZOLE-4-CARBOXAMIDO)METHYL)BENZOATE [BZ02], (E)-N-(3-((1,5-DIMETHYL-3-OXO-2-PHENYL-2,3-DIHYDRO-1H-PYRAZOL-4-YL)AMINO)-3-OXO-1-PHENYLPROP-1-EN-2-YL)BENZAMIDE [BZ03].

Scoring Function	BZ01	BZ02	BZ03
LigScore2_Dreiding	5	5.38	5
-PLP1	56.06	101.82	68.54
-PLP2	55.88	90.39	63.07

A second fragment that is of interest is methyl 3-benzamido-5-((5-methyl-3-phenylisoxazole-4-carboxamido)methyl)benzoate (BZ02; Figure 2.4) which contains the benzamide Ncap, a 5-methyl-3-phenylisoxazole-4-carboxamide Ccap, and benzoate in

place of Arg5. The benzamide Ncap H-bonds with Trp217 and this molecule scores within the top twenty-five percent with scores of 5.38, 101.82, and 90.39 for LigScore2_Dreiding, -PLP1, and –PLP2, respectively (Table 1.1).
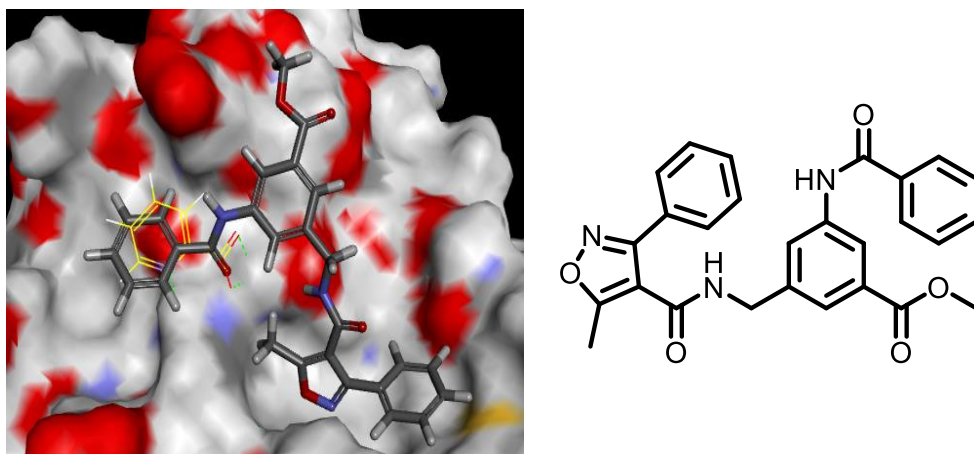
FIGURE 2.4. POTENTIAL SMALL MOLECULE FOR THE REPLACEMENT OF HAKRRLIF (BZ02). Methyl 3-benzamido-5-((5-methyl-3-phenylisoxazole-4-carboxamido)methyl)benzoate [BZ02] modeled into the CBG of cyclin A (PDB 2UUE).

The scores for this fragment rank higher than BZ01 however, BZ02 may not retain the binding affinity as well. The benzoate linker is unable to ion-pair with Asp283 similarly to Arg5 and the 5-methyl-3-phenylisoxazole-4-carboxamide Ccap does not mimic the binding mode of Leu6 and Phe8 well. However, the lack of these interactions has not been determined to be detrimental to the binding affinity and thus would be worth testing to determine the activity this fragment has against both CDK2/cyclin A and CDK4/cyclin D1.

Another compound that is of interest is (E)-N-(3-(((1,5-dimethyl-3-oxo-2-phenyl-2,3-dihydro-1H-pyrazol-4-yl)amino)-3-oxo-1-phenylprop-1-en-2-yl)benzamide   (BZ03; Figure 2.5). This molecule contains the benzamide Ncap, a 4-amino-1,5-dimethyl-2-phenyl-1H- pyrazol-3(2H)-one Ccap and 3-phenylacrylaldehyde in place of Arg5. This fragment H-bonds with Trp217 and ranks within the top twenty-five percent of the

ligands docked. This molecule has scores of 5, 68.54, and 63.07 for LigScore2_Dreiding, -PLP1, and –PLP2, respectively (Table 1.1). Compared to BZ01 this fragment also ranks higher in all scoring functions however, this molecule is also not expected to retain the binding affinity of HAKRRLIF. The 3-phenylacrylaldehyde linker acts more as a spacer and theoretically does not interact with the CBG similarly to Arg5. The 4-amino-1,5-dimethyl-2-phenyl-1H-pyrazol-3(2H)-one Ccap looks to mimic the binding mode of Leu6 and Phe8 better than that of BZ02 and potentially may help retain the binding affinity of these residues.

In addition to potential replacements for HAKRRLIF, this exercise helped generate ideas for the design of novel Ccaps. From BZ01, it is evident that a fused ring system, like naphthalene (Figure 2.6), fits well into the primary pocket and many analogs of this Ccap can be generated. A few modifications can be alkylation or halogenation to help the Ccap reach further into the pocket and potentially enhance the binding mode of these analogs. Another compound identified from ChemBridge® was an adamantane derivative. This compound is also adequate for this pocket and would most likely mimic the binding mode of Phe8 but this group is bulky and may not be suitable for the Leu6 position. Modifications of the adamantane can also be generated by alkylation or halogenation to retain/enhance the binding affinity of the FLIP compound incorporating this Ccap. An alkylated furan group may also be of interest for the replacement of LIF. The five-membered ring will provide a different geometry in the pocket which may benefit the binding affinity and help generate further SAR.
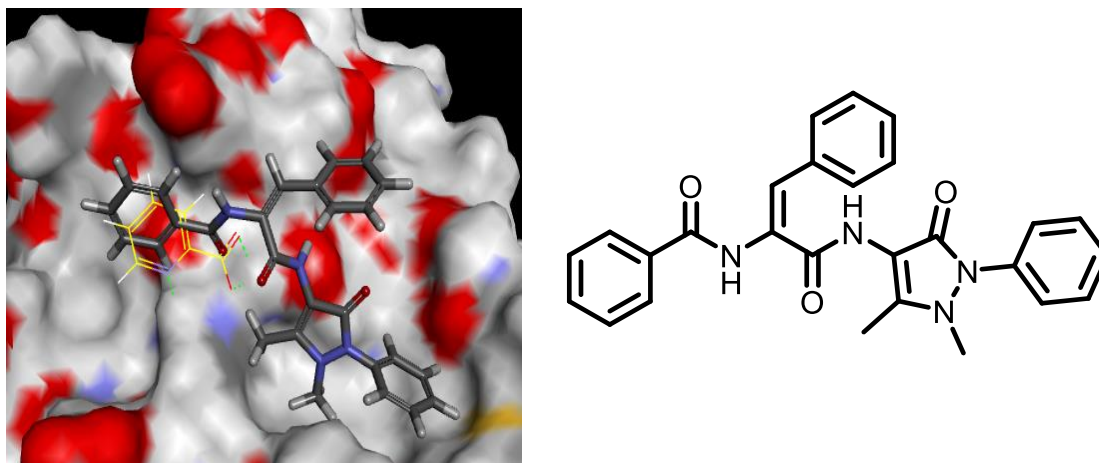
FIGURE 2.5. POTENTIAL SMALL MOLECULE FOR THE REPLACEMENT OF HAKRRLIF (BZ03). (E)-N-(3-((1,5-dimethyl-3-oxo-2-phenyl-2,3-dihydro-1H-pyrazol-4-yl)amino)-3-oxo-1-phenylprop-1-en-2-yl) benzamide [BZ03] modeled into the CBG of cyclin A (PDB 2UUE).

(1R,3S,5r,7r)-adamantan-2-amine	3-(5-methylfuran-2-yl) butan-1-amine	naphthalen-2-amine
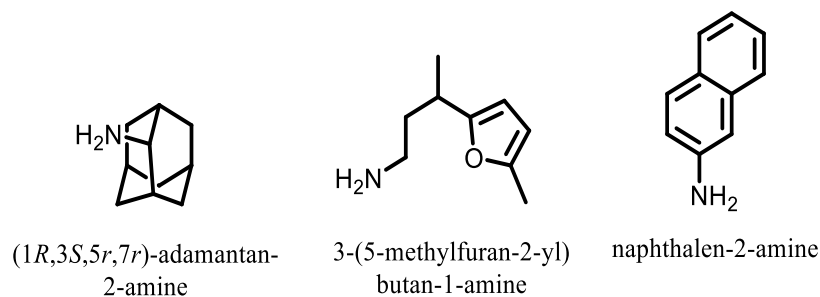
FIGURE 2.6. CHEMICAL STRUCTURES OF CCAP SCAFFOLDS. Chemical structures of adamantane, furan, and naphthalene amine derivatives as scaffolds for Ccap designs.

Obtaining the IC_{50} values for BZ02 and BZ03 will beneficial to the investigation of prospective replacements for HAKRRLIF. BZ01 was determined to be weakly binding and shows that a fused ring system alone may not be sufficient in the primary pocket and that further optimization of this group is needed to regain activity. The ideas generated from this exercise for potential Ccaps have been taken into consideration and the future design of Ccap may incorporate such scaffolds.

2.1.3 MATERIAL AND METHODS

Small molecules identified through the ChemBridge® library search that are of most interest, have been/will be purchased and tested in a competitive binding assay. The

Florescence Polarization (FP) assay was used to evaluate the small molecule's ability to compete with a florescence labeled ligand, known as tracer, against CDK2/cyclin A and CDK4/cyclin D1. This assay monitors the changes in molecular interactions in fluorescent molecules[39]. This type of analysis is advantageous because it allows for direct and rapid measurements of the ratio of bound and free tracer peptide[39] The FP assay is conducted in solution allowing for true equilibrium analysis into the low picomolar range and real time measurements[39].

The theory behind the FP assay is that small fluorescent molecules become excited via plane-polarized light. When the tracer is bound to the protein, the rotation is slower and the emitted light is in the same plane at the excitation energy therefore, giving off a higher fluorescence[39]. Polarization is then calculated by measuring the molecular rotation during the time between excitation (488 nm) and emission (535 nm)[39]. The equation used for calculating the relative polarization (mp) is as follows:

$$\text{relative mp} = \frac{\text{MP(compound)} - \text{MP(DMSO, protein, tracer)}}{\text{MP(DMSO, protein)} - \text{MP(DMSO, protein, tracer)}} \qquad \text{EQ 2.1}$$

The IC_{50} values are then determined by using a logarithmic regression of the relative mp values versus the testing concentrations[3].

The FP assay was conducted as previously reported[3]. In brief, buffer solution, tracer peptide, positive and negative controls, the protein, and the FLIP compound are combined in 384-well plates and the fluorescence of each well is measured by a Beckman Coulter DTX 880 Multimode detector. The C-terminal pentapeptide of the endogenous p21[WAF1] (RRLIF) was previously tested in the FP assay and showed IC_{50} values of 1.4 µM and 16.1 µM for CDK2/cyclin A and CDK4/cyclin D1, respectively[3]. The binding

affinity for CDK2/cyclin A and CDK4/cyclin D1 of the Ccaps generated will be directly compared the binding affinity of these native ligands.

2.2 PHARMACOPHORE BASED DESIGN

Studies using the AnchorQuery™ pharmacophore search technology software have been conducted for the development of potential Ccaps. AnchorQuery™ is an online software program that runs from a webserver that allows pharmacophore features of a peptide sequence to be specified and small molecules from a Multi-Component Reaction (MCR) database that closely mimic the pharmacophore of interest be returned by the software for further analysis. For this study, HAKRRLIF and the receptor (cyclin A) were uploaded into the software and the desired pharmacophore queries of the C-terminal amino acids (RRLIF) were varied to allow the maximum number of potential small molecules to be returned by the software. Example pharmacophore queries include aromatic, hydrogen bond donor, hydrogen bond acceptor, hydrophobic and positive-ion searches. Two types of anchors (leucine/valine and phenylalanine) were used to aid in the preservation of side chains functionality required for binding in the peptide context. An anchor is defined as a functional group that chemically mimics a specific amino acid[40]. Other filters that may be set include specific types of reaction used for synthesis, molecular weight in Daltons, rotatable bond count, or the root mean squared deviation (RMSD; to minimize the compounds returned by the software to those containing the conformation within the query features that were selected) can be varied to help obtain fragments that are of most interest. The molecules returned by the software are all accompanied with the information regarding their synthesis via MCR. Using this strategy, fragments identified should closely match the pharmacophore of the native ligand in order to retain critical

peptide binding determinants and increase the probability of finding an active Ccap.
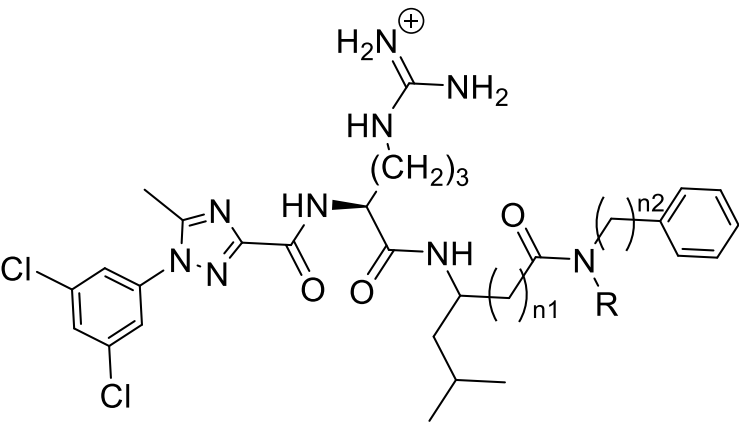
2.2.1 RESULTS

Using this approach, Ccaps of interest have been identified and synthesized. One of the most interesting Ccaps predicted by the software is 2-amino-N-ethyl-4-methyl-N-(3-phenylpropyl)pentanamide (Ccap in SCCP 6005 and 6014; Table 2.4), Figure 2.7 illustrates this capping group superimposed with HAKRRLIF in the primary hydrophobic pocket of Cyclin A. From this image, it is evident that the phenyl propylamine group closely mimics the interactions of Phe8. The predicted binding mode of this group suggests that when incorporated as a FLIP, this compound will aid in retaining the binding affinity of RRLIF in the primary hydrophobic pocket. This synthesis of this small molecule was suggested by AnchorQuery™ to be achieved using a reductive amination MCR however, it was determined that synthesis via a two-step process had better versatility and allowed facile incorporation of the Ncap and arginine residues. This fragment, 2-amino-N-ethyl-4-methyl-N-(3-phenylpropyl)pentanamide, was synthesized via reductive amination followed by peptide synthesis (Scheme 2.1) and purified through semi-preparative High Performance Liquid Chromatography (prep-HPLC). Prep-HPLC and Mass Spectroscopy (MS) data can be found in Appendix A.

In addition to 2-amino-N-ethyl-4-methyl-N-(3-phenylpropyl)pentanamide, other variations have also been synthesized (Table 2.3). Each of these Ccaps have been coupled to 35DCPT-Arg and either Leu or Beta-Leu (Figure 2.8). The variations (Table 2.3) include different length alkyl chains, and a hydrogen or ethyl group at the R position. The natural leucine was used in the synthesis of the analogs with a propyl alkyl chain (SCCP 6004, 6005, and 6014). Natural leucine, with the amine group on the alpha

carbon, helps position these Ccaps in a binding mode similarly to that of the native

ligand, aids in the positioning of these fragments in the primary hydrophobic pocket, and

potentially aids in retaining the binding affinity of LIF. Non-natural β-leucine was used

in the synthesis of the analogs with either methylene or ethylene alkyl chains (SCCP

6000, 6001, 6002, and 6003). Beta amino acids contain an additional methylene group,

placing the amine group on the beta carbon, which theoretically should adjust for the

shorter alkyl chains and help position the fragments in the primary hydrophobic pocket to

closely mimic the native ligand.

TABLE 2.3. **SUMMARY OF CCAPS IDENTIFIED VIA THE ANCHORQUERY™ SOFTWARE.**

SCCP ID	n1	n2	R	CDK2/Cyclin A IC$_{50}$ (μM)	CDK4/Cyclin D1 IC$_{50}$ (μM)
6000	1	1	H	>180	>180
6001	1	1	Et	>180	>180
6002	1	2	H	>180	>180
6003	1	2	Et	85.62	>180
6004	0	3	H	57.74	>180
6005	0	3	Et	>180	>180
6014	0	3	Et	90.19	>180
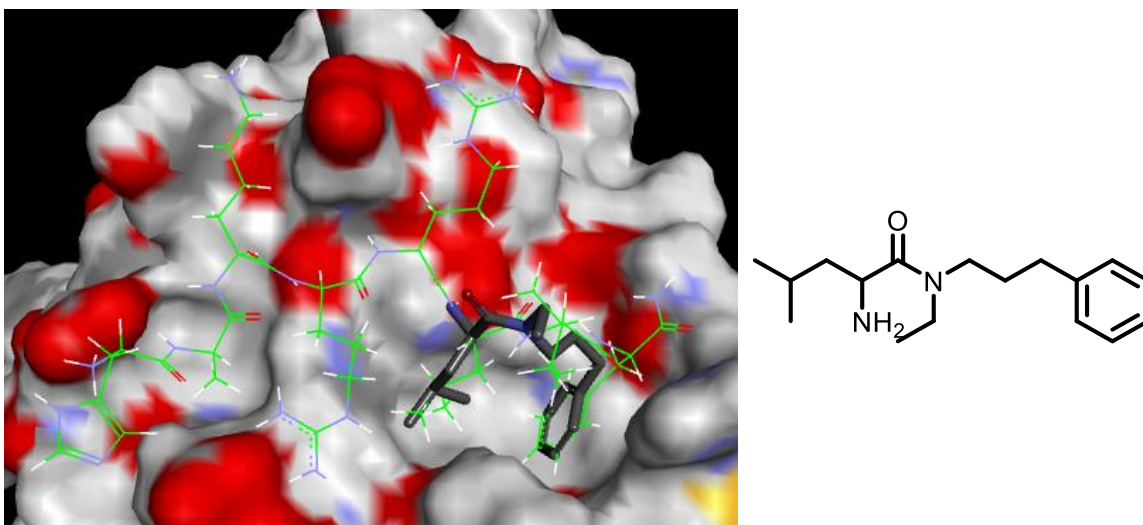
FIGURE 2.7. NOVEL C-TERMINAL CAPPING GROUP FOR THE REPLACEMENT OF LIF. 2-amino-N-ethyl-4-methyl-N-(3-phenylpropyl)pentanamide superimposed with LIF of the CBM in the primary hydrophobic pocket. This small molecule mimics the exact poses of LEU6 and PHE8 in this pocket and thus several derivatives of this small molecule have been designed and tested in a competitive binding assay to determine their binding affinity.

Following the peptide synthesis of Ncap-Arg-Leu/βLeu the Ccaps of Table 2.3 were coupled followed by the deprotection of these guanidine protecting group of arginine and the purification of these FLIP compounds through prep-HPLC. The HPLC data and MS data of the purified FLIPs are located in Appendix A. As shown by the HPLC traces, the FLIPs are 88-98 percent pure, by UV, and the MS results confirm the identity of the desired FLIP. Once the FLIP compounds were characterized, their binding affinities were tested by FP assay as described in Section 2.1.4. The competitive binding assay determined that the ethyl phenylethan-amine Ccap coupled to 35DCPT-R-β-L (SCCP 6003, Table 2.3) has an IC_{50} value of 85.62 μM and the phenylpropyl amine and ethyl phenylpropyl amine Ccaps, coupled with 35DCPT-RL (SCCP 6004 and 6014 respectively), have an IC_{50} values of 57.74 μM, and 90.19 μM against CDK2/cyclin A, respectively. All other FLIP compounds in Table 2.3 have IC_{50} values greater than 180 μM against CDK2/cyclin A.

CCAP SYNTHESIS
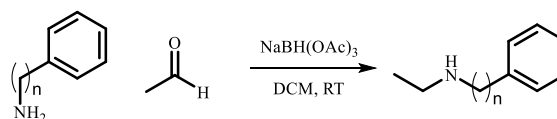
SOLID PHASE SYNTHESIS
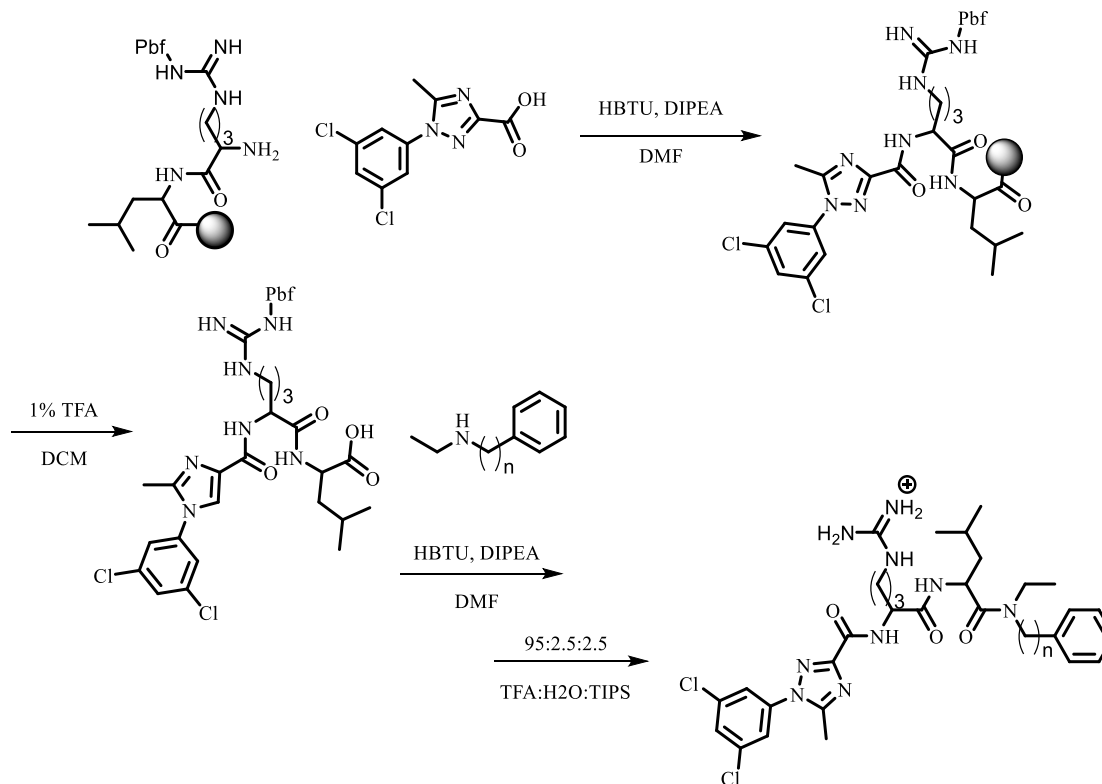
SCHEME 2.1. SYNTHESIS OF THE NOVEL C-TERMINAL CAPPING GROUPS. This scheme illustrates the route of synthesis for the novel C-terminal capping groups. First the amine underwent reductive amination to form a secondary amine. Second, the Ncapped peptide was made using solid phase synthesis. Next, the secondary amine was coupled to the Ncapped peptide in a solution phase coupling reaction. In the final step, the arginine side chain was deprotected.

Leu   Beta-Leu
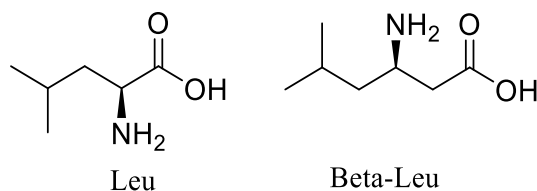
FIGURE 2.8. CHEMICAL STRUCTURES OF LEUCINE AND BETALEUCINE. Chemical structures of natural leucine and non-natural β-Leucine.

2.2.2 DISCUSSION

The replacement of the C-terminal tetrapeptide (RLIF) is necessary for the complete conversion of HAKRRLIF to a non-peptidic, drug-like inhibitor. The pharmacophore of

(R)RLIF was utilized in the AnchorQuery™ software to screen for potential fragment alternatives for the replacement of this peptide sequence. The AnchorQuery™ software is of interest because it specializes in pharmacophore search technology to help users screen for novel PPIs[40].

A library of potential C-terminal capping groups have been identified, through AnchorQuery™, that contains the desired pharmacophore features while maintaining good complementarity with the primary hydrophobic pocket of the CBG. Mimicking and preserving the binding determinants of Leu6 and Phe8 is of utmost importance because these particular residues make important intermolecular interactions with the CBG. Other important interactions between the CBM and the CBG are the H-bonding of Arg4 with Ile281 and ion-pairing interactions of this residue with Glu220, H-bonds between Arg5 and Gln254 and charge-charge interactions with Asp283. In addition, the backbone amide of Leu6 H-bonds with Gln254 while Ile7, of the CBM, acts as a spacer between Leu6 and Phe8, allowing complementary binding of these two residues in the primary hydrophobic pocket (Figure 2.9). P

otential Ccaps for the C-terminal tripeptide LIF have been identified using the AnchorQuery™ software. HAKRRLIF and the receptor (cyclin A) were uploaded into the software and the desired pharmacophore queries of the C-terminus were set. Figure 2.10 illustrates the pharmacophores that were varied to maximize the number of potentially viable small molecules returned by the software. In addition, other filters were applied and varied to refine the fragments returned by the software to those that most closely mimic the pharmacophore queries of interest. A LeuVal anchor was used to preserve the side chain functionality of the Leu6 because it was previously determined

that this residue is the most critical residue in the CBM[10b]. Once the preferred pharmacophore queries (maximum of 20) and filters were set, the query was submitted and the software searched upwards of 25 million compounds to find small molecules that were within the specified parameters. The fragments returned by the software can be viewed interactively on the website or be downloaded as .sdf files to be viewed in preferred software.
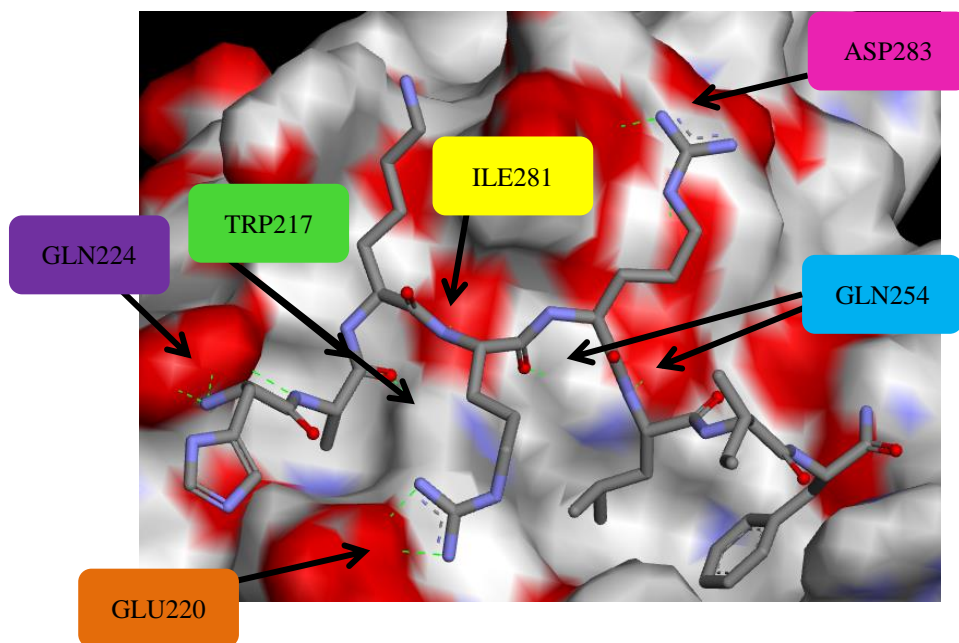
FIGURE 2.9. HAKRRLIF DOCKED INTO THE CBG. The intermolecular interactions of the CBM with the CBG are illustrated here indicated by the light green dotted lines. The known intermolecular interacts are as follows: histidine ion-pairs with GLU224, alanine hydrogen bonds with TRP217, the first arginine hydrogen bonds with ILE281 and GLN254 as well as ion-pairs with GLU220, the second arginine ion-pairs with ASP283, and leucine hydrogen bonds with GLN254.

The AnchorQuery™ website contains sufficient information for the synthesis of the potential capping groups. The fragments returned by the software are categorized by the type of reaction that can be used for their synthesis. The small molecules in the database are part of a MCR library and these reactions differ from standard sequential syntheses in that the desired product may be obtained by a "one-pot" method using three or more starting materials. The single step used has obvious benefits in saving on time and cost

and the overall yield, simplicity of reaction and purification, safety, and environmental acceptability[41]. In MCRs, the starting materials react sequentially rather than at the same time and it is the irreversible steps that drive the reaction to completion. With MCRs, more time is spent on the design and development of the experiment compared to traditional sequential reactions. The most common MCR is the Ugi Reaction (Scheme 2.2). This MCR is a four component reaction that includes an acid component, aldehyde or ketone, amine component and an isocyanide component[41]. In the initial step, the aldehyde or ketone and the amine components condense to form an intermediate imine, followed by protonation of the acid component to increase the electrophilicity of the imine bond[41]. The electrophilic iminium ion and the now nucleophilic conjugate base of the acid, add to the isocyanide component forming an intermediate acid anhydride (not shown). Acid anhydrides are strong acylating agents and following intramolecular acylation and rearrangement of the hydroxylimine intermediate to an amine the stable Ugi product is formed[41].

Previously it has been reported that RRLIF (SCCP 5811, Table 2.4) has an IC_{50} value of 1.4±0.42 µM against CDK2/cyclin A and when Arg4 (the first Arg of RRLIF) was replaced with 35DCPT (SCCP 5773, Table 1.2) the potency decreased by two-fold to give an IC_{50} value of 4.0±0.6 µM against CDK2/cyclin A. Also, RRLF (SCCP 5874; Table 2.4) was reported to have an IC_{50} value of 24.8±12.66 µM, a decrease in potency of approximately twelve-fold, against CDK2/cyclin A. Theoretically, if Arg4 (the first Arg of RRLF) of SCCP 5874 was replaced with 35DCPT (35DCPT-RLF), the IC_{50} value of this FLIP compound would be near 50 µM against CDK2/cyclin A. The novel Ccap, phenylpropyl amine containing FLIP (SCCP 6004; Table 2.3) mimics the binding mode

of Phe8 and is structurally comparable to the hypothetical structure of 35DCPT-RLF. SCCP 6004 has an IC_{50} value of 57.74 µM against CDK2/cyclin A which is comparable to that of the theoretical IC_{50} value of 35DCPT-RLF of approximately 50 µM. This concludes that SCCP 6004 may be the best FLIP compound of this series and the aromatic ring can further be optimized to regain potency.
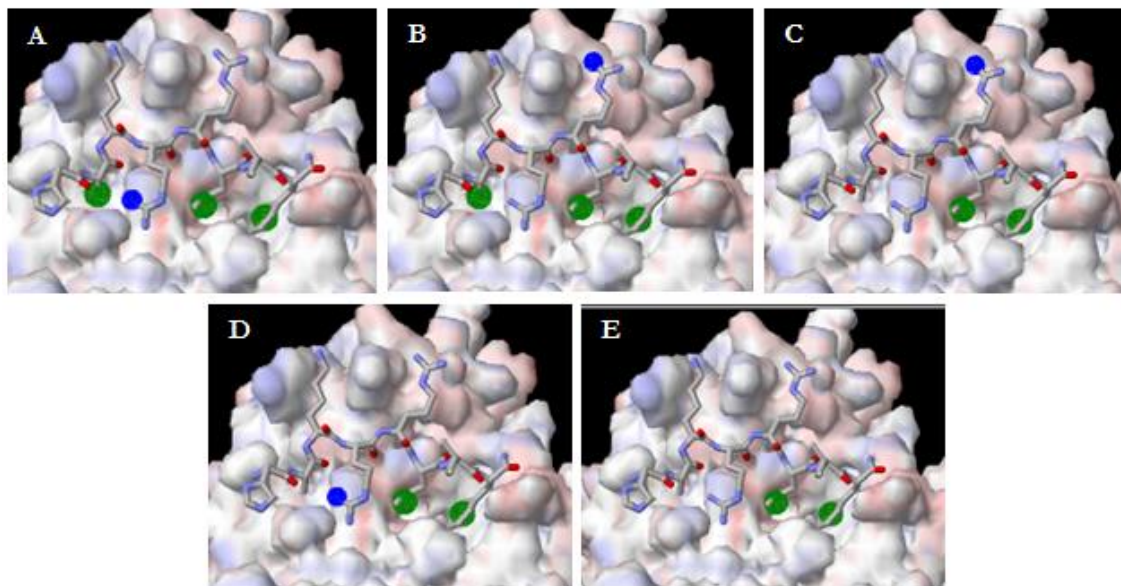
FIGURE 2.10. ILLUSTRATIONS OF THE ANCHORQUERY™ PHARMACOPHORE QUERIES. AnchorQuery™ images of the pharmacophore queries that were used for the pharmacophore search. The variations in the query were as follows: A) $Ala2_{hydrophobic}$, $Arg4_{positiveion}$, $Leu6_{hydrophobic}$, and $Phe8_{hydrophobic}$, B) $Ala2_{hydrophobic}$, $Arg5_{positiveion}$, $Leu6_{hydrophobic}$, and $Phe8_{hydrophobic}$ C) $Arg4_{positiveion}$, $Leu6_{hydrophobic}$, and $Phe8_{hydrophobic}$, D) $Arg5_{positiveion}$, $Leu6_{hydrophobic}$, and $Phe8_{hydrophobic}$, and E) $Leu6_{hydrophobic}$ and $Phe8_{hydrophobic}$.
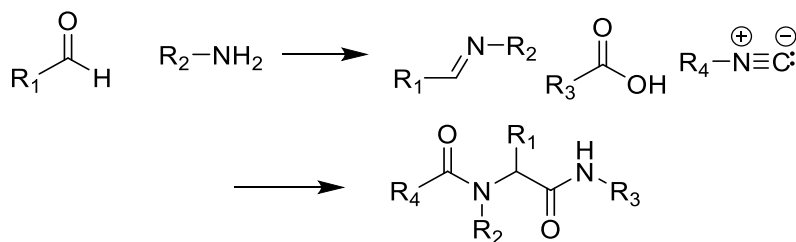
SCHEME 2.2. ILLUSTRATION OF THE UGI REACTION. The Ugi reaction is a four component reaction where an acid component, an aldehyde or ketone, an amine component and an isocyanide are combined to form the Ugi product.

SCCP 6014 differs from SCCP 6004 by a tertiary amine at the R position, seen in Table 2.3. The added ethyl group was originally thought to aid in the

geometry/conformation of this compound however, the addition of this group has abolished most of the activity that is shown by SCCP 6004. The ethyl chain may hinder the activity by steric hindrance, causing a clash with the protein, and resulting in the lower potency of this FLIP. Perhaps a methyl group would be a better substituent at this position. With a methyl there would be less steric bulk and potentially would avoid a clash with the protein. The methyl group would still structurally aid in the geometry of the compound.

TABLE 2.4. SUMMARY OF PREVIOUSLY REPORTED PEPTIDES AND THEIR ACTIVITY AGAINST CDK2/CYCLIN A AND CDK4/ CYCLIN D1.

SCCP ID	Peptide	CDK2/Cyclin A IC_{50} (μM)	CDK4/Cyclin D1 IC_{50} (μM)
5811	RRLIF	1.4±0.42	16.1±1.73
5874	RRLF	24.8±12.66	100~180
5875	RR(βLeu)F	3.3±2.33	20.7±12.45

2.2.3 MATERIAL AND METHODS

Individually, HAKRRLIF and cyclin A (PDB 2UUE) were uploaded into the AnchorQuery™ software, the desired pharmacophore queries of the C-terminal amino acids (RRLIF) and a LeuVal anchor were selected. The hydrophobic pharmacophore of Ala2, Leu6, and Phe8 (the 2nd, 6th, and 8th amino acids of the octamer) and the ion-pairing pharmacophore of Arg4 and Arg5 were varied to obtain numerous small molecules (Figure 2.10). The capping groups returned by the software all closely mimic the binding mode of both Leu6 and Phe8. Retaining the SAR of these amino acids is critical in identifying potential Ccaps to replace LIF of HAKRRLIF.

The initial compound synthesized from the fragments returned by AnchorQuery™ was 2-amino-N-ethyl-4-methyl-N-(3-phenylpropyl)pentanamide. This small molecule

was synthesized in four steps (1) reductive amination, (2) solid phase synthesis, (3) solution phase coupling, and (4) arginine deprotection (Scheme 2.1). In brief, in a round bottom the amine (5 mmol; 5EQ; 676.05 mg) and aldehyde (1 mmol; 1EQ; 44.05 mg) starting materials were coupled via reductive amination in the presents of sodium triacetoxyborohydride (NaBH(OAc)$_3$); 1.4 mmol; 1.4EQ; 296.72 mg) reducing agent in dichloromethane (DCM). The reaction was conducted at room temperature (RT) for two hours. After which 2N sodium hydroxide (NaOH) was added to quench the reaction and the reaction was left to stir for an additional 10 minutes. The organic and aqueous layers were separated and the organic layer was removed under reduced pressure and the product was dried under vacuum. The monoalkylated product was then purified by prep-HPLC yielding 74.7 mg (0.1%) of pure product. MS (EI+) 163.

The Ncap, 35DCPT, was prepared by the following procedure. To a solution of 3,5-dichloroaniline (15 mmol; 1EQ; 2.430 g) in a round bottom in 10 mL of methanol was added 10 mL of 6N hydrochloric acid (HCl) at 0 degrees Celsius. Sodium nitrite (30 mmol; 2EQ; 2.070 g) was then slowly added as a solid. The reaction mixture was stirred for 15 minutes at 0 degrees Celsius, after which sodium acetate was added as a solid to adjust the reaction to pH 5. Subsequent to this, a solution of ethyl 2-chloroacetoacetate (15 mmol; 1EQ; 2.469 g) in 10 mL of methanol was added slowly while the temperature was maintained at 0 degrees Celsius, after which the reaction mixture was allowed to warm to room temperature and stirred for 12 hours. The reaction was monitored for completion by thin-layer chromatography (TLC) with 20 percent ethyl acetate (EtOAc) in hexanes. Methanol was then removed under reduced pressure, diethyl ether was added, and the organic layer was separated and washed with saturated sodium bicarbonate and

water prior to drying over sodium sulfate[3]. The organic layer was concentrated and the product was dried under vacuum yielding 2.107 g (47.6%). ^{1}H NMR (chloroform-d, 300 MHz) δ (ppm) 8.2 (s, 1H), 7.1 (s, 2H), 7.0 (s, 1H), 4.36-4.43 (q, J = 5.46 Hz, 2H), 1.38-1.43 (t, J = 7.05 Hz, 3H).

The second step for the synthesis of 35DCPT is as follows. The step 1 product, ethyl 2-chloro-2-[2-(3,5-dichlorophenyl)hydrazono]acetate (7.129 mmol; 1EQ; 2.107 g), and acetaldehyde oxime (7.129 mmol; 1EQ; 0.421 g) were dissolved in toluene and heated to reflux for 2 h, after which triethylamine (7.129 mmol; 1EQ; 0.721 g) was added. The reaction was monitored by TLC with 20% EtOAc in hexanes. After completion, the reaction mixture was then concentrated and partitioned between EtOAc and water. The layers were separated and the aqueous layer was washed with EtOAc. The combined organic layers were washed with water and brine, dried with sodium sulfate, filtered, concentrated and dried under vacuum yielding 2.2818 g (50.7%)[3]. 1H NMR (chloroform-d, 300 MHz) δ (ppm) 7.43 (d, J = 9 Hz 3H), 2.57 (s, 3H).

The final step in the synthesis of 35DCPT is as follows. The step 2 product, ethyl 1-(3,5-dichlorophenyl)-5-methyl-1H-1,2,4-triazole-3-carboxylate (7.602 mmol; 1EQ; 2.282 g) was refluxed in NaOH (60.820 mmol; 8EQ; 2.433 g) in a 50/50 mixture of ethanol and water for 2 h, and the reaction was monitored by TLC (35% EtOAC in hexanes). After completion, the reaction mixture was cooled, the alcohol was evaporated, and the mixture was diluted with water. The reaction mixture was acidified with 1 N HCl and stirred to precipitate the product yielding 1.032 g (25.3%). 1H NMR (chloroform-d, 300 MHz) δ (ppm) 7.50 (s, 1H), 7.45 (s, 2H), 4.46−4.53 (q, J = 7.26 Hz, 2H), 2.62 (s, 3H), 1.41−1.46 (t, J = 7.08 Hz, 3H). MS (EI+) 271.

Solid phase peptide synthesis was used for the synthesis of 35DCPT-Arg-β-Leu similar to Section 2.3.3 (Scheme 2.3). In brief, Fmoc protected leucine (1.108 mmol; 2EQ; 391.58 mg) in 5 mL of DCM (10 mL/1 gram resin) and a 2-chlorotrityl resin (0.554 mmol; 1EQ; 480 mg) was mixed in a round bottom at room temperature with N,N-Diisopropylethylamine (DIPEA; 5.54 mmol; 1EQ; 715.99 mg) for 5 minutes[42]. After which another 1.662 mmol (1.5EQ; 215.06 mg) of DIPEA was added and mixed for an additional 60 minutes. To endcap any unreacted 2-chlorotrityl groups, HPLC grade methanol (0.4 mL; 0.8mL/1 gram of resin) was added and stirred for 15 minutes. The resin was then filtered and washed three times with DCM, twice with dimethylformamide (DMF), twice with DCM and three times with methanol[42]. The resin was placed into a solid phase peptide ynthesis vessel and the Fmoc group of the Leu was deprotected using 20 percent piperidine in DMF while nitrogen was bubbled into the vessel for stirring. After 30 minutes, the resin was filtered and washed thoroughly with DMF.

The second amino acid, Fmoc-Arginine(Pmc) (1.108 mmol; 2EQ; 764.38 mg) was added to the vessel in the presence of a coupling agent (O-benzotriazole-N,N,N',N'-tetramethyl-uronium-hexafluoro-phosphate , HBTU; 2.438 mmol; 4.4EQ; 924.587 mg) and a base, DIPEA (3.324 mmol; 6EQ; 429.59 mg) in DMF and was bubbled with nitrogen at room temperature for 4-6 hours. Upon a negative ninhydrin test, the resin was filtered and washed several times with DMF. The Fmoc group was deprotected using 20 percent piperidine in DMF for 30 minutes. The resin was filtered and washed with DMF. The Ncap, 35DCPT (1.108 mmol; 2EQ; 301.48 mg) was then added to the resin with HBTU (2.438 mmol; 4.4EQ; 924.587 mg) and DIPEA (3.324 mmol; 6EQ; 429.59 mg) in DMF and bubbled with nitrogen at room temperature for 4-6 hours. When the reaction

47

was complete, the resin was thoroughly washed with DMF. The resin was removed from the vessel and placed into a round bottom flask to be cleaved using 3-5 percent TFA in DCM for approximately three minutes. The resin was filtered and rinsed until the resin returned to a yellow in color and the filtrates was collected and was removed under reduced pressure and left to dry under vacuum. The product was purified through FLASH chromatography yielding 240.10 mg (54%).

In a round bottom, the Ccap 2-amino-N-ethyl-4-methyl-N-(3-phenylpropyl) pentanamide (0.272 mmol; 2EQ; 36.78 mg) was coupled the 35DCPT-Arg(Pmc)-Leu (0.136 mmol; 1EQ; 110 mg) peptide in the presence of HBTU (0.299 mmol; 2.2EQ; 113.47 mg) and DIPEA (0.408 mmol; 4EQ; 52.73 mg). HPLC was used to monitor the reaction and upon completion the reaction mixture was concentrated and partitioned between EtOAc and water. The aqueous layer was back extracted with EtOAc. The organic layers were combined and washed with 1N sodium hydroxide (NaOH), 1N HCl, and brine (saturated sodium chloride solution). The organic layer was dried with sodium sulfate (Na_2SO_4), filter, concentrated, and dried under vacuum. Lastly, the side chain of the Arg was deprotected using 95:2.5:2.5 TFA:water:TIPS overnight. Once the HPLC confirmed deprotection the solvents were removed under reduced pressure and the final product was purified by prep-HPLC resulting 36.0 mg (40%) of SCCP 6004. MS (EI+) 658.

2.3 LEU-PHE MIMETICS

Based on commercially available compounds with appropriate functionality to mimic both Leu6 and Phe8, FLIPs have been computationally designed (Table 2.5), synthesized and coupled to 35DCPT-Arg5. These Leu-Phe mimetics contain either isobutyl or

isopropyl groups at the R2 position (Table 2.5) to help retain the interactions of Leu6 in the primary hydrophobic pocket which was shown to be the most important residue of the CBM. Also, there are varying alkyl groups at the R1 position to mimic Phe8 in the pocket.
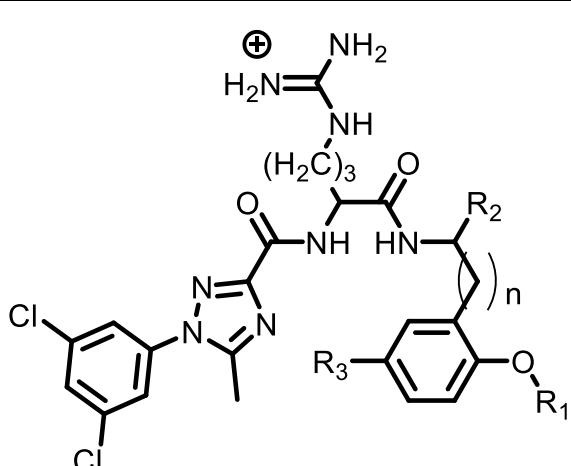
2.3.1 RESULTS

Following solid phase synthesis and coupling with the Ccap, the Leu-Phe mimetics were purified via prep-HPLC. As these compounds have a chiral center and were purchased as a racemic mixture, diastereomers were formed for the FLIPs during synthesis. However, not all of the FLIP isomers were able to be successfully separated by prep-HPLC but the diastereomers that were separated the first isomers that eluted were those that showed activity against CDK2/cyclin A. The isomers with activity would be the R isomer, as the S isomer would not be expected to have activity against the CDK/cyclin complexes because only R amino acids have been shown to be active. The HPLC data and MS data of the purified FLIPs are located in Appendix B. As shown by HPLC, the FLIP compounds are 79-98 percent pure by UV and the MS results confirm the identity of desired FLIP compounds. Subsequent to full characterization of the FLIP compounds their binding affinities were tested via FP assay as described in Section 2.1.4.

Of the FLIPs listed in Table 2.5, only SCCP 5977, 5979 and 5983 showed activity against CDK2/cyclin A while none displayed significant binding to CDK4/cyclin D1. The isobutyl group mimicking Leu6, in all the compounds, retained some of the binding affinity and the various alkoxy groups mimicking Phe8 had a significant effect on the activity of each FLIP on CDK2/cyclin A. SCCP 5977 contains an isobutyl group to mimic the Phe8 position in the primary pocket. This compound had an IC_{50} value of

49

148.4 µM against CDK2/cyclin A. SCCP 5979 has a propyl group reaching in to the pocket in replacement of Phe8 and has an IC_{50} value of 181.2 µM against CDK2/cyclin A. Lastly, SCCP 5983 contains an ethyl group which was shown to be slightly less potent against CDK2/cyclin A with an IC_{50} value of 164.02 µM. All other compounds (SCCP 5978, 5980-5982, 5984, and 5985) are not active against either CDK2/cyclin A or CDK4/cyclin D1.

TABLE 2.5. SUMMARY OF THE LEU-PHE MIMETICS

SCCP ID	n	R1	R2	R3	CDK2/Cyclin A IC_{50} (µM)	CDK2/Cyclin A $IC0_{50}$ (µM)
5977	0	iBut	iBut	H	148.4	>180
5978	0	iBut	iBut	H	>180	>180
5979	0	Pr	iBut	H	181.2	>180
5980	0	Pr	iBut	H	>180	>180
5981	1	Me	iBut	Me	>180	>180
5982	1	Me	iBut	H	>180	>180
5983	0	Et	iBut	H	164.02	>180
5984	0	Et	iBut	H	>180	>180
5985	0	Me	iBut	H	>180	>180

2.3.2 DISCUSSION

The computationally designed Ccaps, based on commercially available compounds with appropriate functionality to mimic both Leu6 and Phe8 of HAKRRLIF, have been coupled to the 35DCPT-Arg. The binding affinity of these novel Ccaps have been measured via the FP assay to determine the ability of the FLIP compounds to compete with a peptidic inhibitor (tracer peptide) against CDK2/cyclin A and CDK4/cyclin D1. Compounds SCCP 5977, 5979, and 5983 (Figure 2.11) are the only FLIPs out of this series to show activity against CDK2/cyclin A. No FLIPs were active against CDK4/cyclin D1.

The isobutyl group replacement for Phe8 (SCCP 5977) appears to be the best alkyl group compared to the propyl group (SCCP5979) and the ethyl group (SCCP 5983). The additional methyl group of the isobutyl seems to be a contributor to the retention of potency compared to the propyl group. SCCP 5977 showed an IC_{50} value of 148.4 μM, SCCP 5979 with 181.2 μM and SCCP 5983 with 164.02 μM against CDK2/cyclin A. The isobutyl side chain (SCCP 5977) proves to be most potent against CDK2/cyclin A.

SCCP 5977   SCCP 5979   SCCP 5983
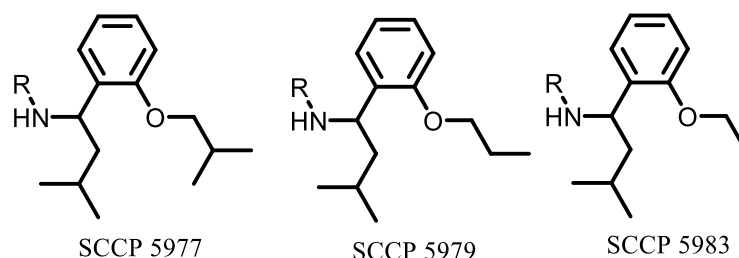
FIGURE 2.11. CHEMICAL STRUCTURES OF SCCP 5977, 5979, AND 5983. Listed are the chemical structures for the Ccaps of SCCP 5977, 5979, and 5983. SCCP 5977 showed an IC_{50} value of 148.4 μM, SCCP 5979 has an IC_{50} value of 181.2 μM, and SCCP 5983 with an IC_{50} value of 164.02 μM all against CDK2/cyclin A. These compounds are not active against CDK4/cyclin D1. The R group for each of these compounds is 35DCPT-Arg.

We can compare these results to a previously reported FLIP (SCCP 5923; Table 1.3) that contains 4CPT-Arg5-Leu6 and the 4-(4-fluorophenoxy)pyridin-2-

yl)methanamine Ccap. This FLIP compound has an IC_{50} value of 18.1±4.0 μM. Section 1.5 introduced both 35DCPT and 4CPT as Ncaps and when coupled to RLIF (5773 and 5774, respectively) showed IC_{50} values of 4.0±0.6 μM and 11.5±3.3 μM, respectively. There is a slight difference in the expected binding affinities between SCCP 5979 and SCCP 5923 due to the different Ncaps but even with these differences SCCP 5923 is still significantly more potent against CDK2/cyclin A.

2.3.3 MATERIAL AND METHODS

The computationally designed Ccaps have been coupled to 35DCPT-Arg and their binding affinities have been evaluated in a competitive binding assay. The peptide synthesis in which these small molecules were synthesized is illustrated in Scheme 2.3. In a round bottom, an arginine (1.32 mmol; 1EQ; 3.935 g) (protected by Pbf and coupled to a 2-Chlorotrityl resin) was coupled to 1-(3,5-dichlorophenyl)-5-methyl-1H-1,2,4-triazole-3-carboxamide (35DCPT; 2EQ; 2.64 mmol; 0.718 g) in the presence of a coupling agent (HBTU, 5.808 mmol; 4.4EQ; 2.202 g) and a base (DIPEA, 7.92 mmol; 6EQ; 1.023 g) in DMF. The reaction was left to stir overnight and when HPLC confirmed the consumption of starting materials the resin was filtered and washed thoroughly with DMF. The resin was then cleaved with 3-5 percent TFA in DCM for 3 minutes. The resin was then filtered and washed several times with DCM until the resin returned to a yellow color. The filtrate was collected and the organic layer was removed under reduced pressure yielding 581.26 mg (64.7%).

The Leu-Phe mimetic Ccaps were then coupled. In brief, 1-(2-isobutoxyphenyl)-3-methylbutan-1-amine (0.07346 mmol; 1EQ; 17.29 mg) was coupled to 35DCPT-Arg(Pbf) (0.07346 mmol; 1EQ; 50 mg) in the presence of HBTU (0.1469 mmol; 2.2EQ;

55.72 mg) and DIPEA (0.2938 mmol; 4EQ; 37.971 mg) in DCM. The reaction was left overnight and when HPLC confirmed the consumption of starting materials the reaction mixture was concentrated and partitioned between EtOAc and water. The aqueous layer was back extracted with EtOAc. The organic layers were combined and washed with 1N NaOH, 1N HCl, and brine, dried over sodium sulfate, filtered concentrated, and dried under vacuum. Lastly, the side chain of the Arg was deprotected using 95:2.5:2.5 TFA:water:TIPS overnight. Once deprotection was confirmed the solvents were removed under reduced pressure. Due to this compound having a chiral center, diastereomers were synthesized and were separated by prep-HPLC resulting in 0.940 mg (0.02%; SCCP 5977) and 1.180 mg (0.025%; SCCP 5978). MS (EI+) 645. The FP assay was used to measure the binding affinity of these novel Ccaps. In this assay, each FLIP compound was tested against CDK2/cyclin A and CDK4/cyclin D1.
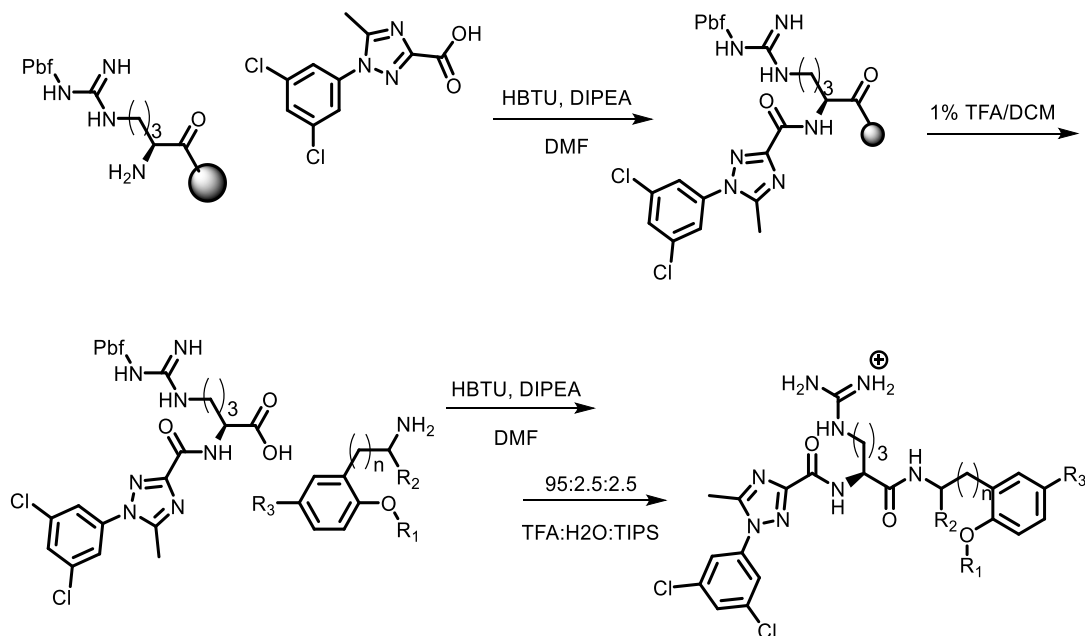
SCHEME 2.3. GENERAL REACTION SCHEME FOR THE SYNTHESIS OF THE LEU-PHE MIMETICS. As seen in this scheme, the arginine linker attached to a resin was coupling with the desired Ncap of 35DCPT. This product was then cleaved from the resin and coupled with the novel Leu-Phe mimetic Ccaps.

.

53

CHAPTER 3
DEVELOPMENT OF FRAGMENT LIGAND INHIBITORY PEPTIDES CONTAINING NON-NATURAL AMINO ACIDS

In the effort to convert HAKRRLIF into a more drug-like molecule by the REPLACE strategy, the C-terminal amino acids (RLIF) need to be replaced by small molecules for the complete conversion of the octamer into a cell permeable, non-peptidic inhibitor. Chapter 2 describes a valid approach in the replacement of LIF of the octamer. Chapter 3 introduces the replacement of the critical arginine amino acid by an alternative approach. The replacement of Arg5 has been attempted by the inclusion of non-natural arginine derivatives. These isosteres have been utilized to explore their effects on the binding affinity of the FLIP molecules, further establish SAR for this interaction, and potentially improve drug-likeness through enhancing stability and cell permeability.

3.1 ARGININE ISOSTERES

Isosteric arginine derivatives have been utilized as linkers between 35DCPT and a C-terminal dipeptide, β-Leu-NMethylPhe-NH$_2$. These non-natural amino acids form amide bonds similarly to natural amino acids but have side chains that distinguish them[43]. The non-natural amino acids have been synthesized and incorporated into the FLIP compounds to enhance pharmacokinetics and the inhibitory activities of peptides[37a]. The library of non-natural arginine derivatives obtained may (1) potentially mimic the interactions that are made between the CBM (Arg5) and the CBG (Asp283), (2) evaluate the steric requirements of this position, (3) improve drug-like properties, and (4) most

likely improve the binding affinity of the FLIPs through favoring increased ion-pairing interactions. Currently, structure-activity relationship (SAR) data for this interaction is at the initial stages. The replacement of Arg5 with various amino acids has been done with activity still present however at a decreased amount of 4-fold or greater. The arginine at this position is important for the binding affinity of HAKRRLIF and therefore varying the functionality of these arginine derivative side chains will aid in the further development of the SAR and possibly the replacement for this position.

3.2 RESULTS AND DISCUSSION

The arginine isosteres listed in Table 3.1 were Fmoc-protected prior to solid phase synthesis with the dipeptide Ccap, β-Leu-NMethylPhe-NH$_2$. These FLIPs were then Ncapped with 35DCPT. The alkylation of the guanidine group in these isosteres provide functionality and should protect the guanidine groups from reacting during peptide synthesis. These side chains are expected to interact with Asp283 of the CBG and help establish further SAR.

Peptides composed of naturally occurring amino acids are useful as lead compounds in discovering new drug therapies but generally speaking are limited as therapeutics by their undesirable pharmacokinetic profiles. These are caused by their poor permeability (blood brain barrier, cell membrane, etc.) and lack of metabolic stability including protease-mediated degradation[37]. While naturally occurring amino acids are not ideal for novel drug therapies, their non-natural counterparts allow modification to improve drug-likeness. Appropriate non-natural amino acids, such as these arginine isosteres, can be incorporated into compounds in order to increase lipophilicity and potentially improve the pharmacokinetic parameters, the

agonist/antagonist behaviors, and may promote ion-pairing[37a]. This ion-pairing interaction is enhanced by incorporating alkyl groups on the side chains of guanidine containing residues. The alkyl groups destabilize solvation of the charged side chain promoting ion-pairing and the binding to the target[44].

TABLE 3.1. SUMMARY OF THE ARGININE ISOSTERES
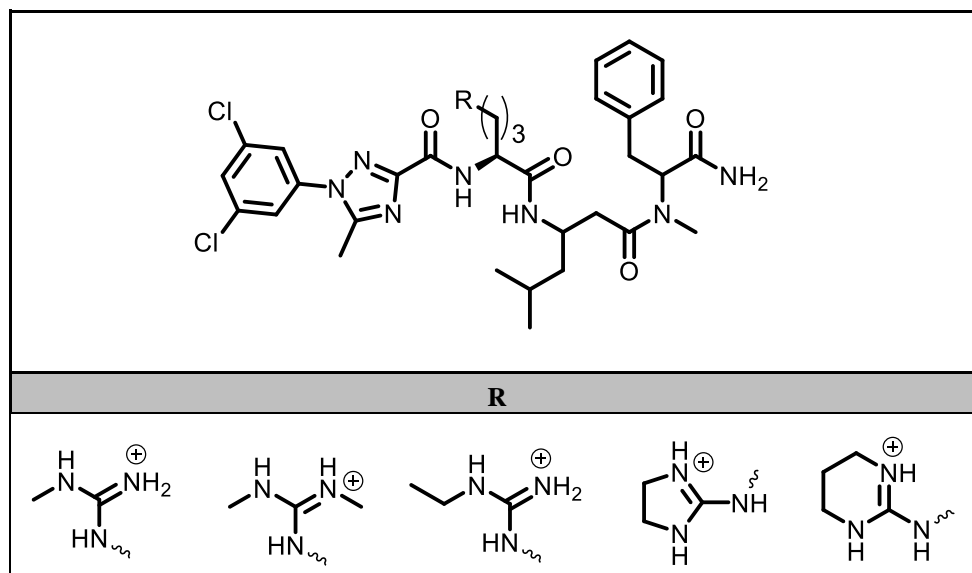
The incorporation of non-natural amino acids can allow compounds to evade peptidase digestion thus creating a more stable compound[44]. Having a more stable compound should result in an increased half-life of the compound in the circulatory system of patients[44]. This improved stability can potentially be achieved through modifications to the side chains of amino acids and may include, but are not limited to, the incorporation of halogens, unsaturated hydrocarbons, heterocycles, silicon, and organometallic units[45]. By adding appropriate non-natural amino acids in the non-peptidic inhibitor, functionality can be incorporated to help enhance pharmacokinetic parameters, enhance the inhibitory abilities of peptides and promote favorable ion-pairing [37a, b]. Varying the side chains can also provide SAR data to further optimize the

functionality of these side chains.

Non-natural arginine derivatives, gifted to the McInnes lab from the Dix laboratory at the Medical University of South Carolina, have been utilized to replace Arg5 of the C-terminal pentapeptide (RRLIF; Table 3.1). The side chains of these arginine derivatives contain functional groups such as acyclic (methyl and ethyl) and cyclic (4,5-dihydro-1H-imidazole and 1,4,5,6-tetrahydropyrimidine) groups. These groups may provide protection to the guanidine group to elude reactivity during peptide synthesis. These modified guanidines will help establish further SAR data for the interactions between the Arg5 of the CBM and Asp283 of the CGB.

The arginine derivatives have been Fmoc-protected prior to solid phase peptide synthesis with a C-terminal dipeptide, β-Leu-NMethylPhe-NH$_2$ and Ncapped with 35DCPT. The C-terminal dipeptide has been previously tested in the FP assay as RR(β-Leu)NMePhe-NH$_2$ (SCCP 5941) and is a potent inhibitor of CDK2/cyclin A with an IC$_{50}$ value of 0.405±0.091 μM. To incorporate this C-terminal dipeptide with the current isosteres, the natural arginine was been replaced with an arginine derivative. The identity of the Arg isostere-dipeptide was confirmed by Liquid Chromatography-Mass Spectrometry (LCMS), was Ncapped with 35DCPT and the final FLIP compound was cleaved from the resin but the M+S did not confirm the desired product but indicates that, in this case, the guanidine group was able to react readily with the activated 35DCPT and resulted in double Ncapped FLIP compounds (Appendix C). During purification two peaks were isolated and identified through MS. The first isolated peak has an m/z of 1010 (Appendix C; C1) which theoretically corresponds to the addition of 35DCPT twice. It is believed that the additional Ncap is coupled to the guanidine side chain;

further analysis will confirm the exact structure that relates to this mass. The other fraction that was isolated has an m/z of 559 (data not shown). This mass corresponds to 35DCPT-βL-NMethylF indicating that the addition of the arginine isosteres was not complete.

To address this issue several different parameters will be varied to elude such outcomes. During the initial synthesis 35DCPT was used in excess and the reaction occurred overnight. To resolve the current issue, the Ncap and Arg isosteres-dipeptide will be used at the same scale (1:1 ratio) and the reaction will be monitored closely through HPLC until the starting materials are consumed. If the guanidine still proves to be readily reactive, protection of this group will be employed. Common protecting groups for guanidines are 2,2,4,6,7-pentamethyl-dihydrobenzofuran-5-sulfonyl (Pbf) and 2,2,5,7,8-pentamethylchroman-6-sulfonyl (Pmc). The addition of the sulfonamide group masks the reactivity of the guanidine and these groups are easily removed with high concentrations of acid.

3.3 MATERIALS AND METHODS

Following the synthesis of the arginine derivatives, the amine group on the alpha carbon was protected by 9-Fluorenylmethyl *N*-succinimidyl carbonate (Fmoc-O Suc) via Fmoc protection in aqueous solution. For example, N-methyl arginine (1.328 mmol; 1EQ; 250 mg) was combined with Fmoc-O Suc (1.859 mmol; 1.4EQ; 627.10 mg) in a 3:1 ratio of water and ethanol[46]. The reaction mixture was stirred for 4 to 6 hours at 60 degrees Celsius. Once complete, the reaction mixture was cooled to zero degrees Celsius, acidified to pH 4-5, and extracted with EtOAc[46]. The aqueous layer was evaporated under reduced pressure and purified by FLASH chromatography.

The Fmoc-N-methyl arginine was then coupled to 35DCPT and a C-terminal dipeptide sequence of β-Leu-NMethylPhe-NH$_2$ via solid phase peptide synthesis (Scheme 3.1). In brief, Fmoc protected Rink Amide Resin (0.75 mmol; 1EQ; 1.19 g) was pre-swelled in DMF for 30 minutes. The resin was then placed into a solid phase peptide synthesis vessel, and the Fmoc group protecting the resin was deprotected with 20% piperidine in DMF for 30 minutes[47]. The resin was then filtered and rinsed thoroughly with DMF. Fmoc-N-MethylPhe (1.5 mmol; 2EQ; 0.6022 g) was then coupled using dry DMF, HBTU as the coupling agent (3.375 mmol; 4.4EQ; 1.280 g), and DIPEA as base (4.5 mmol; 6EQ; 0.5816 g) with nitrogen was bubbled into the vessel for stirring. After 4 to 6 hours a ninhydrin test confirmed consumption of the starting material and the resin was filtered and rinsed several times with DMF and the Fmoc group was deprotected using 20% piperidine in DMF under nitrogen. Next, the Fmoc-β-Leu (1.5 mmol; 2EQ; 0.5512 g) was coupled in the same manner and the Fmoc protecting group was deprotected.

The Fmoc-N-methyl arginine (0.561 mmol; 5EQ; 0.230 g) was coupled to the dipeptide-resin (0.112 mmol; 1EQ; 0.277 g) for 24 to 36 hours in the presence of HBTU (1.008 mmol; 11EQ; 382.27 mg), DIPEA (1.380 mmol; 15EQ; 178.35 mg), DNF and nitrogen was bubbled into the vessel for stirring. When the ninhydrin test confirmed the consumption of the starting materials, the resin was then filtered and washed thoroughly with DMF. The Ncap, 35DCPT, (0.240 mmol; 2EQ; 0.0653 g) was then attached by the same procedure for 12 hours. To complete the synthesis, the rink amide resin was removed from the vessel, placed into a round bottom and was cleaved using 20% TFA in DCM for 20 minutes and rinsed several times with DCM. Following resin cleavage, the

filtrate was collected and the organic solvent was removed under reduced pressure. The

product was purified by prep-HPLC and tested in the FP assay for their binding.
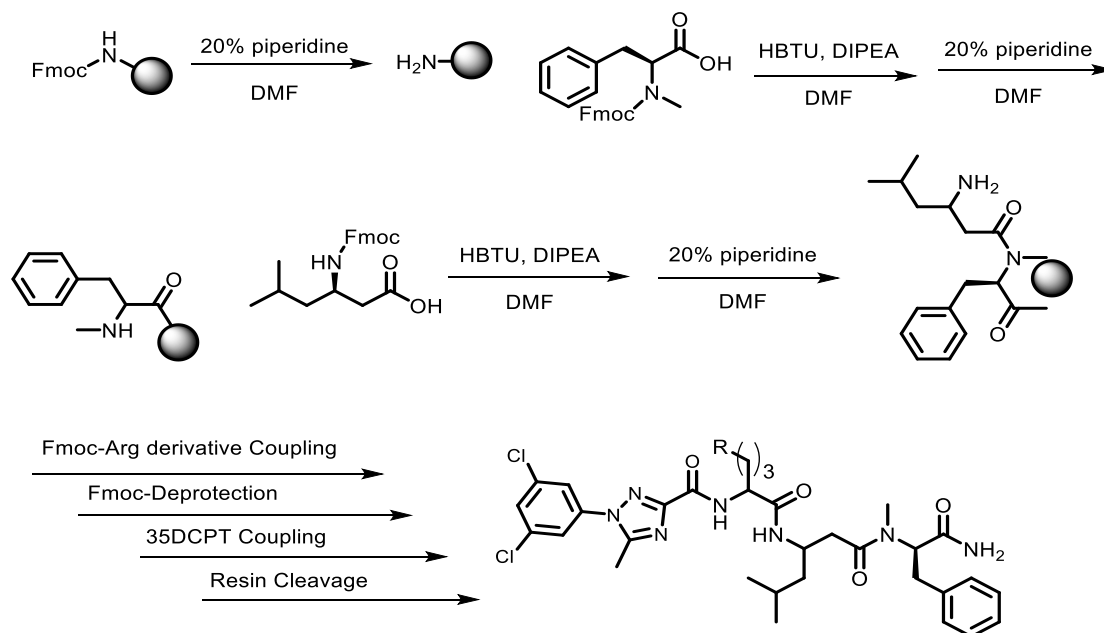
SCHEME 3.1. GENERAL REACTION SCHEME FOR THE PEPTIDE SYNTHESIS OF THE ARGININE ISOSTERS.
An amide rink resin was deprotected and coupled with the coupled with NMethyl-Phe and β-Leu. This
dipeptide was then coupled with an arginine isosteres and Ncapped with 35DCPT. These peptides were
synthesized via solid phase peptide synthesis.

CHAPTER 4
ALTERNATIVE APPROACHES AND THE FUTURE
DIRECTION OF CDK INHIBITORS

SECTION 4.1 ALTERNATIVE APPROACHES

Another strategy for the development of CDK inhibitors for use in oncology beyond targeting the ATP binding pocket and the cyclin binding groove is to inhibit the formation of the CDK/cyclin complex. Such inhibitors interfere with the protein-protein interface between CDK2 and cyclin A. Cyclin A binds to CDK2 by interacting with the N- and C-terminal lobes through PPI[48]. When the α3 and α5 helices of cyclin A bind to the PSTAIRE helix of CDK2 major conformational rearrangements occur resulting in an inactive intermediate complex[48]. This process is the initial step in the CDK/cyclin complex formation followed by a gradual conformational reorganization to expose the T loop of CDK2. The T-loop is then phosphorylated by the cyclin activating kinase (CAK) to form the substrate binding site[48]. A peptide was developed, C1, based on the α5 helices of the cyclin, to target this interface and has shown to inhibit CDK2/cyclin A activity towards histone H1 and pRb fused with GST[48]. A derivative of this peptide, C4, containing a point mutation to increase solubility, was shown to inhibit CDK2 kinase activity when associating with either cyclin A or cyclin E[48]. Figure 4.1 illustrates the binding placement for C4 on the cyclin subunit. However, CDK1/cyclin B, protein kinase A and protein kinase C were not affected by C4[48]. C4 was shown to adopt an α-helical conformation that mimics the hydrophobic interactions between CDK2 and cyclin

A and this is understood as to how the inhibition of this complex occurs[48]. C4 promotes a conformational change that induces the CDK2/cyclin A complex into an inactive conformation and was shown to not bind to pre-existing CDK2/cyclin A complexes or free CDK2[48]. Concluding that C4 is potentially a selective inhibitor of CDK2/cyclin A and this was validated when tested in estrogen-independent MDA-MB-231 breast cancer cells[48]. C4 was able to completely inhibit cellular proliferation[48].
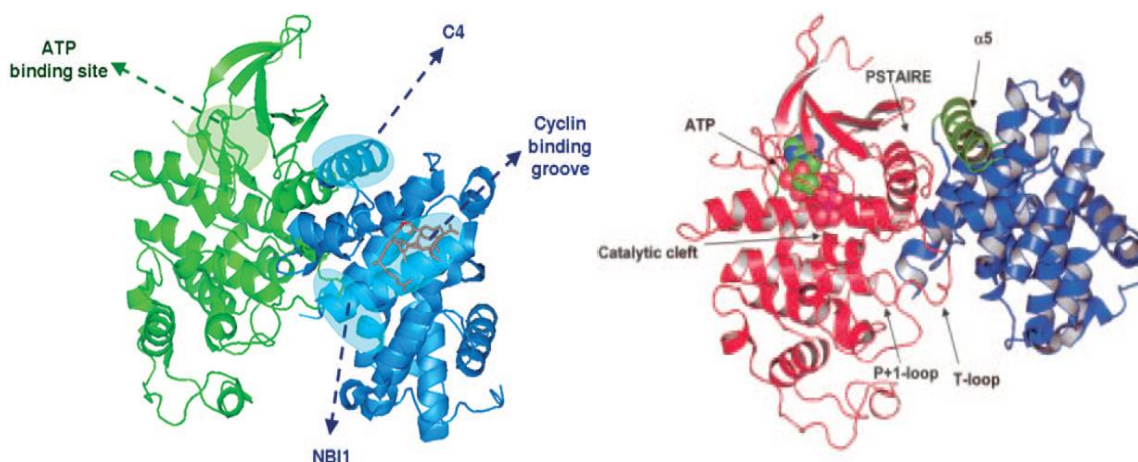

FIGURE 4.1. ILLUSTRATION OF A CDK/CYCLIN COMPLEX. A. The ATP binding site is located on the CDK and the cyclin binding groove on the cyclin. C4 and NBI1 bind to the interface between CDK2 and cyclin A. [Reprinted with permission from Orzaez, M., A. Gortat, et al. (2009). "ATP-noncompetitive inhibitors of CDK-cyclin complexes." ChemMedChem **4**(1): 19-24.] **B.** The three major sites discussed in this section are illustrated; α5 helix, PSTAIRE, and the T-loop all located on the interface between CDK2 and cyclin A. [Gondeau, C., S. Gerbal-Chaloin, et al. (2005). "Design of a novel class of peptide inhibitors of cyclin-dependent kinase/cyclin activation." The Journal of biological chemistry **280**(14): 13793-13800.]

A second compound, NBI1, has also been identified as a CDK2/cyclin A inhibitor that targets neither the ATP binding pocket nor the CBG[48]. NBI1 is a hexapeptide that contains all D-amino acids and is known to only interact with the cyclin subunit by binding to the region containing the α3, α4, and α5 helices, illustrated in Figure 4.1[48-49]. NBI1 showed an IC$_{50}$ value against CDK2/cyclin A of 1.1 μM[49] and it is believed that NBI1 affects the stability of the CDK/cyclin complex[48]. Inhibition of CDK2/cyclin A results in elevated E2F-1 activity leading to cell cycle arrest in S phase resulting in apoptosis[49]. Unlike C4, NBI1 was shown to inhibit CDK1/cyclin B and CDK6/cyclin D3

but did not show inhibition against a panel of other serine/threonine protein kinases[48]. A derivative of NBI1, TAT-NBI1 (TAT is a cell penetrating carrier), was tested against numerous cell lines at various concentrations and CDK1 and CDK2 activities were significantly decreased whereas CDK4 was only minimally inhibited and demonstrated to have cells arrest in the S or G2/M phases[48]. TAT-NBI1 in a concentration and time dependent manner inhibited cell proliferation by inducing S phase arrest and apoptosis in glioblastoma, colon, and ovarian cancer cells[49].

NB11 has been proven to be a selective inhibitor of the association between CDK2/cyclin A with remarkable affinity however, this small molecule is a weak inhibitor of CDK2/cyclin E[49]. Both cyclins associate with the same CDK therefore the different selectivity between the two complexes must be due to structural differences amongst the cyclins[49]. This suggests that the development for an alternative inhibitor for the inhibition of CDK2/cyclin E is necessary. A potential advantage of targeting the CBG is the inhibition of all the cell cycle CDKs due to the conserved sequence recognition (CBM) across cyclins A, E and D-type.

SECTION 4.2 FUTURE DIRECTIONS

The REPLACE methodology has successfully aided in the identification of novel Ccaps. The most potent FLIP compound reported here is SCCP 6004 with an IC_{50} value of 57.74 µM against CDK2/cyclin A. The Ccap of this FLIP and many other potential Ccaps were identified by the AnchorQuery™ software. The fragments chosen for the work in this thesis closely mimic the position of Leu6 and Phe8 in the primary hydrophobic pocket. The software also returned a similar small molecule to 2-amino-N-ethyl-4-methyl-N-(3-phenylpropyl)pentanamide (Ccap of SCCP 6005 and 6014; Figure 2.7). This fragment 3-

amino-N-phenethyl-3-phenyl-N-(2,2,2-trifluoroethyl)propanamide (Figure 4.2) and is of interest to further build the SAR. The trifluoroethyl group of this small molecule could be replaced with a small alkyl group because it does not make intermolecular interactions within the pocket, although having a group at this position may be important geometrically. The aromatic ring positioned in the Leu6 position is expected to have a binding mode similarly to Leu6 and be space-filling.
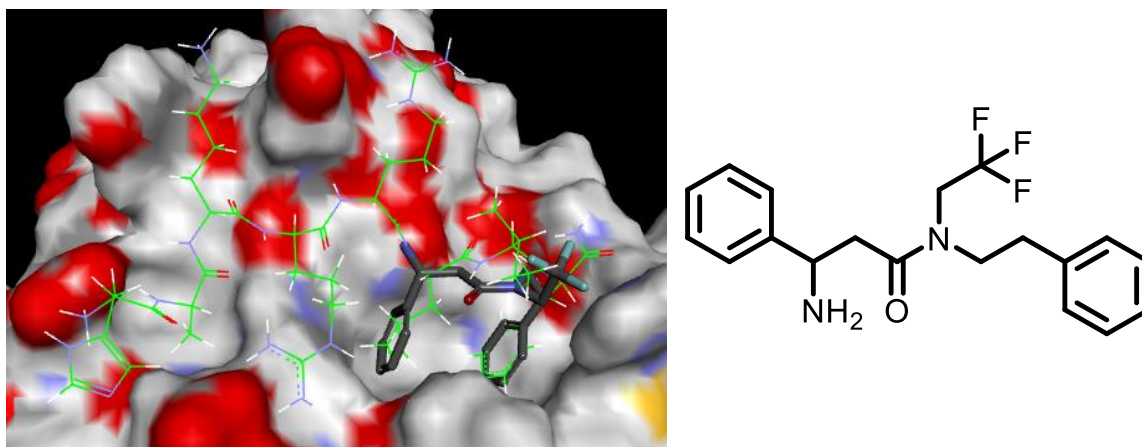

FIGURE 4.2. POTENTIAL FRAGMENT SUPERIMPOSED WITH HAKRRLIF IN THE PRIMARY HYDROPHOBIC POCKET. 3-amino-N-phenethyl-3-phenyl-N-(2,2,2-trifluoroethyl)propanamide superimposed with HAKRRLIF in the primary hydrophobic pocket. This small molecule closely mimics the pose of LEU6 and PHE8 and therefore is a potential Ccap of interest.

Based on the results from the Ccaps tested in Chapter 2, a series of Ccaps have been designed that are of interest (Table 4.1). These Ccaps (Table 4.1) will be synthesized and undergo solid phase synthesis similarly to that which is illustrated in Scheme 2.1. The Ccaps (No. 1-4) differ from SCCP 6000 – 6005 and 6014 (Table 2.3) by the group in the Leu6 position which is either leucine or β-leucine. The new Ccaps will contain phenylalanine, histidine, β-phenylalanine, or β-histidine depending on the length of the alkyl chain at the n2 position seen in Table 2.3. These derivatives will help further establish the SAR for the Leu6 position. The variation of the ring size plus the addition of potential ion-pairing interaction of the imidazole ring of histidine will aid in

the determination of which functional group(s) would best retain or enhance the binding affinity of this position. Leu6 has previously been determined to be the most critical amino acid of the octamer (HAKRRLIF) and therefore its replacement has been challenging but has also been shown that this position is capable of being replaced with a small molecule.

SCCP 6004 has shown to be the most potent FLIP of the compounds reported here. SCCP 6004 has been structurally modified (Table 4.1; No. 5-8) to help regain activity that was lost due to fragment replacement. These modified FLIP compounds will contain the addition of halogens on the aromatic ring at either the 4-position or the 3,5-position. Previously, a library of bis(aryl) ether Ccaps were generated. The first of this series was a FLIP compound contained 4CPT-RL-(3-phenoxyphenyl)methanamine (SCCP 5807) showed an IC_{50} value of 106.1±26.2 μM against CDK2/cyclin A. Following the addition of halogens on the aromatic ring the binding affinities for these compounds increased 2-5 fold compared to SCCP 5807. SCCP 5824 and 5823 (Table 1.3) contain fluoro groups at the 3 and 4 position with IC_{50} values of 53.2±11.6 μM and 18.1±4.0 μM against CDK2/cyclin A, respectively.

Of Table 4.1, compounds No. 5 and 7 contain a chlorine and fluorine at the 3 and 5 positions, respectively. Modeling these compounds using Discovery Studio showed that the addition of halogens to these fragments does not clash with the protein and therefore may potentially enhance the current activity of SCCP 6004. Compounds No. 6 and 8 have either a chlorine or fluorine at the 4 position of the aromatic ring, respectively. Having a chlorine at this position severely clashed with the protein when structurally designed in Discovery Studio and thus a compound containing this functional group may result in a

loss of activity that SCCP 6004 currently has. The fluorine at the 4 position however has a good complementarity with the binding pocket. Such compounds will be tested in the competitive binding assay to determine the effects of halogenation.

TABLE 4.1. SUMMARY OF C-TERMINAL CAPPING GROUPS OF INTEREST.

No.	n1	n2	R1	R3	R4	R5
1	0	3	phenyl	H	H	H
2	1	3		H	H	H
3	0	3	imidazole	H	H	H
4	1	3		H	H	H
5	0	3	isopropyl	Cl	H	Cl
6	0	3		H	Cl	H
7	0	3		F	H	F
8	0	3		H	F	H

SECTION 4.3 PREDICTION OF CELLULAR ACTIVITY OF NOVEL CCAPPED FLIPS

The work reported here has identified a series of FLIP compounds that further validate the REPLACE methodology through the replacement of the C-terminal amino acids with fragments that have IC_{50} values comparable to those previously reported. With further modification these Ccaps have the potential to be 2-fold or more potent than the bis(aryl) ether Ccaps which has an IC_{50} value of 18.1±4.0 µM against CDK2/cyclin A. The next major step in this project is to generate cell permeable compounds.

Mendoza *et al.* (2003) reported that RXL peptides have the ability to block the recruitment of E2F-1 and its phosphorylation through the inhibition of CDK2/cyclin A as well as selectively promote apoptosis in cells with deregulated CDK4/6-cyclin D-INK4-pRb pathway[50]. The peptides PVKRRLDL and PVKRRLFL were coupled to fusion peptides (penetratin) to promote entry into cells[50]. During standard cell viability assays both PEN-PVKRRLDL and PEN-PVKRRLFG peptide inhibited the proliferation of an osteosarcoma (U2OS) cell line in a concentration-dependent manner[50].

Cell proliferation assays were conducted in house with HeLa (p53 defective), prostate cancer Du145 (pRb null), and osteosarcoma U2OS (p16 defective which should upregulate E2F-1 activity) cell lines. Peptides containing the fusion peptide or peptide alone showed that both a peptide alone (SCCP 5995; SAKRR-βL-3TA-G) and a scrambled fusion peptide (SCCP 5991; PEN-ETDHQYLAESS) have no effect on growth inhibition, both with IC_{50} values greater than 100 μM (Table 4.2). A weakly binding control (SCCP 5990; PEN-PVKRRAFG) shows growth inhibition against all three cell lines with IC_{50} values of 49.9±0.6 μM (HeLa), 24.9±1.9 μM (Du145) and 42.5±1.9 μM (U2OS). A positive control (SCCP 5994; PEN-SAKRR-βL-3TA-Gly) has growth inhibition in only Du145 (38.5±4.3 μM) and U2OS (43.1±1.1 μM) cell lines. SCCP 5989 a fusion peptide used by Mendoza *et al.* (2003) with the peptide sequence of PEN-PVRRLFG showed to have an IC_{50} values of approximately 30 μM in all three cell lines.

Efforts are also being made to put FLIP compounds with well-established competitive binding assay IC_{50} values into cancer cell lines. Prostate (DU145) and osteosarcoma (U2OS) cell lines have been treated with SCCP 5963 and 5964 (Table 4.3). These FLIPs showed IC_{50} values of 6.49±0.27 μM and 7.91±5.08 μM against

CDK2/cyclin A, respectively. When DU145 prostate cells were treated with SCCP 5963 and 5964 the IC$_{50}$ values obtained were 36.5±2.6 μM and 21.8±0.32 μM, respectively. The U2OS osteosarcoma cells had similar results with IC$_{50}$ values of 30.7±2.7 μM for SCCP 5963 and 18.3±1.5 μM for SCCP 5964. SCCP 5963 has comparable growth inhibition compared to SCCP 5989 however, SCCP 5964 has a greater growth inhibition than SCCP 5989.
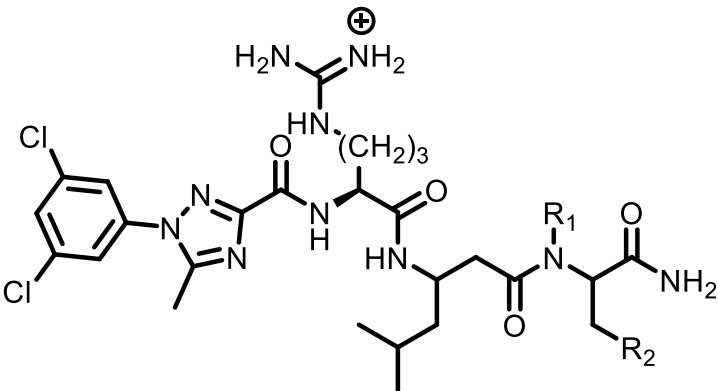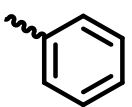
TABLE 4.2. SUMMARY OF VARIOUS PEPTIDE ACTIVITIES IN CELL LINES.

SCCP	HeLa IC$_{50}$ (μM)	Du145 IC$_{50}$ (μM)	U2OS IC$_{50}$ (μM)
5990	49.9±0.6	24.9±1.9	42.5±1.9
5995	>100		
5989	30.3±1.4	32.3±3.2	28.9±2.2
5991	>100	>100	>100
5994	>100	38.5±4.3	43.1±1.1

To aid in the prediction of cell permeability, ADMET (absorption, distribution, metabolism, excretion, and toxicity) parameters have been calculated for SCCP 5963, 5964, and 6004 as well as the new FLIP compounds of interest for the future (Table 4.4). ADMET parameters such as solubility between 0-1, absorption between 3-4, Lipinski's Rule of 5 (molecular weight (MW) <500, logP <5, the number of hydrogen bond donors (HBD) <5, and the number of hydrogen bond acceptors (HBA) <10), the number of rotatable bonds (≤10), and the polar surface area (PSA) (≤140) are ideal for cell permeability. SCCP 5964 (Table 4.4) was the most active in the cell proliferation assay and when compared to SCCP 5963, it has a more ideal solubility level, lowest logP value, fewer HBA and fewer rotatable bonds but has the highest PSA.

The most active compound from the novel Ccaps reported here is SCCP 6004. This FLIP has comparable solubility and absorption levels and has fewer HBD, HBA,

and rotatable bonds to SCCP 5964. The logP value for SCCP 6004 is significantly higher than that of SCCP 5964 and has almost 1.5 fold less PSA. This may conclude that SCCP 6004 will be more cell permeability compared to SCCP 5964. With these ADMET values it can be predicted that SCCP 6004 will have greater cell permeability but may have slightly less activity based on its binding affinity in the FP assay.

TABLE 4.3. SUMMARY OF FLIP ACTIVITY IN COMPETITIVE BINDING AND CELL PROLIFERATION ASSAYS

			Competitive Binding Assay		Cell proliferation Assay	
SCCP	R1	R2	CDK2/Cyclins A IC50 (μM)	CDK4/Cyclins D1 IC50 (μM)	DU145 IC50 (μM)	U2OS IC50 (μM)
5963	Me		6.49±0.27	>100	36.5±2.6	30.7±2.7
5964	H		7.91±5.08	>100	21.8±0.32	18.3±1.5

The FLIP compounds of interest for the future also have comparable solubility and absorption levels (Table 4.4). Compounds No. 3 and 4 have comparable logP values and lower PSA values than SCCP 5964 which may indicate a slight increased in cell permeability. All other FLIPs have greater logP values, similar number of HBD, HBA

and rotatable bonds, and lower PSA values. This may contend that these FLIPs may have cell permeability and activity but will most likely not be greater than that of SCCP 5964. Compound No. 6 has the highest logP value (without exceeding the limit of 5) and one of the lowest PSAs, therefore this FLIP can be predicted to be the most cell permeable of Table 4.4).
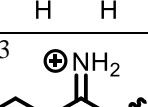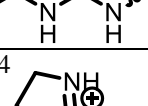
TABLE 4.4. ADMET RESULTS FOR CURRENT AND FUTURE FLIPS.

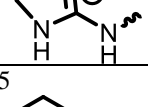| SCCP	Molecular Weight (<500)	Solubility Level (0-1)	Absorption Level (3-4)	logP ≤5	Number of HBD (<5)	Number of HBA (<10)	Number of Rotatable Bonds (≤10)	Polar Surface Area (≤140)
5963	714.292	2	3	3.163	8	14	18	214.21
5964	706.233	1	3	2.255	9	14	18	251.25
6004	658.279	2	3	4.044	8	12	17	181.65
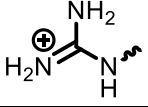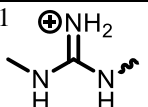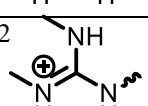
	No.	Molecular Weight (<500)	Solubility Level (0-1)	Absorption Level (3-4)	logP ≤5	Number of HBD (<5)	Number of HBA (<10)	Number of Rotatable Bonds (≤10)	Polar Surface Area (≤140)
Future Ccaps of Interest	1	706.279	2	3	4.510	8	12	18	181.65
	2	692.263	2	3	4.054	8	12	17	181.65
	3	682.254	2	3	2.398	9	14	17	210.33
	4	696.64	2	3	2.083	9	14	17	210.33
	5	726.201	1	3	5.373	8	12	17	181.65
	6	692.240	1	3	4.708	8	12	17	181.65
	7	694.260	1	3	4.455	8	12	17	181.65
	8	676.269	2	3	4.250	8	12	17	181.65

As for the arginine isosteres, changing the functionality at this position affects mainly logP and PSA (Table 4.5). The solubility and absorption levels remain consistent with the altered side chains and the number of HBD, HBA, and rotatable bonds are comparable across the table. However, the PSA values decrease by 13 to 25 units and the logP values increase with added functionality. With the increase in logP and the decrease

in PSA, these arginine isosteres are expected to be promising replacements for natural arginine. Theoretically, if arginine isosteres 2 or 3 were introduced into a compound like SCCP 5964 the cell permeability and potentially the activity would increase due to the effects of the altered side chain.

TABLE 4.5. RESULTS FOR ARGININE ISOSTERES.

Structure of Side Chain	Molecular Weight (<500)	Solubility Level (0-1)	Absorption Level (3-4)	logP ≤5	Number of HBD (<5)	Number of HBA (<10)	Number of Rotatable Bonds (≤10)	Polar Surface Area (≤140)
Natural Arg	116.12	5	0	0.308	5	3	4	63.64
1	130.13	5	0	0.514	4	3	5	49.65
2	144.15	4	0	0.720	3	3	5	38.03
3	144.15	5	0	0.863	4	3	6	49.65
4	142.13	4	0	0.538	3	3	4	38.03
5	156.15	4	0	0.601	3	3	4	38.03

SECTION 4.4 CONCLUSIONS

There are frequent deregulations of endogenous CDKIs in human cancers and the development of novel CDK inhibitors is being investigated by targeting the CBG. Currently, non-peptidic inhibitors are being developed based on the HAKRRLIF which is derived from the C-terminal peptide sequence of the CDK inhibitor p21[WAF1]. Reported

here, computational design (structure- and pharmacophore-based) and the incorporation of arginine isosteres have been utilized to identify PLAs to replace the C-terminal amino acids (RLIF) by the REPLACE methodology. These FLIPs have been synthesized, coupled with a potent Ncap, and their binding affinities have been tested using an FP assay. Of the FLIP compounds generated, SCCP 6004 was determined to have the greatest potency against CDK2/cyclin A with and IC_{50} value of 57.74 μM. Furthermore, ADMET values have been calculated for SCCP 6004 for the comparison with a known cell permeable FLIP, SCCP 5964. SCCP 6004 may have comparable or greater cell permeability than SCCP 5964 however further optimization of SCCP 6004 is needed for this compound to be more active in cells. ADMET values were also calculated to compare natural arginine with the arginine isosteres listed here. Isostere number 2 is expected to have the greatest impact on cell permeability and cellular activity if it were to be incorporated into a compound similar to SCCP 5964.

The results reported here have enhanced the development of a selective, drug-like, cell permeable CDK inhibitors by generating promising Ccaps and by identifying a novel approach for the design of PLAs. Furthermore, these results bring this project closer to achieving the ultimate goal of developing a novel class of cancer therapeutics based on cell cycle inhibition.

REFERENCES

1.   Vermeulen, K.; Van Bockstaele, D. R.; Berneman, Z. N., The cell cycle: a review of regulation, deregulation and therapeutic targets in cancer. *Cell Prolif* **2003,** *36* (3), 131-49.

2.   (a) Shapiro, G. I., Cyclin-Dependent Kinase Pathways As Targets for Cancer Treatment. *Journal of Clinical Oncology* **2006,** *24* (11), 1770-1783; (b) Fischer, P. M.; Lane, D. P., Inhibitors of Cyclin-Dependent Kinases as Anti-Cancer Therapeutics. *Current Medicinal Chemistry* **2000,** *7*, 1213-1245.

3.   Liu, S.; Premnath, P. N.; Perkins, T.; Bolger, J. K.; Kirkland, L. O.; Kontopidis, G. A.; McInnes, C., Optimization of Non-ATP Competitive CDK/Cyclin Groove Inhibitors through REPLACE-Mediated Fragment Assembly. *J. Med. Chem.* **2013,** *56*, 1573-1582.

4.   Kontopidis, G.; McInnes, C.; Pandalaneni, S. R.; McNae, I.; Gibson, D.; Mezna, M.; Thomas, M.; Wood, G.; Wang, S.; Walkinshaw, M. D.; Fischer, P. M., Differential binding of inhibitors to active and inactive CDK2 provides insights for drug design. *Chemistry & Biology* **2006,** *13* (2), 201-11.

5.   Napolitano, G.; Majello, B.; Lania, L., Role of cyclinT/Cdk9 complex in basal and regulated transcription (review). *Int J Oncol* **2002,** *21* (1), 171-7.

6.   Knudsen, E. S.; Knudsen, K. E., Tailoring to RB: tumour suppressor status and therapeutic response. *Nat Rev Cancer* **2008,** *8* (9), 714-24.

7.   Pollard, T. D.; Earnshaw, W. C.; Lippincott-Schwartz, J., Introduction to the Cell Cycle. In *Cell Biology*, 2nd ed.; Saunders Elsevier: Philadelphia, 2008; pp 731-746.

8.   Lodish, H.; Berk, A.; Kaiser, C. A.; Krieger, M.; Scott, M. P.; Bretscher, A.; Ploegh, H.; Matsudaira, P., Molecular Cell Biology. 6th ed.; W. H. Freeman and Company: New York, NY, 2008; p 888.

9.   (a) Kirkland, L. O.; McInnes, C., Non-ATP competitive protein kinase inhibitors as anti-tumor therapeutics. *Biochemical Pharmacology* **2009,** *77*, 1561-1571; (b) Singh, S.

K.; Tripathi, S. K.; Dessalew, N.; Singh, P., Cyclin Dependent Kinase as Significant Target for Cancer Treatment. *Current Cancer Therapy Reviews* **2012,** *8*, 225-235.

10.   (a) Atkinson, G. E.; Cowan, A.; McInnes, C.; Zheleva, D. I.; Fischer, P. M.; Chan, W. C., Peptide Inhibitors of CDK2-cyclin A that Target the Cyclin Recruitment-Site: Structural Variants of the C-Terminal Phe. *Bioorg Med Chem Lett* **2002,** *12*, 2501-2505; (b) Andrews, M. J. I.; Kontopidis, G.; McInnes, C.; Plater, A.; Innes, L.; Cowan, A.; Jewsbury, P.; Fischer, P. M., REPLACE: A Strategy for Iterative Design of Cyclin-Binding Groove Inhibitors. *ChemBioChem* **2006,** *7*, 1909-1915; (c) McInnes, C.; Andrews, M. J. I.; Zheleva, D. I.; Lane, D. P.; Fischer, P. M., Peptidomimetic Design of CDK Inhibitors Targeting the Recruitment Site of the Cyclin Subunit. *Curr. Med. Chem. - Anti-Cancer Agents* **2003,** *3*, 57-69.

11.   Shan, B.; Lee, W. H., Deregulated expression of E2F-1 induces S-phase entry and leads to apoptosis. *Mol Cell Biol* **1994,** *14* (12), 8166-73.

12.   Yu, Q.; Sicinska, E.; Geng, Y.; Ahnstrom, M.; Zagozdzon, A.; Kong, Y.; Gardner, H.; Kiyokawa, H.; Harris, L. N.; Stal, O.; Sicinski, P., Requirement for CDK4 kinase function in breast cancer. *Cancer Cell* **2006,** *9* (1), 23-32.

13.   (a) McInnes, C., Recent Advances in the Structure-Guided Deisgn of Protein Kinase Inhibitors. *Frontiers in Drug Design & Discovery* **2007,** *3*; (b) McInnes, C.; Wang, S.; Anderson, S.; O'Boyle, J.; Jackson, W.; Kontopidis, G.; Meades, C.; Mezna, M.; Thomas, M.; Wood, G.; Lane, D. P.; Fischer, P. M., Structural Determinants of CDK4 Inhibition and Design of Selective ATP Competitve Inhibitors. *Chemistry & Biology* **2004,** *11*, 525-534; (c) McInnes, C.; Fischer, P. M., Strategies for the Design of Potent and Selective Kinase Inhibitors. *Current Pharmaceutical Design* **2005,** *11*, 1845-1863.

14.   McIntyre, N. A.; McInnes, C.; Griffiths, G.; Barnett, A. L.; Kontopidis, G.; Slawin, A. M. Z.; Jackson, W.; Thomas, M.; Zheleva, D. I.; Wang, S.; Blake, D. G.; Westwood, N. J.; Fischer, P. M., Design, Synthesis, and Evaluation of 2-Methyl- and 2-Amino-*N*-aryl-4,5-dihydrothiazolo[4,5-*h*]quinazolin-8-amines as Ring-Constraiined 2-Anilino-4-(thiazol-5-yl)pyrimidine Cyclin-Dependent Kinase Inhibitors. *J Med Chem* **2010,** *53*, 2136-2145.

15.   McInnes, C., Progress in the evaluation of CDK inhibitors as anti-tumor agents. *Drug Discov Today* **2008,** *13* (19-20), 875-881.

16.   Pfizer Pfizer's Palbociclib (PD-0332991) Receives Food And Drug Administration Breakthrough Therapy Designation For Potential Treatment Of Patients

With Breast Cancer. http://pfizer.newshq.businesswire.com/press-release/pfizera%E2%82%ACs-palbociclib-pd-0332991-receives-food-and-drug-administration-breakthrough-th.

17.   Flaherty, K. T.; LoRusso, P. M.; DeMichele, A.; Abramson, V. G.; Courtney, R.; Randolph, S. S.; Shaik, M. N.; Wilner, K. D.; O'Dwyer, P. J.; Schwarts, G. K., Phase I, Dose-Escalation Trial of the Oral Cyclin-Dependent Kinase 4/6 Inhibitor PD 0332991, Administered Using a 21-Day Schedule in Patients with Advanced Cancer. *Clin Cancer Res* **2012,** *18* (2), 568-576.

18.   Fry, D. W.; Harvey, P. J.; Keller, P. R.; Elliott, W. L.; Meade, M.; Trachet, E.; Albassam, M.; Zheng, X.; Leopold, W. R.; Pryer, N. K.; Toogood, P. L., Specific inhibition of cyclin-dependent kinase 4/6 by PD 0332991 and associated antitumor activity in human tumor xenografts. *Mol Cancer Ther* **2004,** *3* (11), 1427-1437.

19.   Schwartz, G. K.; LoRusso, P. M.; Dickson, M. A.; Randolph, S. S.; Shaik, M. N.; Wilner, K. D.; Courtney, R.; O'Dwyer, P. J., Phase I study of PD 0332991, a cyclin-dependent kinase inhibitor, administered in 3-week cycles (Schedule 2/1). *British Journal of Cancer* **2011,** *104*, 1862-1868.

20.   Guhna, M., Blockbuster dreams for Pfizer's CDK inhibitor. *Nature Biotechnology* **2013,** *31* (3), 187.

21.   Baughn, L. B.; Di Liberto, M.; Wu, K.; Toogood, P. L.; Louie, T.; Gottschalk, R.; Niesvizky, R.; Cho, H.; Ely, S.; Moore, M. A. S.; Chen-Kiang, S., A Novel Orally Active Small Molecule Potently induces G_1 Arrest in Primary Myeloma Cells and Prevents Tumor Growth by Specific Inhibition of Cyclin-Dependent Kinase 4/6. *Cancer Res* **2006,** *66* (15), 7661-7667.

22.   Carlson, B. A.; Dubay, M. M.; Sausville, E. A.; Brizuela, L.; Worland, P. J., Flavopiridol Induces G_1 Arrest with Inhibition of Cyclin-dependent Kinase (CDK) 2 and CDK4 in Human Breast Carcinoma Cells. *Cancer Res* **1996,** *56*, 2973-2978.

23.   Patel, V.; Senderowicz, A. M.; Pinto, D. J.; Igishi, T.; Raffeld, m.; Quintanilla-Martinez, L.; Ensley, J. F.; Sausville, E. A.; Gutkind, J. S., Flavopiridol, a Novel Cyclin-dependent Kinase Inhibitor, Suppresses the Growth of Head and Neck Squamous Cell Carcinomas by Inducing Apoptosis. *The Journal of Clinical Investigation* **1998,** *102* (9), 1674-1681.

24.   Wang, S.; Midgley, C. A.; Scaerou, F.; Grabarek, J. B.; Griffiths, G.; Jackson, W.; Kontopidis, G.; McClue, S. J.; McInnes, C.; Meades, C.; Mezna, M.; Plater, A.; Stuart, I.;

Thomas, M. P.; Wood, G.; Clarke, R. G.; Blake, D. G.; Zheleva, D. I.; Lane, D. P.; Jackson, R. C.; Glover, D. M.; Fischer, P. M., Discovery of *N*-Phenyl-4-(thiazol-5-yl)pyrimidin-2-amine Aurora Kinase Inhibitors. *J Med Chem* **2010,** *53*, 4367-4378.

25.   Fischer, P. M.; Gianella-Borradori, A., CDK inhibitors in clinical development for the treatment of cancer. *Expert Opin. Investig. Drugs* **2003,** *12* (6), 955-970.

26.   Drees, M.; Dengler, W. A.; Roth, T.; Labonte, H.; Mayo, J.; Malspeis, L.; Grever, M.; Sausville, E. A.; Fiebig, H. H., Flavopiridol (L86-8275): Selective Antitumor Activity *in Vitro* and Activity *in Vivo* for Prostate Carcinoma Cells. *Clin Cancer Res* **1997,** *3*, 273-279.

27.   Arguello, F.; Alexander, M.; Sterry, J. A.; Tudor, G.; Smith, E. M.; Kalavar, N. T.; Greene, J. F. J.; Koss, W.; Morgan, C. D.; Stinson, S. F.; Siford, T. J.; Alvord, W. G.; Klabansky, R. L.; Sauville, E. A., Flavopiridol Induces Apoptosis of Normal Lymphoid Cells, Causes Immunosuppression, and Has Potent Antitumor Activity In Vivo Against Human Leukemia and Lymphoma Xenografts. *Blood* **1998,** *91* (7), 2482-2490.

28.   Senderowicz, A. M.; Headlee, D.; Stinson, S. F.; Lush, R. M.; Kalil, N.; Villalba, L.; Hill, K.; Steinberg, S. M.; Figg, W. D.; Tompkins, A.; Arbuck, S. G.; Sausville, E. A., Phase I Trial of Conitnuous Infusion Flavopiridol, a Novel Cycline-Dependent Kinase Inhibitor, in Patients With Refractory Neoplasms. *Journal of Clinical Oncology* **1998,** *16* (9), 2986-2999.

29.   (a) Schwartz, G. K.; Ilson, D.; Saltz, L.; O'Reilly, E.; Tong, W.; Maslak, P.; Werner, J.; Perkins, P.; Stoltz, M.; Kelsen, D., Phase II Study of the Cyclin-Dependent Kinase Inhibitor Flavopiridol Administered to Patients With Advanced Gastric Carcinoma. *Journal of Clinical Oncology* **2001,** *19* (7), 1985-1992; (b) Shapiro, G. I.; Supko, J. G.; Patterson, A.; Lynch, C.; Lucca, J.; Zacarola, P. F.; Muzikansky, A.; Wright, J. J.; Lynch, T. J. J.; Rollins, B. J., A Phase II Trial of the Cyclin-dependent Kinase Inhibitor Flavopiridol in Patients with PReviously Untreated Stage IV Non-Small Cell Lung Cancer. *Clin Cancer Res* **2001,** *7*, 1590-1599; (c) Aklilu, M.; Kindler, H. L.; Donehower, R. C.; Mani, S.; Vokes, E. E., Phase II study of flavopiridol in patients with advanced colorectal cancer. *Annals of Oncology* **2003,** *14*, 1270-1273; (d) Burdette-Radoux, S.; Tozer, R. G.; Lohmann, R. C.; Quirt, I.; Ernst, D. S.; Walsh, W.; Wainman, N.; Colevas, A. D.; Eisenhauer, E. A., Phase II trial of flavopiridol, a cyclin-dependent kinase inhibitor, in untreated metastatic malignant melanoma. *Investigational New Drugs* **2004,** *22*, 315-322; (e) Liu, G.; Gandara, D. R.; Lara, P. N. J.; Raghavvan, D.; Doroshow, J. H.; Twardowski, P.; Kantoff, P.; Oh, W.; Kim, K.; Wilding, G., A Phase II Trial of Flavopiridol (NSC #649890) in Patients with Previously Untreated Metastatic Androgen-Independent Prostate Cancer. *Clin Cancer Res* **2004,** *10*, 924-928; (f) Morris, D. G.; Bramwell, V. H. C.; Turcotte, R.; Figueredo, A. T.; Blackstein, M. E.; Verma, n.; Matthews, S.; Eisenhauer, E. A., A Phase II Study of Flavopiridol in Patients With

Previously Untreated Advanced Soft Tissue Sarcoma. *Sarcome* **2006,** *2006*, 1-7.

30.   (a) Grendys, E. C.; Blessing, J. A.; Burger, R.; Hoffman, J., A phase II evaluation of flavopiridol as second-line chemotherapy of endemetrial carcinoma: A Gynecologic Oncology Group Study. *Gynecologic Oncology* **2005,** *98*, 249-253; (b) Veldhuizen, P. J. V.; Faulkner, J. R.; Lara, P. N. J.; Gumerlock, P. H.; Goodwin, J. W.; Dakhil, S. R.; Gross, H. M.; Flanigan, R. C.; Crawford, E. D., A phase II study of flavopiridol in patients with advanced renal cell carcinoma: results of Southwest Oncology Group Trial 0109. *Cancer Chemother Pharmacol* **2005,** *56*, 39-45.

31.   Fekrazad, H. M.; Verschraegen, C. F.; Royce, M.; Smith, H. O.; Chyi Lee, F.; Rabinowitz, I., A phase I study of flavopiridol in combination with gemcitabine and irinotecan in patients with metastatic cancer. *Am J Clin Oncol* **2010,** *33* (4), 393-7.

32.   Seamon, J. A.; Rugg, C. A.; Emanuel, S.; Calcogno, A. M.; Ambudkar, S. V.; Middleton, S. A.; Butler, J.; Borowski, V.; Greenberger, L. M., Role of the ABCG2 drug transporter in the resistance and oral bioavailability of a potent cyclin-dependent kinase/Aurora kinase inhibitor. *Mol Cancer Ther* **2006,** *5*, 2459-2467.

33.   Emanuel, S.; Rugg, C. A.; Gruninger, R. H.; Lin, R.; Fuentes-Pesquera, A.; Connolly, P. J.; Wetter, S. K.; Hollister, B.; Kruger, W. W.; Napier, C.; Jolliffe, L.; Middleton, S. A., The *In vitro* and *In vivo* Effects of JNJ-7706621: A Dual Inhibitor of Cyclin-Dependent Kinases and Aurora Kinases. *Cancer Res* **2005,** *65*, 9038-9046.

34.   Danhier, F.; Ucakar, B.; Magotteaux, N.; Brewster, M. E.; Preat, V., Active and passive tumor targeting of a novel poorly soluble cyclin dependent kinase inhibitor JNJ-7706621. *International Journal of Pharmaceutics* **2010,** *392*, 20-28.

35.   McInnes, C., Progress in the Development of Non-ATP-Competitive Protein Kinase Inhibitors for Oncology. *Annual Reports in Medicinal Chemistry* **2012,** *47*, 459-474.

36.   Castanedo, G.; Clark, K.; Wang, S.; Tsui, V.; Wong, M.; Nicholas, J.; Wickramasinghe, D.; Marsters, J. C., Jr.; Sutherlin, D., CDK2/cyclinA inhibitors: targeting the cyclinA recruitment site with small molecules derived from peptide leads. *Bioorg Med Chem Lett* **2006,** *16* (6), 1716-20.

37.   (a) Kennedy, K. J.; Lundquist, J. T., IV; Simandan, T. L.; Kokko, K. P.; Beeson, C. C.; Dix, T. A., Design rationale, synthesis, and characterization of non-natural analogs of the cationic amino acids arginine and lysine. *J. Peptide Res.* **2000,** *55*, 348-358; (b) Kokko, K. P.; Arrigoni, C. E.; Dix, T. A., Selectivity Enhancement Induced by

Substitution of Non-natural Analogues of Arginine and Lysine in Arginine-Based Thrombin Inhibitors. *Bioorg Med Chem Lett* **2001,** *11*, 1947-1950; (c) Rafi, S. B.; Hearn, B. R.; Vedantham, P.; Jacobson, M. P.; Renslo, A. R., Predictin and Improving the Membrane Permeability of Peptidic Small Molecules. *J. Med. Chem.* **2012,** *55*, 3163-3169; (d) Dix, T. A. Non-Natural Amino Acids. 2006; (e) Gfeller, D.; Michielin, O.; Zoete, V., Expanding Molecular Modeling and Design Tools to Non-Natural Sidechains. *Journal of Computational Chemistry* **2012,** *33*, 1525-1535.

38.   Liu, S.; Bolger, J. K.; Kirkland, L. O.; Premnath, P. N.; McInnes, C., Structural and Functional Analysis of Cyclin D1 Reveals p27 and Substrate Inhibitor Binding Requirements. *ACS Chemical Biology* **2010,** *5* (12), 1169-1182.

39.   Invitrogen, Technical Resource Guide: Fluorescence Polarization. 4th ed.; 2006.

40.   Camacho;   Domling;   Pittsburgh,   U.   o.   AnchorQuery. http://anchorquery.ccbb.pitt.edu/.

41.   Domling, A.; Ugi, I., Multicomponent Reactions with Isocyanides. *Angew. Chem. Int. Ed.* **2000,** *39*, 3168-3210.

42.   aapptec 2-Chlorotrityl Resin (CTC Resin). http://www.2-chlorotritylresins.com/.

43.   Grabstein, K. H.; Wang, A.; Nairn, N. W.; Graddis, T. J. Amino Acid Substituted Molecules. 2009.

44.   Dix, T. A. Positively Charged Non-Natural Amino Acids, Methods of Making and Using Thereof in Peptides. 2002.

45.   Tirrell, D. A.; Tang, Y. Method for Stabilization of Proteins Using Non-Natural Amino Acids. 2004.

46.   Gawanda, M. B.; Branco, P. S., An efficient and expedious Fmoc protection of amines and amino acids in aqueous media. *Green Chemistry* **2011,** *13*, 3355-9.

47.   Stathopoulos, P.; Papas, S.; Tsikaris, V., C-terminal N-alkylated peptide amides resulting from the linker decomposition of the Rink amid resin. A new cleavage mixture prevents their formation. *J. Peptide Sci.* **2006,** *12*, 227-232.

48.   Orzaez, M.; Gortat, A.; Mondragon, L.; Bachs, O.; Perez-Paya, E., ATP-noncompetitive inhibitors of CDK-cyclin complexes. *ChemMedChem* **2009,** *4* (1), 19-24.

49.   Canela, N.; Orzaez, M.; Fucho, R.; Mateo, F.; Gutierrez, R.; Pineda-Lucena, A.; Bachs, O.; Perez-Paya, E., Identification of an hexapeptide that binds to a surface pocket in cyclin A and inhibits the catalytic activity of the complex cyclin-dependent kinase 2-cyclin A. *J Biol Chem* **2006,** *281* (47), 35942-53.

50.   Mendoza, N.; Fong, S.; Marsters, J.; Koeppen, H.; Schwall, R.; Wickramasignhe, D., Selective Cyclin-dependent Kinase 2/Cyclin A Antagonists that Differ from ATP Site Inhibitors Block Tumor Growth. *Cancer Res* **2003,** *63*, 1020-1024.

ANCHORQUERY™ IDENTIFIED CCAP CHARACTERIZATION

SCCP 6000
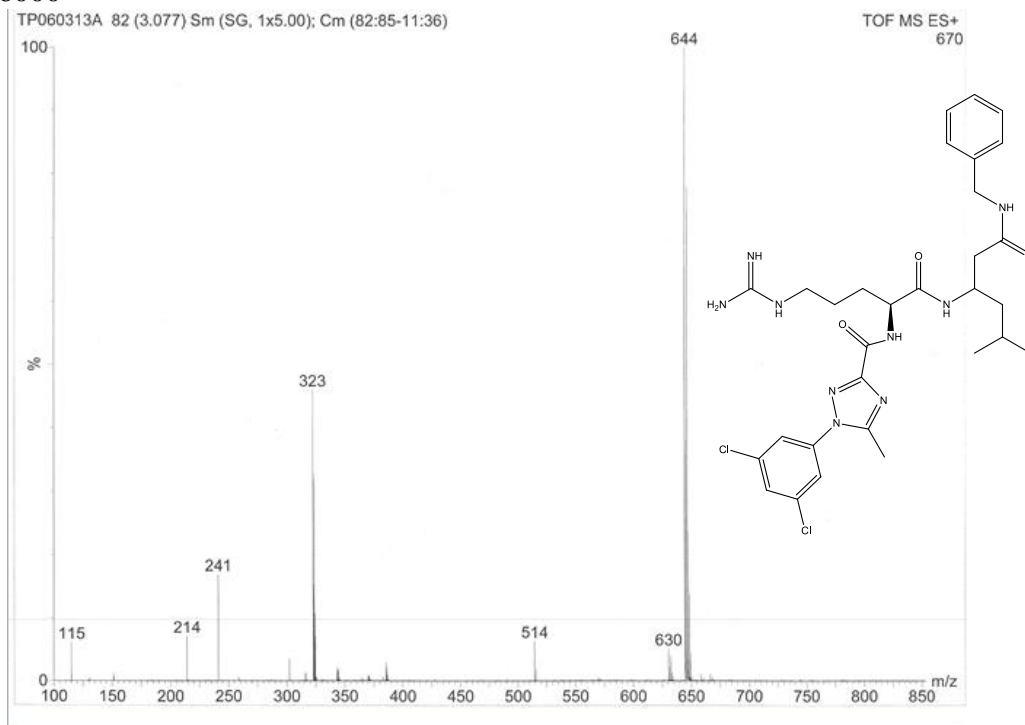
A1. MS results for N-((2S)-1-((1-(benzylamino)-5-methyl-1-oxohexan-3-yl)amino)-5-guanidino-1-oxopentan-2-yl)-1-(3,5-dichlorophenyl)-5-methyl-1H-1,2,4-triazole-3-carboxamide (SCCP 6000). MS(ES): m/z: 644 [M+H]$^+$ (100%)
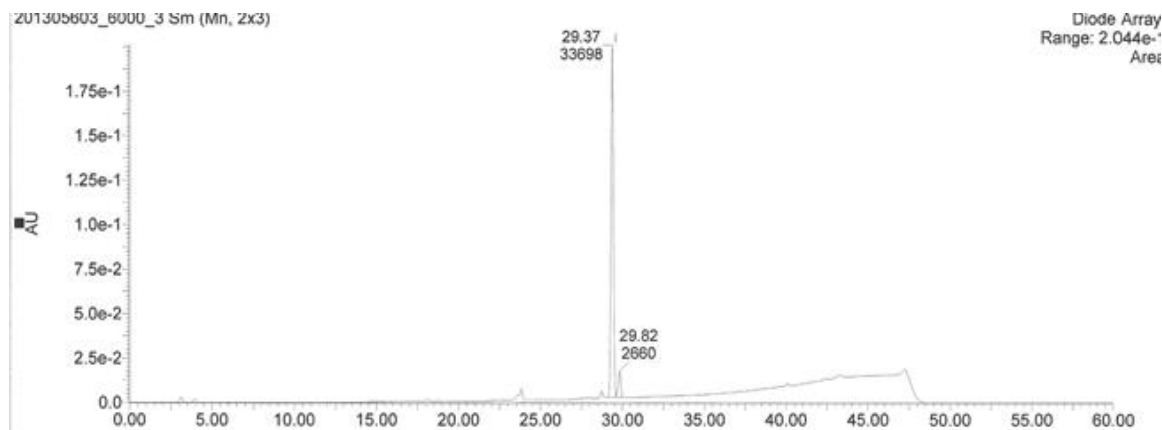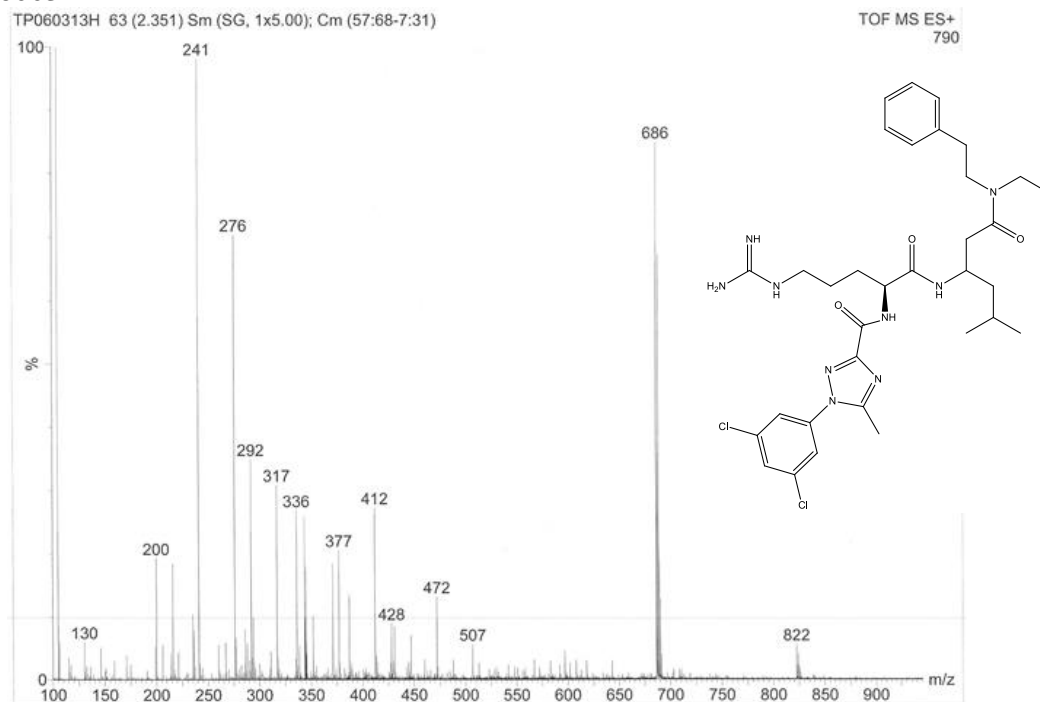

A2. HPLC trace of N-((2S)-1-((1-(benzylamino)-5-methyl-1-oxohexan-3-yl)amino)-5-guanidino-1-oxopentan-2-yl)-1-(3,5-dichlorophenyl)-5-methyl-1H-1,2,4-triazole-3-carboxamide (SCCP 6000).

SCCP 6001
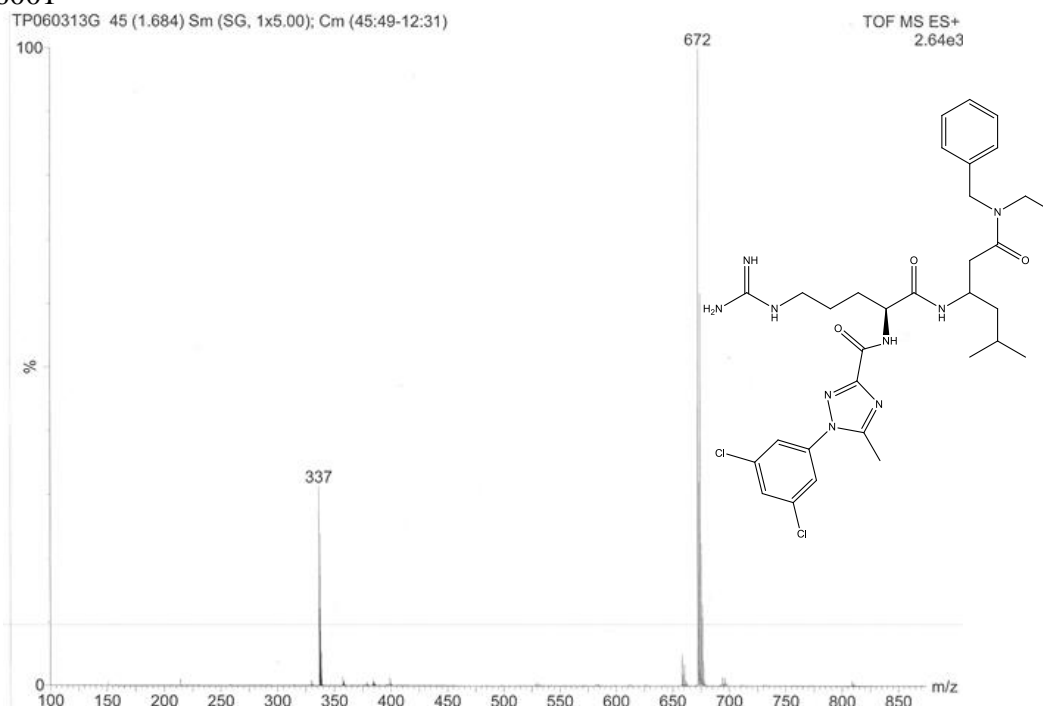
A3. MS results for N-((2S)-1-((1-(benzyl(ethyl)amino)-5-methyl-1-oxohexan-3-yl)amino)-5-guanidino-1-oxopentan-2-yl)-1-(3,5-dichlorophenyl)-5-methyl-1H-1,2,4-triazole-3-carboxamide (SCCP 6001). MS(ES): m/z: 672 [M+H]$^+$ (100%)
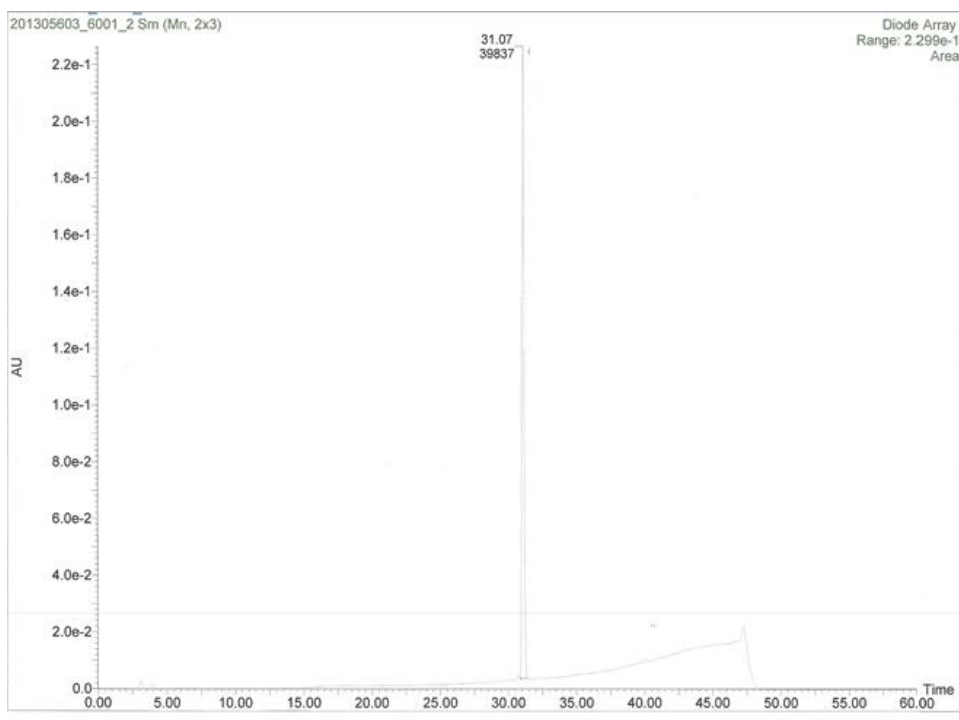
A4. HPLC results for N-((2S)-1-((1-(benzyl(ethyl)amino)-5-methyl-1-oxohexan-3-yl)amino)-5-guanidino-1-oxopentan-2-yl)-1-(3,5-dichlorophenyl)-5-methyl-1H-1,2,4-triazole-3-carboxamide (SCCP 6001).

SCCP 6002
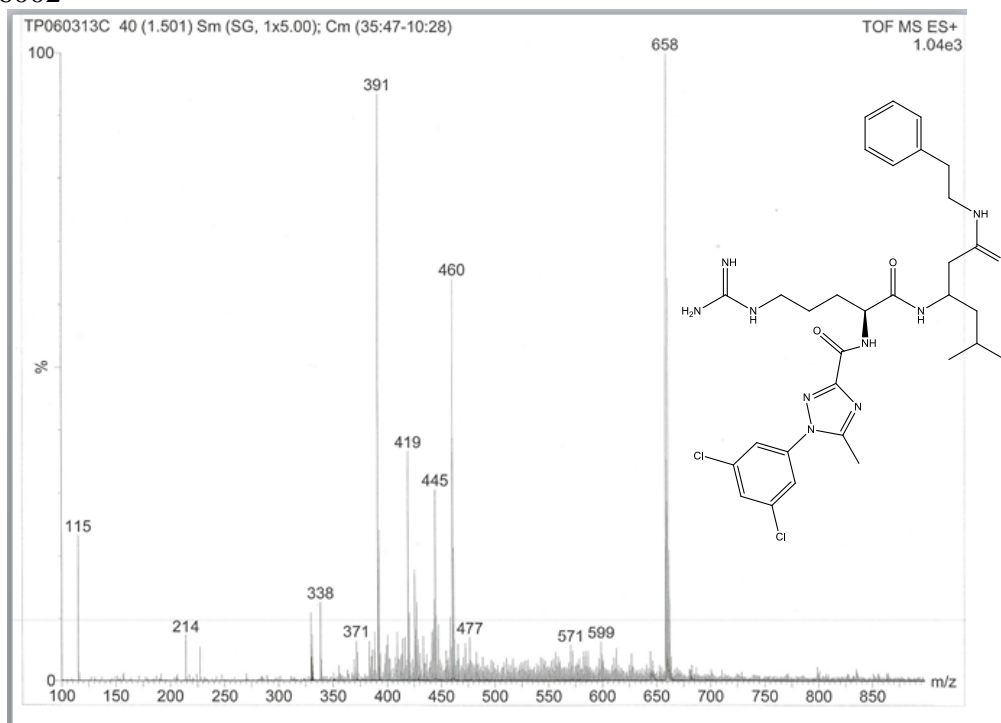
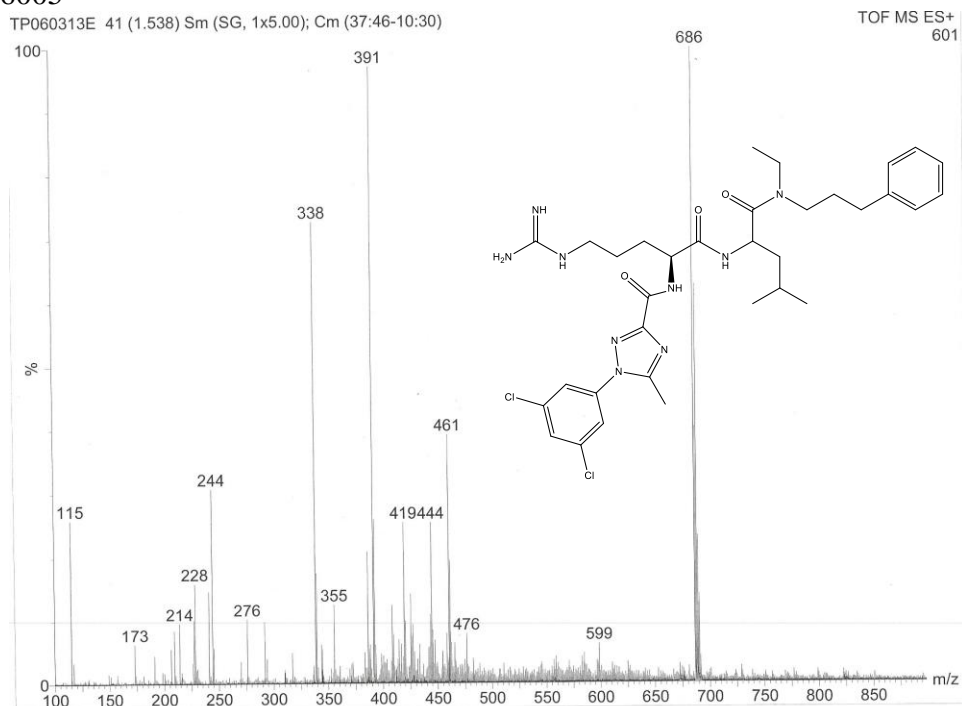**A5.** MS results for 1-(3,5-dichlorophenyl)-N-((2S)-5-guanidino-1-((5-methyl-1-oxo-1-(phenethylamino)hexan-3-yl)amino)-1-oxopentan-2-yl)-5-methyl-1H-1,2,4-triazole-3-carboxamide (SCCP 6002). MS(ES): m/z: 658 [M+H]$^+$ (100%)
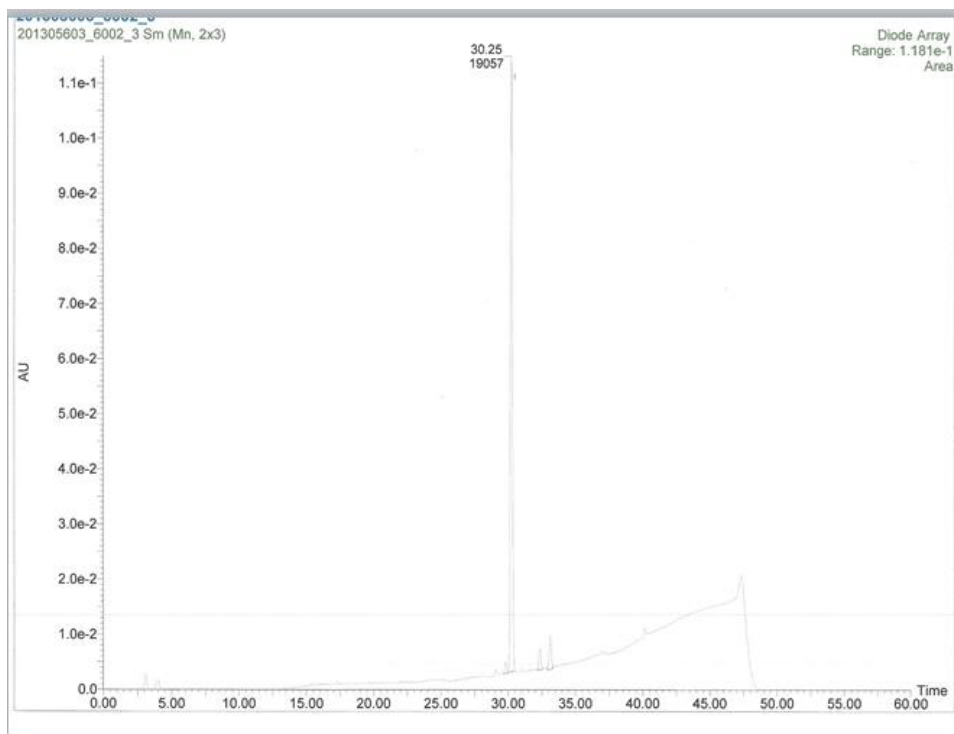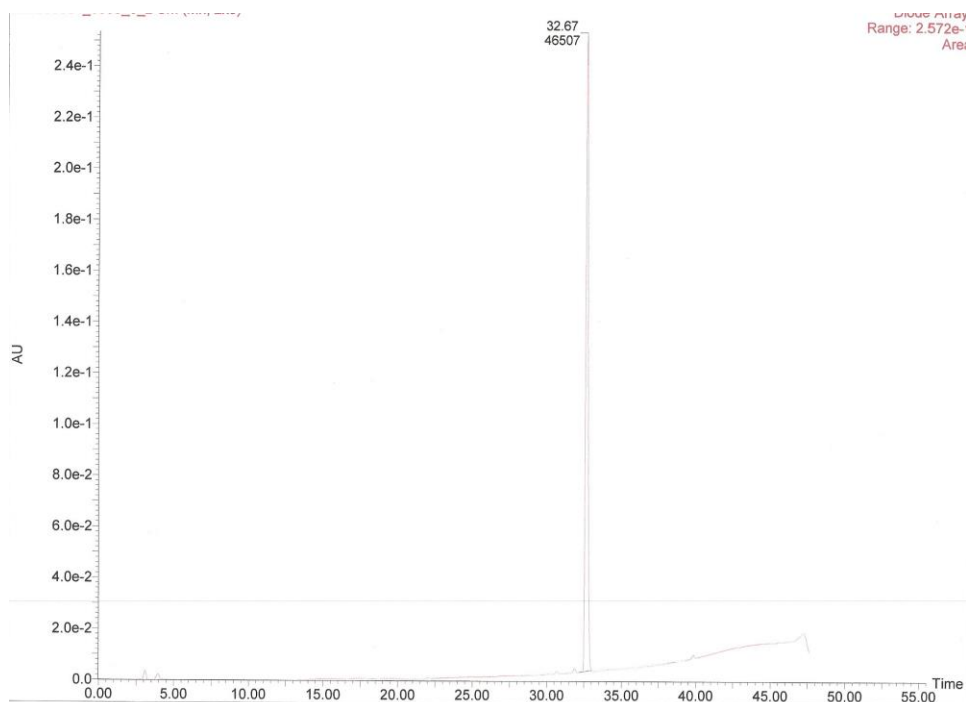

A6. HPLC results for 1-(3,5-dichlorophenyl)-N-((2S)-5-guanidino-1-((5-methyl-1-oxo-1-(phenethylamino)hexan-3-yl)amino)-1-oxopentan-2-yl)-5-methyl-1H-1,2,4-triazole-3-carboxamide (SCCP 6002). MS(ES):

SCCP 6003

TP060313H 63 (2.351) Sm (SG, 1x5.00); Cm (57:68-7:31)   TOF MS ES+
                                                                                                     790

A7. MS results for 1-(3,5-dichlorophenyl)-N-((2S)-1-((1-(ethyl(phenethyl)amino)-5-methyl-1-oxohexan-3-yl)amino)-5-guanidino-1-oxopentan-2-yl)-5-methyl-1H-1,2,4-triazole-3-carboxamide   (SCCP   6003).
MS(ES): m/z: 686 [M+H]$^+$ (100%)

201305604_6003_2_2 Sm (Mn, 2x3)   Diode Array
                                                                                         Range: 6.752e-2
                                                                                                     Area
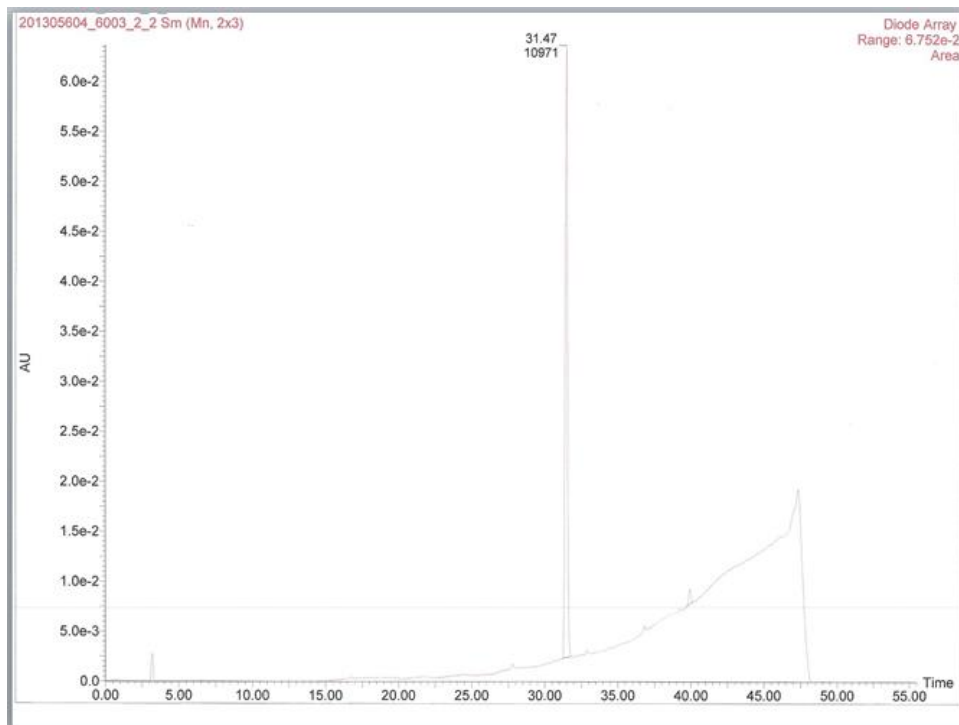
A8.   HPLC   results   for   1-(3,5-dichlorophenyl)-N-((2S)-1-((1-(ethyl(phenethyl)amino)-5-methyl-1-oxohexan-3-yl)amino)-5-guanidino-1-oxopentan-2-yl)-5-methyl-1H-1,2,4-triazole-3-carboxamide   (SCCP 6003).

SCCP 6004
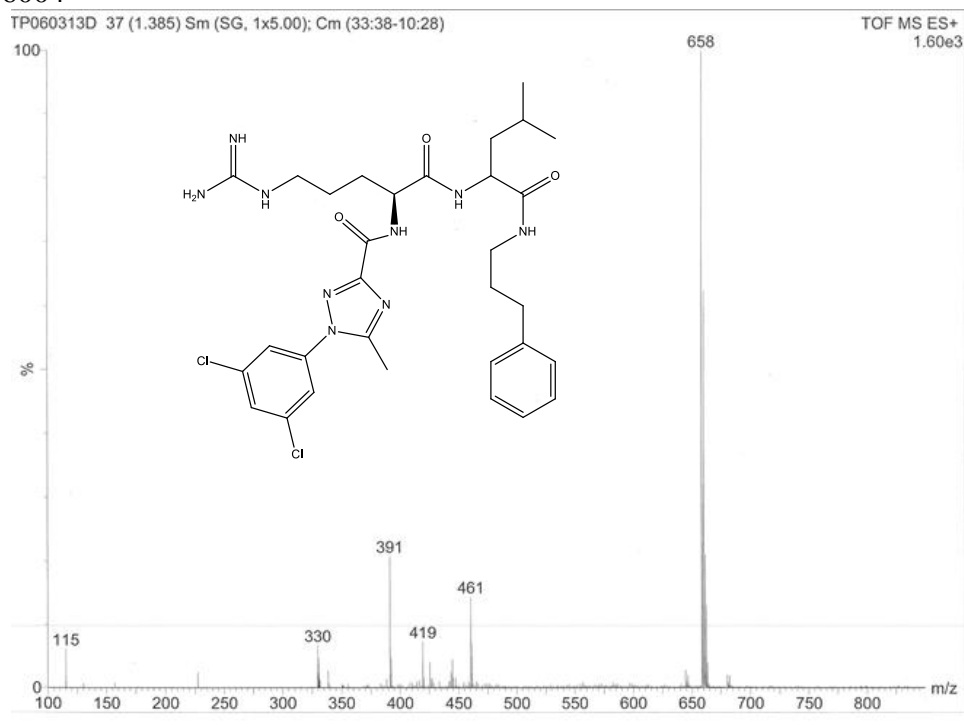
A9. MS results for 1-(3,5-dichlorophenyl)-N-((2S)-5-guanidino-1-((4-methyl-1-oxo-1-((3-phenylpropyl)amino)pentan-2-yl)amino)-1-oxopentan-2-yl)-5-methyl-1H-1,2,4-triazole-3-carboxamide (SCCP 6004). MS(ES): m/z: 658 [M+H]$^+$ (100%)
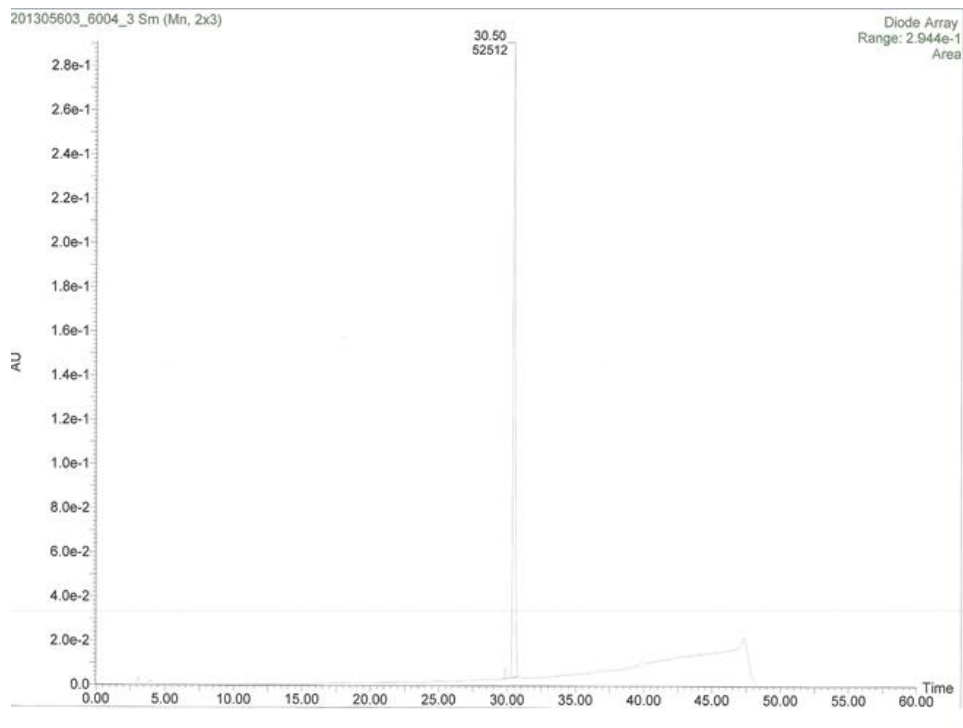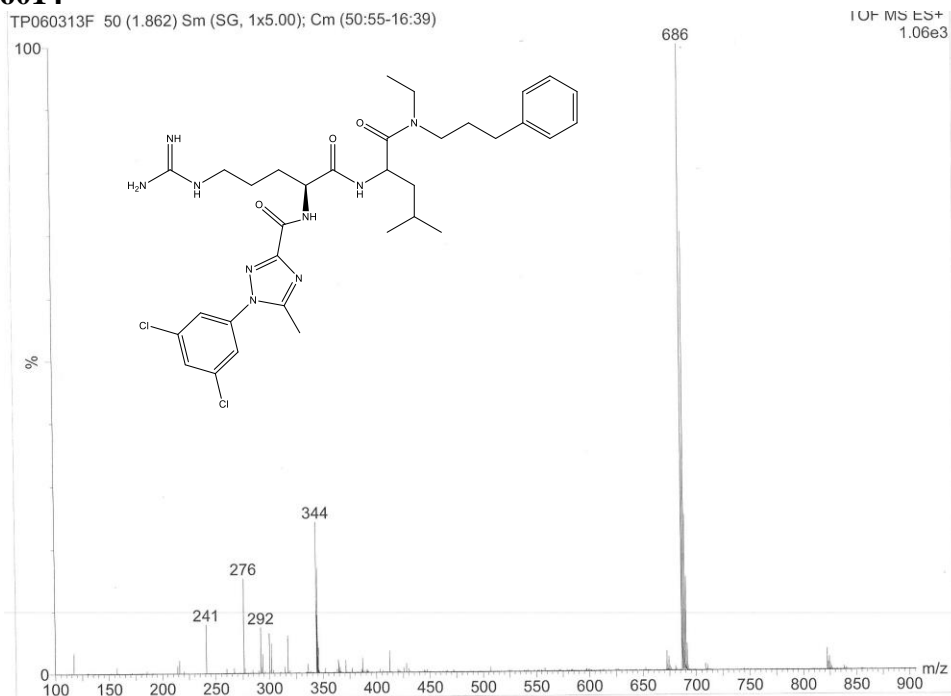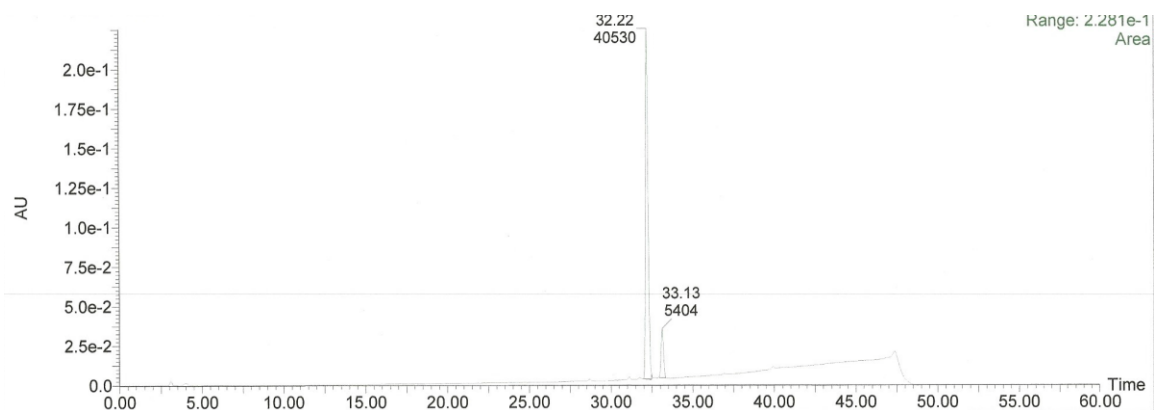

A10. HPLC results for 1-(3,5-dichlorophenyl)-N-((2S)-5-guanidino-1-((4-methyl-1-oxo-1-((3-phenylpropyl)amino)pentan-2-yl)amino)-1-oxopentan-2-yl)-5-methyl-1H-1,2,4-triazole-3-carboxamide (SCCP 6004).

84

A11. MS results for 1-(3,5-dichlorophenyl)-N-((2S)-1-((1-(ethyl(3-phenylpropyl)amino)-4-methyl-1-oxopentan-2-yl)amino)-5-guanidino-1-oxopentan-2-yl)-5-methyl-1H-1,2,4-triazole-3-carboxamide (SCCP 6005). MS(ES): m/z: 686 [M+H]$^+$ (100%)
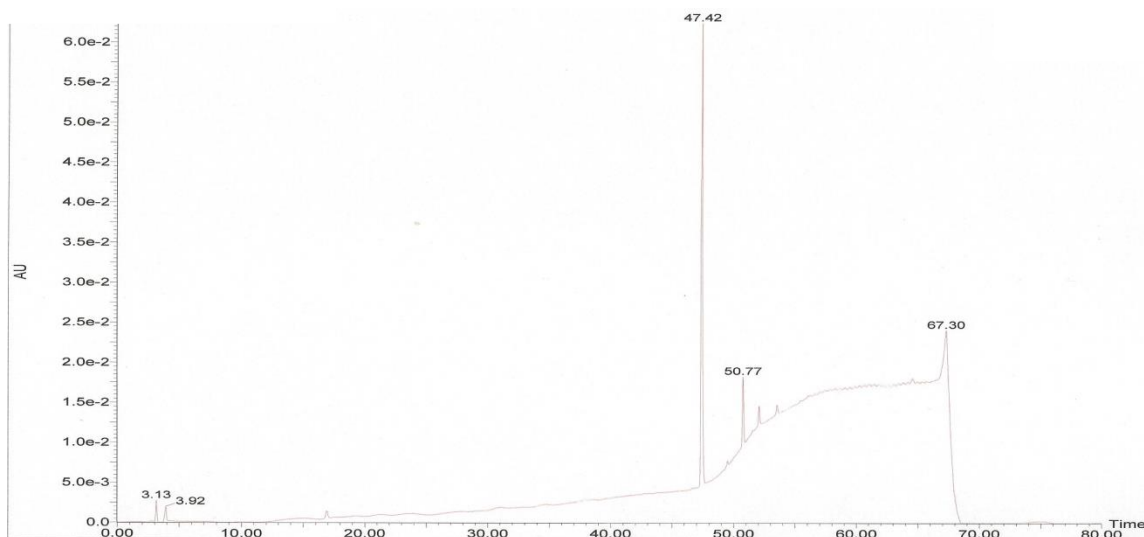

A12. HPLC results for 1 1-(3,5-dichlorophenyl)-N-((2S)-1-((1-(ethyl(3-phenylpropyl)amino)-4-methyl-1-oxopentan-2-yl)amino)-5-guanidino-1-oxopentan-2-yl)-5-methyl-1H-1,2,4-triazole-3-carboxamide (SCCP 6005).

SCCP 6014

A13. MS results for 1-(3,5-dichlorophenyl)-N-((2S)-1-((1-(ethyl(3-phenylpropyl)amino)-4-methyl-1-oxopentan-2-yl)amino)-5-guanidino-1-oxopentan-2-yl)-5-methyl-1H-1,2,4-triazole-3-carboxamide (SCCP 6014). MS(ES): m/z: 686 [M+H]$^+$ (100%)

A14. HPLC results for 1 1-(3,5-dichlorophenyl)-N-((2S)-1-((1-(ethyl(3-phenylpropyl)amino)-4-methyl-1-oxopentan-2-yl)amino)-5-guanidino-1-oxopentan-2-yl)-5-methyl-1H-1,2,4-triazole-3-carboxamide (SCCP 6014).

A Table 1.

SCCP	Purity	Column Dimensions	Method	Flow Rate	HPLC RT	Theoretical MW
6000	>92.7%	4.6 × 250 mm	5-95% acetonitrile/water/ 0.1%TFA	1ml/min	29.37	644.60
6001	>98.0%	4.6 × 250 mm	5-95% acetonitrile/water/ 0.1%TFA	1ml/min	31.07	672.65
6002	>90.0%	4.6 × 250 mm	5-95% acetonitrile/water/ 0.1%TFA	1ml/min	30.25	658.62
6003	>98.0%	4.6 × 250 mm	5-95% acetonitrile/water/ 0.1%TFA	1ml/min	31.47	686.67
6004	>95.0%	4.6 × 250 mm	5-95% acetonitrile/water/ 0.1%TFA	1ml/min	30.50	658.62
6005		4.6 × 250 mm	5-95% acetonitrile/water/ 0.1%TFA	1ml/min		
6014		4.6 × 250 mm	5-95% acetonitrile/water/ 0.1%TFA	1ml/min		

LEU6/PHE8 MIMETIC CHARACTERIZATION

SCCP 5977 and 5978

B1. HPLC trace of 1-(3,5-dichlorophenyl)-N-((2S)-5-guanidino-1-((1-(2-isobutoxyphenyl)-3-methylbutyl)amino)-1-oxopentan-2-yl)-5-methyl-1H-1,2,4-triazole-3-carboxamide (SCCP 5977 and 5978).
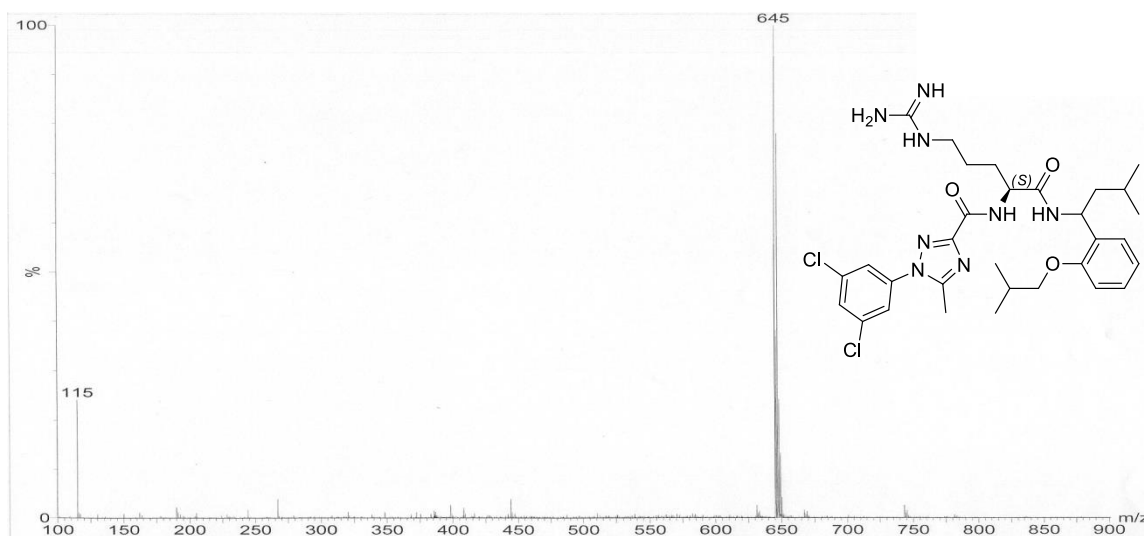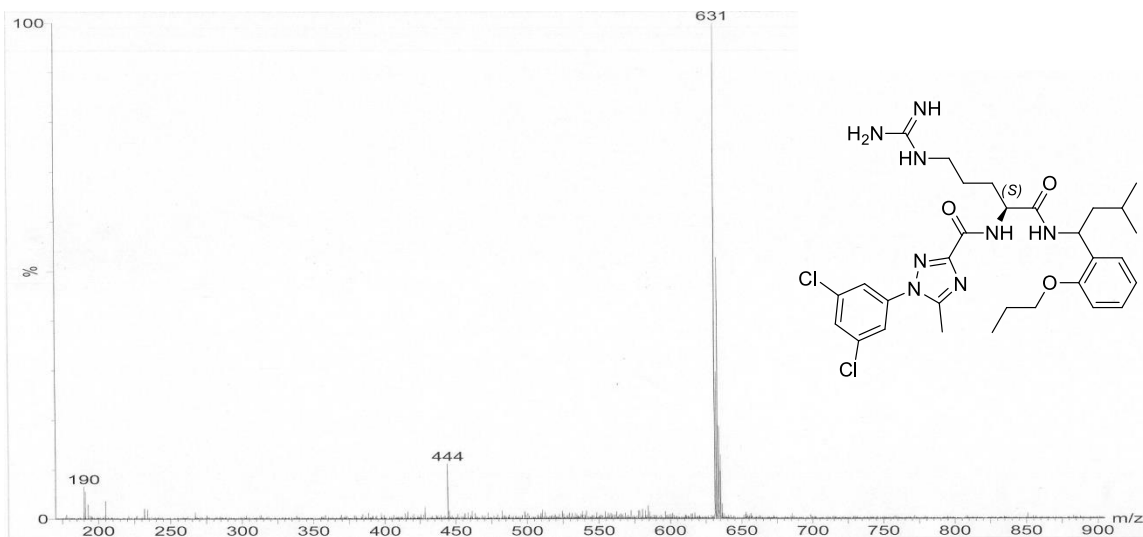

B2. MS results for 1-(3,5-dichlorophenyl)-N-((2S)-5-guanidino-1-((1-(2-isobutoxyphenyl)-3-methylbutyl)amino)-1-oxopentan-2-yl)-5-methyl-1H-1,2,4-triazole-3-carboxamide (SCCP 5977 and 5978). MS(ES): m/z: 645 [M+H]$^+$ (100%)
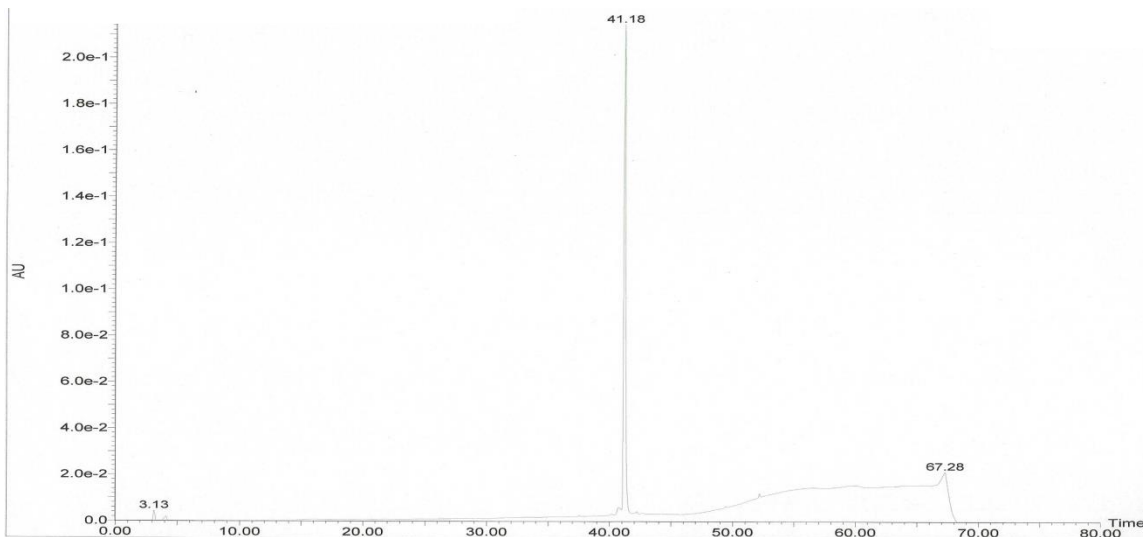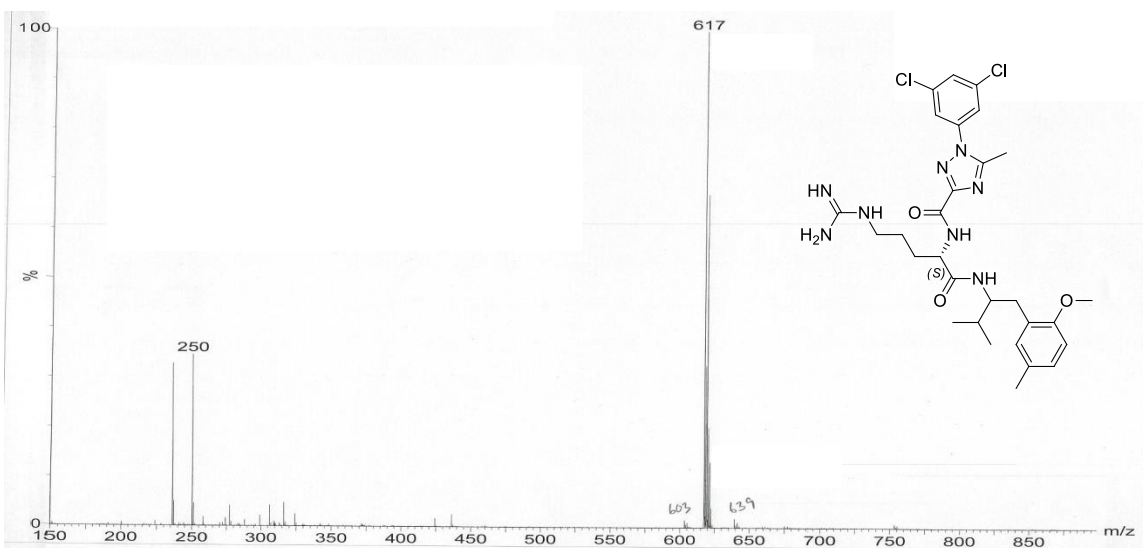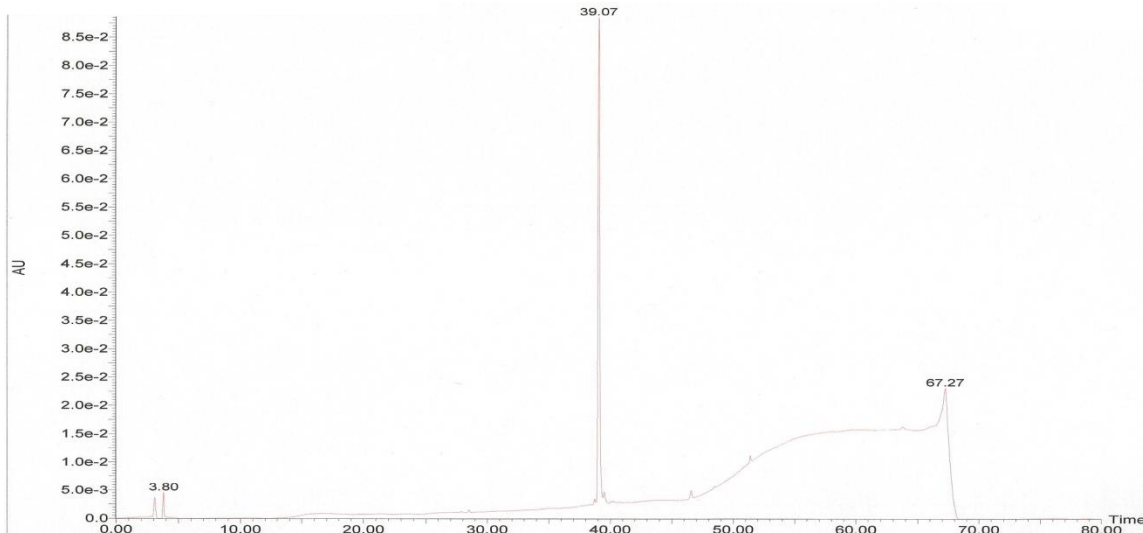
SCCP 5979 and 5980
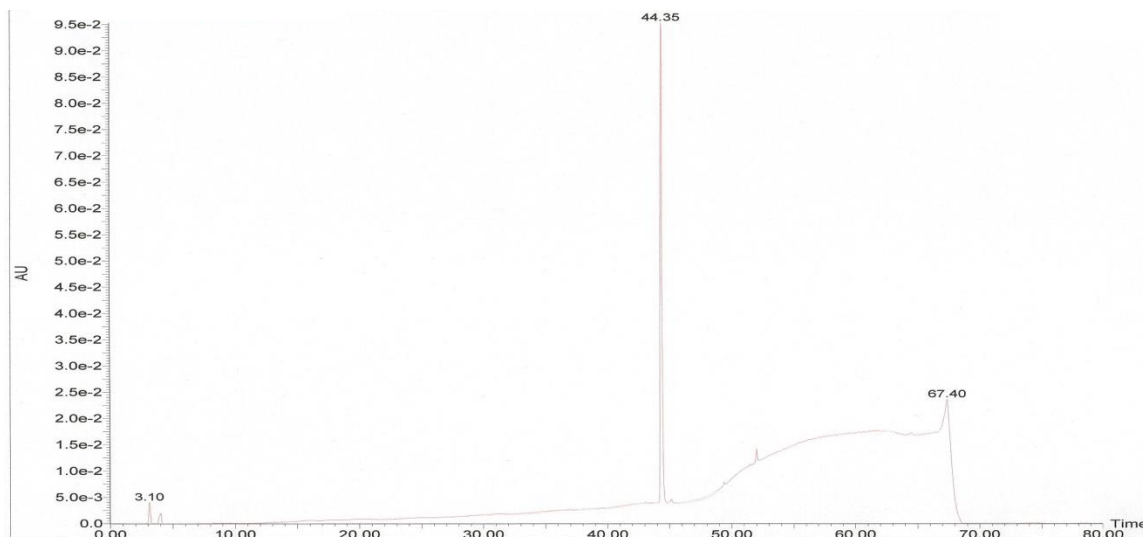
B3. HPLC trace of 1-(3,5-dichlorophenyl)-N-((2S)-5-guanidino-1-((3-methyl-1-(2-propoxyphenyl)butyl)amino)-1-oxopentan-2-yl)-5-methyl-1H-1,2,4-triazole-3-carboxamide (SCCP 5979 and 5980).

B4. MS results for 1-(3,5-dichlorophenyl)-N-((2S)-5-guanidino-1-((3-methyl-1-(2-propoxyphenyl)butyl)amino)-1-oxopentan-2-yl)-5-methyl-1H-1,2,4-triazole-3-carboxamide (SCCP 5979 and 5980). MS(ES): m/z: 631 [M+H]$^+$ (100%)

SCCP 5981

B5. HPLC trace of 1-(3,5-dichlorophenyl)-N-((2S)-5-guanidino-1-((1-(2-methoxy-5-methylphenyl)-3-methylbutan-2-yl)amino)-1-oxopentan-2-yl)-5-methyl-1H-1,2,4-triazole-3-carboxamide (SCCP 5981).
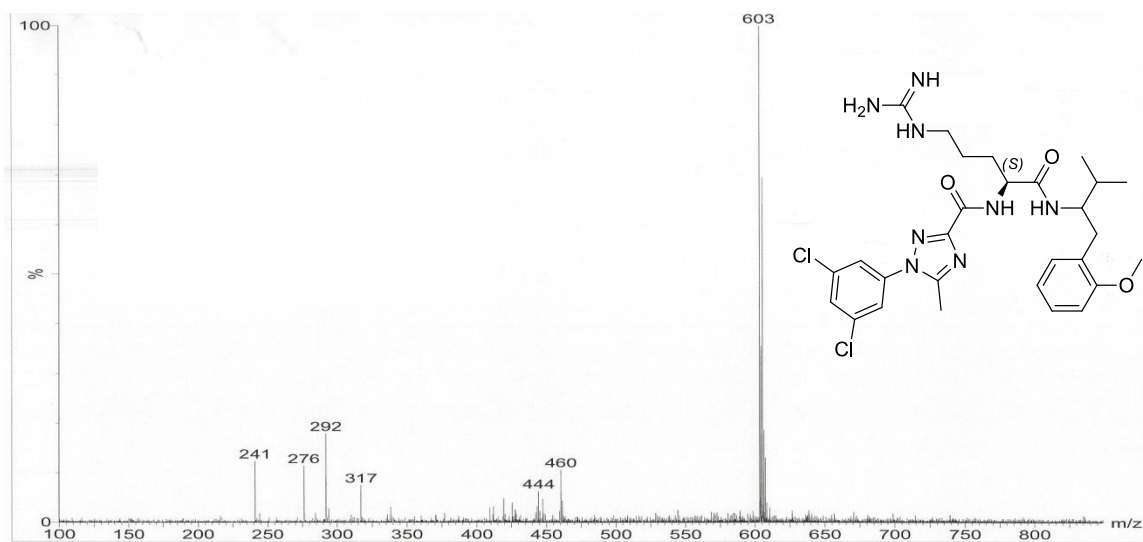

B6. MS results for 1-(3,5-dichlorophenyl)-N-((2S)-5-guanidino-1-((1-(2-methoxy-5-methylphenyl)-3-methylbutan-2-yl)amino)-1-oxopentan-2-yl)-5-methyl-1H-1,2,4-triazole-3-carboxamide (SCCP 5981).
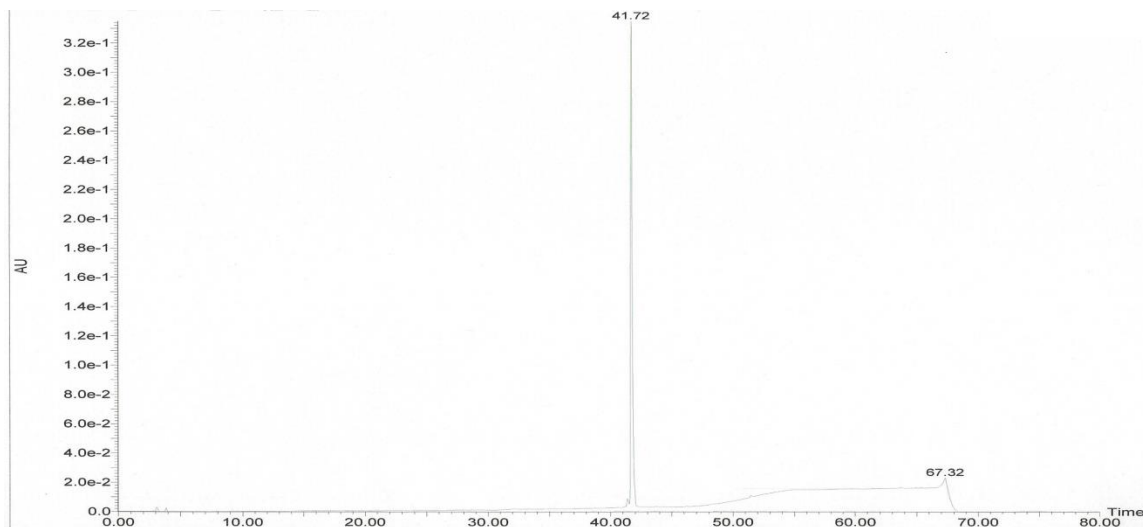MS(ES): m/z: 617 [M+H]$^+$ (100%)

SCCP 5982

B7. HPLC trace of 1-(3,5-dichlorophenyl)-N-((2S)-5-guanidino-1-((1-(2-methoxyphenyl)-3-methylbutan-2-yl)amino)-1-oxopentan-2-yl)-5-methyl-1H-1,2,4-triazole-3-carboxamide (SCCP 5982).
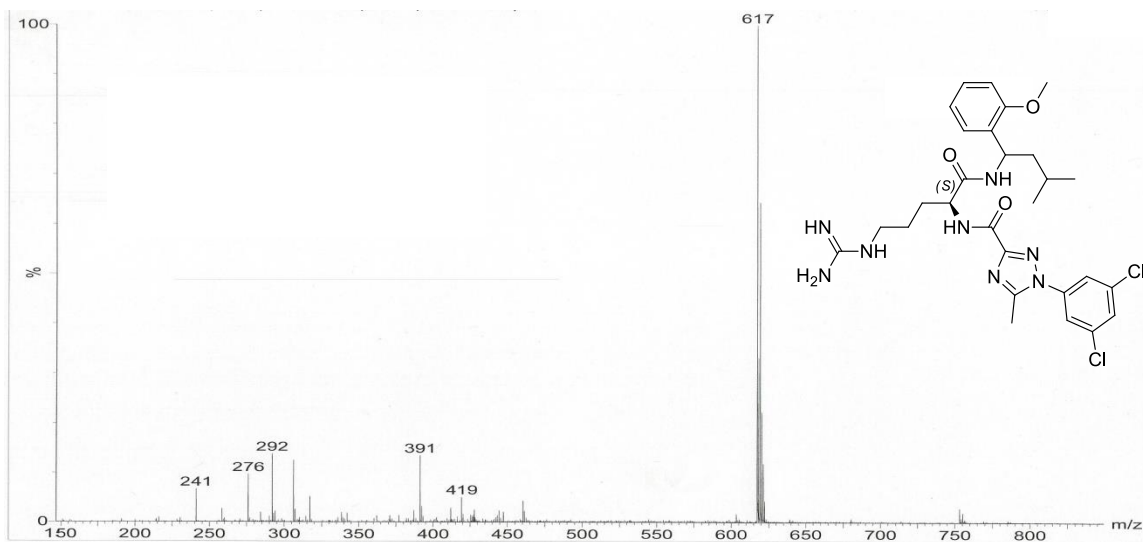

B8. MS results for 1-(3,5-dichlorophenyl)-N-((2S)-5-guanidino-1-((1-(2-methoxyphenyl)-3-methylbutan-2-yl)amino)-1-oxopentan-2-yl)-5-methyl-1H-1,2,4-triazole-3-carboxamide (SCCP 5982). MS(ES): m/z: 603 [M+H]$^+$ (100%)
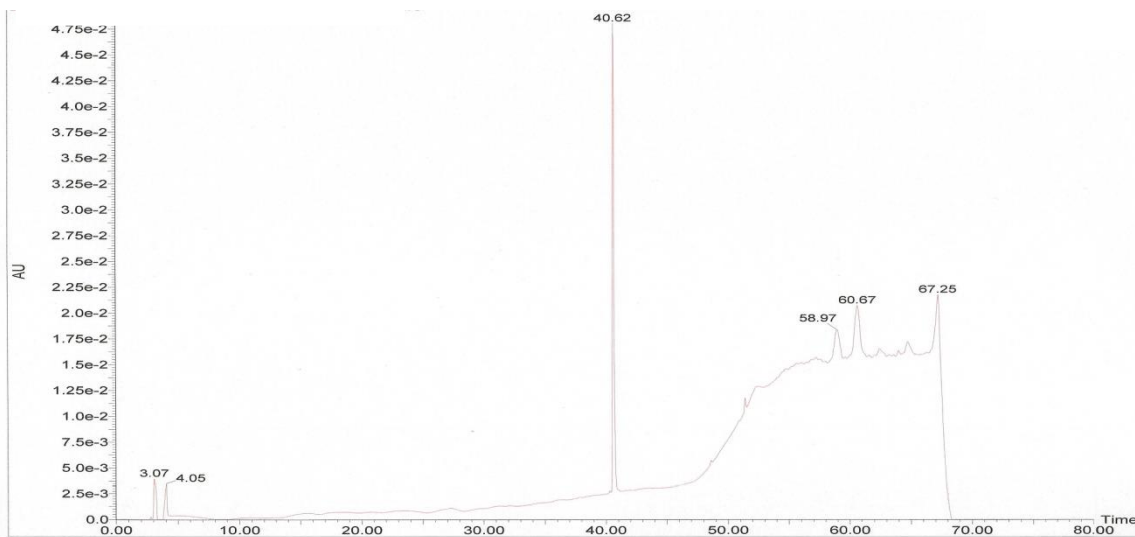
SCCP 5983 and 5984

B9. HPLC trace of 1-(3,5-dichlorophenyl)-N-((2S)-1-((1-(2-ethoxyphenyl)-3-methylbutyl)amino)-5-guanidino-1-oxopentan-2-yl)-5-methyl-1H-1,2,4-triazole-3-carboxamide (SCCP 5983 and 5984).

B10. MS results for 1-(3,5-dichlorophenyl)-N-((2S)-1-((1-(2-ethoxyphenyl)-3-methylbutyl)amino)-5-guanidino-1-oxopentan-2-yl)-5-methyl-1H-1,2,4-triazole-3-carboxamide (SCCP 5983 and 5984). MS(ES): m/z: 617 [M+H]$^+$ (100%)
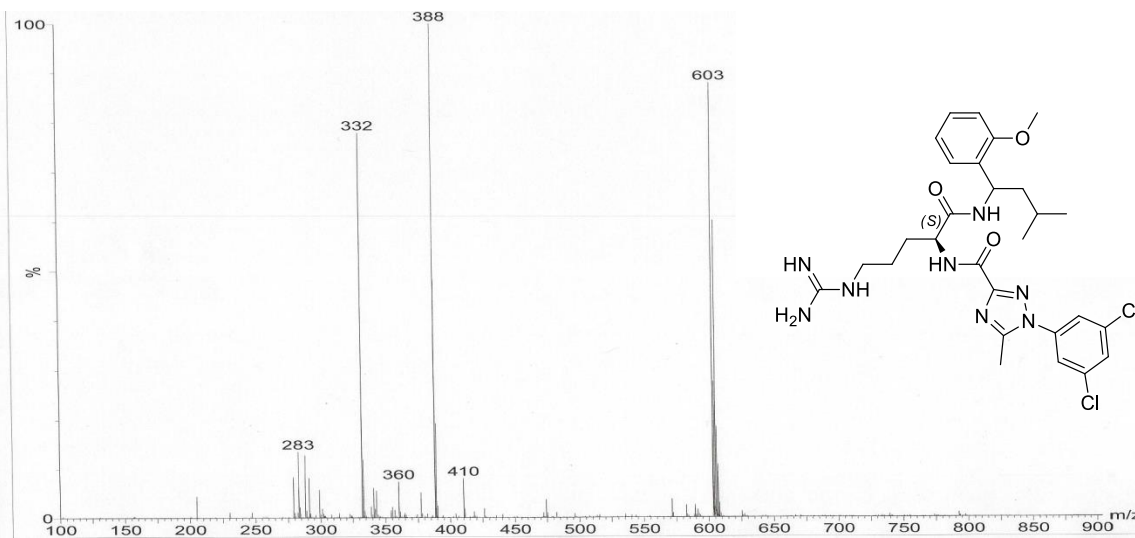
SCCP 5985

B11. HPLC trace of 1-(3,5-dichlorophenyl)-N-((2S)-5-guanidino-1-((1-(2-methoxyphenyl)-3-methylbutyl)amino)-1-oxopentan-2-yl)-5-methyl-1H-1,2,4-triazole-3-carboxamide (SCCP 5985).

B12. MS results for 1-(3,5-dichlorophenyl)-N-((2S)-5-guanidino-1-((1-(2-methoxyphenyl)-3-methylbutyl)amino)-1-oxopentan-2-yl)-5-methyl-1H-1,2,4-triazole-3-carboxamide (SCCP 5985). MS(ES): m/z: 603 [M+H]$^+$ (90%)

B TABLE 1.

SCCP	Purity	Column Dimensions	Method	Flow Rate	HPLC RT	Theoretical MW
5977	>79.20	4.6 × 250 mm	5-95% acetonitrile/water/ 0.1%TFA	1ml/min	46.63	645.62
5978	>83.50	4.6 × 250 mm	5-95% acetonitrile/water/ 0.1%TFA	1ml/min	47.42	645.62
5979	>97.70	4.6 × 250 mm	5-95% acetonitrile/water/ 0.1%TFA	1ml/min	44.35	631.60
5980	>96.00	4.6 × 250 mm	5-95% acetonitrile/water/ 0.1%TFA	1ml/min	45.42	631.60
5981	>98.00	4.6 × 250 mm	5-95% acetonitrile/water/ 0.1%TFA	1ml/min	41.18	617.57
5982	>98.00	4.6 × 250 mm	5-95% acetonitrile/water/ 0.1%TFA	1ml/min	39.07	603.54
5983	>82.90	4.6 × 250 mm	5-95% acetonitrile/water/ 0.1%TFA	1ml/min	41.82	617.57
5984	>98.00	4.6 × 250 mm	5-95% acetonitrile/water/ 0.1%TFA	1ml/min	41.72	617.57
5985	>82.60	4.6 × 250 mm	5-95% acetonitrile/water/ 0.1%TFA	1ml/min	40.62	603.54
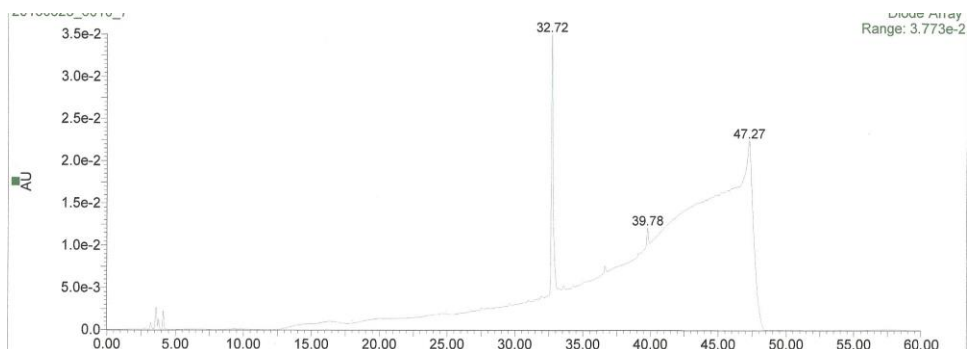
C1. HPLC trace of N-((2S)-1-((1-(((S)-1-amino-1-oxo-3-phenylpropan-2-yl)(methyl)amino)-5-methyl-1-oxohexan-3-yl)amino)-5-((1-(1-(3,5-dichlorophenyl)-5-methyl-1H-1,2,4-triazole-3-carbonyl)-1,4,5,6-tetrahydropyrimidin-2-yl)amino)-1-oxopentan-2-yl)-1-(3,5-dichlorophenyl)-5-methyl-1H-1,2,4-triazole-3-carboxamide.

Proposed Structure of Isolated Product
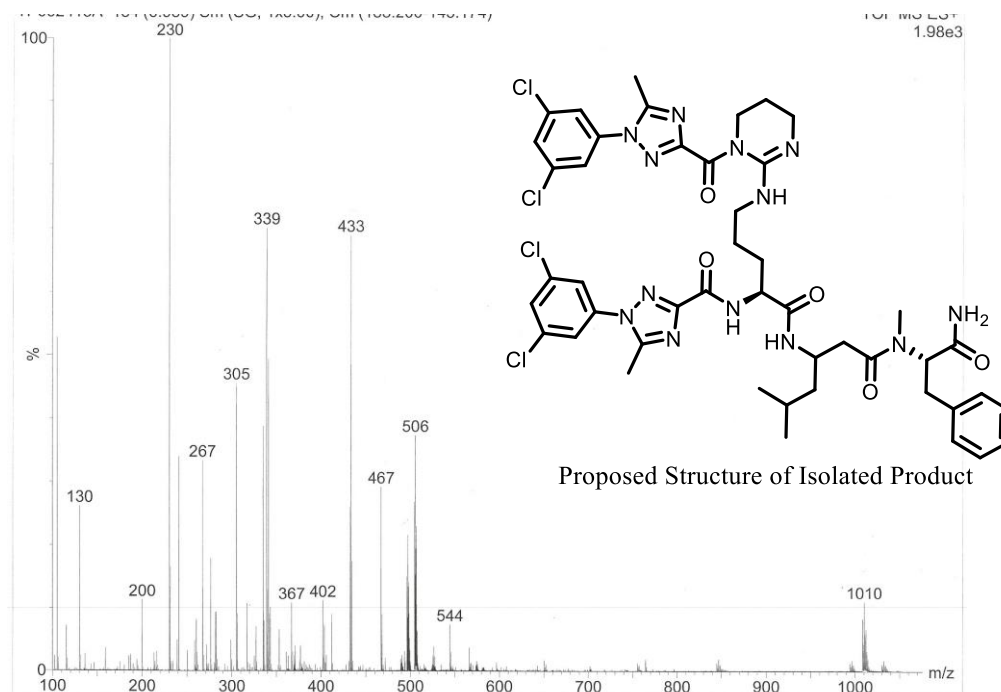
C2. MS results for N-((2S)-1-((1-(((S)-1-amino-1-oxo-3-phenylpropan-2-yl)(methyl)amino)-5-methyl-1-oxohexan-3-yl)amino)-5-((1-(1-(3,5-dichlorophenyl)-5-methyl-1H-1,2,4-triazole-3-carbonyl)-1,4,5,6-tetrahydropyrimidin-2-yl)amino)-1-oxopentan-2-yl)-1-(3,5-dichlorophenyl)-5-methyl-1H-1,2,4-triazole-3-carboxamide. MS(ES): m/z: 1010 [M+H]$^+$ (10-15%)